# Natural evolution of intermale sexual behavior by multiple pheromone switches among *Drosophila* species

Youcef Ouadah [1], Thomas H. Naragon [2], Hayley Smihula [2], Emily L. Behrman [3,†], Mohammed A. Khallaf [4,‡], Yun Ding [5], David L. Stern [3], Joseph Parker [2], and David J. Anderson [1,*]

[1] Division of Biology and Biological Engineering, Tianqiao and Chrissy Chen Institute for Neuroscience, and Howard Hughes Medical Institute, Caltech, Pasadena, CA, USA
[2] Division of Biology and Biological Engineering, Caltech, Pasadena, CA, USA
[3] Janelia Research Campus, Howard Hughes Medical Institute, Ashburn, VA, USA
[4] Department of Evolutionary Neuroethology, Max Planck Institute for Chemical Ecology, Jena, Germany
[5] Department of Biology, University of Pennsylvania, Philadelphia, PA, USA

[†] Present address: Department of Biological Sciences, Dartmouth College, Hanover, NH, USA
[‡] Present Address: Molecular Physiology of Somatic Sensation Laboratory, Max Delbrück Center for Molecular Medicine, Berlin, Germany and Department of Zoology and Entomology, Faculty of Science, Assiut University, Assiut, Egypt
[*] Correspondence: wuwei@caltech.edu

**Abstract**

We have identified a *Drosophila* species in which males exhibit spontaneous, elaborate, and robust intermale sexual behavior. Males of *D. santomea*, a West African island endemic, distinguish conspecific sexes but court males and females promiscuously and seldom attack. Elevated intermale courtship derives from at least three changes in two separate pheromone systems. In males, the sexually monomorphic cuticular pheromone 7-tricosene promotes rather than inhibits courtship and the courtship-inhibiting olfactory pheromone cVA is reduced 84-92% compared to close relatives, including the sibling species *D. yakuba*. The third change is surprisingly in *D. santomea* females, where cVA suppresses rather than promotes sexual receptivity. The female cVA switch and male cVA reduction may have co-evolved to maintain efficient intraspecific mating in *D. santomea* but prevent sympatric hybridization with *D. yakuba*, or to reduce intraspecific aggression. We find that high intermale courtship and low cVA also co-occur and appear selectively derived in a distant monomorphic species *D. persimilis*, implying pheromonal and behavioral convergence in the two recently speciated taxa. The data suggest that sequential changes in the behavioral valence and levels of pheromones explain the recent evolutionary emergence of intermale sexual behavior in *Drosophila*.

## Introduction

Social behaviors, including aggregation, aggression, courtship, mating, parenting, and cooperation (*1*), are remarkably diverse in the animal kingdom, and can vary between closely related sibling species (*2*) or even entire orders (*3*). The ultimate causes of social behaviors (in terms of natural and sexual selection) have received considerable theoretical attention (*4*, *5*) and proximate causes (including genetic loci, hormones, neural circuits, pheromones, and sensory releasers) identified (*6–15*). The ~2,000 species of the genus *Drosophila* (*16*) have historically excelled in this regard as models for intersexual social behaviors (*17–22*), providing notably an unparalleled genetic, neural, and pheromonal understanding of the iconic courtship dance of *D. melanogaster* males (*23–25*). Comparisons of male courtship elsewhere in the genus have revealed flexible substrates, in genomes (*26–29*) and nervous systems (*30–33*), of its rapid evolution and revealed general principles of reproductive function and isolation (*34*, *35*). However, systematic investigations of intrasexual social behaviors between *Drosophila* males or females have comparatively lagged.

Interactions between same-sex conspecifics can vary greatly across species, strains, individuals, and time (*36*, *37*), and can be as opposed as altruistic cooperation (*38*) versus lethal aggression (*39*). Such flexibility implies that intrasexual social behaviors can evolve quickly under varying selection pressures or neutral drift, but underlying changes in pheromone systems, neural circuits, and genomes are often difficult to pinpoint. We sought to identify phylogenetic patterns of variation in intermale social behavior in *Drosophila* and, by leveraging experimental strengths of the genus, reveal proximate and ultimate evolutionary causes. We have found a species, *D. santomea*, in which males show promiscuous sexual behavior toward other males that includes all species-typical motor and acoustic features of the female-directed courtship dance, and is accompanied only rarely by overt aggression. Three distinct changes in pheromone levels or behavioral valence compared to *D. melanogaster* have occurred during *D. santomea* evolution, both before and after divergence from the sibling species *D. yakuba*. Together these changes have highly and selectively amplified intermale courtship without eliminating sex discrimination or the latent potential for intense attack, which can be revealed by optogenetic activation of conserved aggression-promoting neural circuits. The results, together with information from natural history and phylogenetic inference, provide insight into the pheromonal mechanism and evolutionary logic of recent social evolution in *Drosophila* that may apply broadly to other taxa.

## Results

### Evolutionary variation in male-male social behavior within the genus *Drosophila*

In the presence of food or a female, pairs of single-housed *D. melanogaster* males will fight (*40–47*), employing a stereotyped set of contact- and non-contact-mediated motor actions including lunging, tussling, and wing threat (*48–50*). We assessed aggression (and other intermale social behaviors) comparatively in 15 *Drosophila* species, screening for qualitative and quantitative variation in male social engagement, frequency, and motor pattern. We sampled species densely within the *melanogaster* subgroup (7 tested of 9 assigned) (*51*) to monitor potential behavior variation at close phylogenetic distance to *D. melanogaster* with high resolution. At larger evolutionary distances we sampled sparsely (typically one species per subgenus group or subgroup) to broadly survey genus social evolution, apart from including both members of the *D. pseudoobscura* / *D. persimilis* sibling species pair from the *obscura* group (*52*). We standardized assay conditions but occasionally varied the food source over which flies competed to account for host specializations (*53*). Fly behavior was measured in dyadic male-male interactions, by combining manual scoring on a subset of representative recordings (Fig. 1A,B, 1-S1A) with automated behavior classification for the remainder (Fig. 1-S2A,B) (*54–56*).

Aggression among *D. melanogaster* males was the most prominent and intense of any *melanogaster* subgroup species tested (Fig. 1A-C, 1-S2C,E). Species in the neighboring *simulans* clade (*D. simulans*, *D. mauritiana*, and *D. sechellia*) also fought, though less frequently, using a similar set of actions (Fig. 1A-C, 1-S2C,E). Varying foods usually had little effect on the behavior of specialists, with the notable exception of *D. sechellia* which fought significantly more over *Morinda* than the standard apple juice (Fig. 1-S3A), consistent with its specialization (*53*). Male-male interactions in *D. melanogaster* and *simulans* clade species all included very little recognizable courtship, and the few bouts we observed never progressed to attempted copulations (Fig. 1A,B). Thus, intermale aggressive actions in the subgroup branch that includes *D. melanogaster* are almost entirely distinct from the courtship that males perform toward females (Fig. 1E,F, 1-S4).

The other branch of the *melanogaster* subgroup, which includes *D. erecta*, *D. yakuba*, and *D. santomea*, exhibited dramatically different male-male dynamics. *D. erecta* males hardly interacted or locomoted, even on the preferred *Pandanus* substrate (Fig. 1A,B, 1-S1B, 1-S3) (*57*). *D. yakuba* and *D. santomea,* by contrast, exhibited low levels of aggression and multiple distinct, clearly recognizable courtship actions (Fig. 1A,B). Male-male courtship in both species was visually similar as toward females (Fig. 1G,H, 1-S4), but the two sibling species differed markedly from each other in penetrance and expressivity. Courtship and attack between *D. yakuba* males were both infrequent, whereas *D. santomea* males courted other males considerably more than they fought them and far more than did *D. yakuba* or

any other subgroup species (Fig. 1B,D, 1-S2D,F). High levels of male-directed courtship and low aggression were conserved in three additional *D. santomea* strains (Fig. 1-S2C-F), were not limited to the initial moments of an encounter when sex identification might be incomplete (Fig. 1D) (*58*, *59*), and sometimes culminated in copulation attempts (Fig. 1A). Audio recordings (*60*) confirmed that *D. santomea* males sang to males as they did to females, emitting both "pulse" and "clack" song (*61–63*) with similar (though not identical) acoustic features (Fig. 1I,J, 1-S5).

Thus, under the conditions tested there exists a near-qualitative difference in intermale social behavior between *D. melanogaster* and *D. santomea*. *D. melanogaster* and *simulans* clade relatives attack males with varying frequencies using a conserved set of actions, whereas *D. santomea* courts both males and females nearly indistinguishably. While widely described in other taxa (*64*), the frequent courtship among wildtype adult males shown by *D. santomea* in naturalistic settings is, to the best of our knowledge, novel in the *Drosophila* genus. Importantly, *D. santomea* male-directed courtship is not due to sex misidentification, because individual flies that courted and sometimes also attacked males immediately switched to exclusive courtship with significantly increased vigor when encountering a female, no matter the presentation order (Fig. 1K-O).

**The abundant and monomorphic cuticular pheromone 7-tricosene is sexually attractive to *D. santomea* males**

Five of the nine *melanogaster* subgroup species (*D. simulans*, *D. santomea*, *D. yakuba*, *D. teissieri*, and *D. orena*) are considered pheromonally monomorphic because the same cuticular hydrocarbon (CHC) is the most abundant compound on the cuticles of females and males (*65–67*). For all five the defining monomorphism is of (Z)-7-tricosene (7-T) (Fig. 2A, 2-S1), a nonvolatile compound detected via contact chemosensation (*68*, *69*). *D. santomea* courts in the dark (Fig. 2B) (*70*) and removing CHCs in bulk from either females or males strongly diminishes their attractiveness (Fig. 2C), implying the existence of courtship-promoting pheromone(s) shared between sexes. That 7-T is an aphrodisiac signal for *D. santomea* males is supported by monomolecular add-back following bulk CHC removal from *D. santomea* females (Fig. 2D), ectopic addition to intact females of species lacking endogenous 7-T (*D. melanogaster* and others) (Fig. 2E, 2-S2), and positive correlation between 7-T presence and courtship elicited from *D. santomea* males in a variety of heterospecific male-male pairings (Fig. 2F). Thus, 7-T appears necessary and is sufficient to evoke sexual attraction towards males as well as females in *D. santomea.* The inversion from 7-T suppressing courtship in *D. melanogaster* (where it is male-specific) (*71–74*) to promoting courtship in *D. santomea* is shared with *D. yakuba* (*32*), suggesting that the 7-T valence switch arose in tandem with monomorphism in the *D. santomea / D. yakuba* (or *yakuba* clade) common ancestor on mainland Africa (Fig. 2G) (*75*).

115

116 **Selectively low cVA abundance on *D. santomea* males amplifies intermale courtship**

117 If *D. santomea* sexual attraction uses an abundant and monomorphic signal (7-T), then it would
118 seem unsurprising that male-directed courtship is a corollary outcome of this relatively simple pheromone
119 arrangement. However, intermale courtship in *D. yakuba* and other 7-T monomorphic species is rare (Fig.
120 2G) (*30*, *32*, *76*), hinting that *D. santomea* males have either gained an additional courtship-promoting
121 signal absent in the other species or lost a courtship-inhibiting signal otherwise present. We found that *D.*
122 *santomea* males express significantly less (Z)-11-octadecenyl acetate (cVA) than other subgroup members
123 (84-92% reduction, 89% less than *D. yakuba*) (Fig. 3A, 3-S1). cVA is a semi-volatile pheromone
124 produced in the ejaculatory bulb of male drosophilids (*67*, *77*, *78*) and has pleiotropic roles in social
125 behavior including promoting aggregation (*79–81*) and aggression (*82–85*) and suppressing courtship
126 (*86–90*), either natively on males or after transfer to females during copulation. Behavioral dose-response
127 curves with cVA applied onto a piece of filter paper indicated that cVA indeed suppresses courtship in *D.*
128 *santomea* (Fig. 3B-D), with the primary effect being to increase latency to initiation (Fig. 3C). In a choice
129 assay, *D. santomea* males showed nearly universal preference for courting solvent control treated males or
130 females over flies directly coated with cVA (Fig. 3E). Triggering fictive cVA sensation in *D. santomea*
131 males by phasic optogenetic activation of Or67d-expressing olfactory sensory neurons (OSNs) (Fig. 3-S2)
132 (*89*, *91–95*) was sufficient to interrupt natural courtship towards conspecific partners of both sexes (Fig.
133 3F-I), as also observed in *D. melanogaster* (*96*). Interestingly, the photostimulation light intensity needed
134 to pause ongoing courtship was lower with male targets than with females (Fig. 3J), consistent with some
135 courtship suppression even by the low endogenous amount of cVA present on *D. santomea* males.

136 Unlike its courtship-inhibiting function, cVA's aggression-promoting function does not appear to
137 be conserved in *D. santomea* males. cVA addition experiments, either onto filter paper or directly onto
138 live target males, showed no effect of inducing aggression (Fig. 3K,L), nor did strong and direct
139 photoactivation of Or67d OSNs (Fig. 3M). Pairings with unmanipulated heterospecific male partners
140 presenting high endogenous cVA levels also failed to significantly increase attack behavior by *D.*
141 *santomea* males (Fig. 3-S3). The ineffectiveness of cVA to promote aggression in *D. santomea* males may
142 be due to the 7-T valence switch described above (Fig. 3N-P and see Discussion).

143 The combination of sexual attraction by monomorphic 7-T, which likely evolved in the *yakuba*
144 clade common ancestor, and low levels of the male-specific anti-aphrodisiac cVA, uniquely derived in *D.*
145 *santomea,* thus provides a pheromonal basis for selectively elevated courtship among *D. santomea* males.
146 One curious additional effect was observed, presumably also due at least in part to low cVA signaling.
147 When paired with males of other *melanogaster* subgroup species that find cVA sexually aversive (*32*, *67*,
148 *89*) and show minimal sexual behavior in conspecific male-male pairs (*D. melanogaster*, *D. simulans*, *D.*

149 *yakuba*), *D. santomea* males elicited 200-580% higher levels of courtship and 53-91% reduced levels of
150 aggression (Fig. 3-S4) from the heterospecific males. Thus, *D. santomea* male attractiveness extends even
151 across species boundaries to multiple other *Drosophila* males.
152
153 **Central aggression circuits in *D. santomea* can evoke intense attack when photoactivated**
154 *D. santomea* intermale sexual behavior is frequent but does not fully saturate the time that two
155 males interact (Fig. 1B). Even so very little attack occurs outside of courtship periods, which in addition
156 to the ineffectiveness of cVA to promote aggression prompts the question of whether *D. santomea*
157 aggression circuitry is conserved in form and function.
158 Multiple aggression-promoting neurons have been identified in *D. melanogaster* males (*50*),
159 among which are P1/pC1 (and subsets therein) (*56*, *85*, *96–101*) and AIP (also called CL062) (*102*, *103*).
160 We generated transgenic reagents necessary to access P1/pC1 (referred to here as $P1^{dsx}$ to reflect the split
161 driver combination used) and AIP in *D. santomea* by combination CRISPR-Cas9 knock-in (*104*, *105*) and
162 phiC31 recombination into existing landing site lines (*106*, *107*), and tested photoactivation effects in
163 single or paired flies using CsChrimson as the opsin effector (*108*). AIP neurons had the expected position
164 and morphology in *D. santomea* males (Fig. 4A), and photoactivation in solitary flies elicited bilateral
165 wing elevation (i.e. threat display, the major non-contact-mediated form of aggression in male
166 *Drosophila*) (*41*) time-locked to the onset and offset of photostimulation (Fig. 4B-D, 4-S1). $P1^{dsx}$ neurons
167 were similarly present (Fig. 4E) and photostimulation evoked reliable time-locked courtship measured by
168 unilateral wing extension in solitary flies (Fig. 4F, 4-S2), as expected given their dual roles in courtship
169 and aggression (*109*).
170 In same-genotype pairs of *D. santomea* males both experiencing titrated photoactivations, $P1^{dsx}$
171 stimulation induced a mix of aggressive and courtship actions similar to the effects seen in *D.*
172 *melanogaster* (Fig. 4G-J, 4-S3) (*56*). Lunge attacks, the major contact-mediated aggressive action in
173 males (*43*), initiated during low frequency stimulations (significantly at 2 Hz) and escalated in intensity as
174 the stimulus frequency increased (Fig. 4H,I, 4-S3A-C). Fighting remained persistently elevated following
175 the final photostimulation period for the duration of the recording. High frequency stimulations (>10 Hz)
176 at one-minute intervals interrupted the otherwise monotonic increase in attack intensity with temporary
177 phases of courtship and locomotor arrest time-locked to photostimulation (Fig. 4H,J, 4-S3D,E), as also
178 observed in solitary flies. Mixed-genotype pairs (in which one of the two photoactivated males was
179 replaced with a wildtype male prepared to be passive during the assay by group-housing) confirmed that
180 stimulated aggression was fly-autonomous and not exclusively caused by social feedback (Fig. 4-S4A)
181 and revealed some contextual flexibility in its expression. $P1^{dsx}$ photoactivated flies in mixed pairs
182 required slightly higher stimulation frequency to initiate attack (5 instead of 2 Hz, Fig. 4-S4A vs. 4I) and

183 their attack intensity remained ~50-60% lower throughout the trials (Fig. 4-S4B). The delay in attack
184 latency allowed for an intermediate period when attack and courtship were co-expressed (Fig. 4-S4C,D),
185 which contrasted with the largely mutually exclusive action patterns observed in same-genotype pairs
186 controlled by the photostimulation pattern (Fig. 4H). This resulted in a shift from nearly equal balance
187 between flies exhibiting attack or courtship first to a majority of cases where courtship preceded attack
188 (Fig. 4-S4E).

189 Thus, major nodes within at least two distinct aggression-promoting circuits ($P1^{dsx}$ and AIP) are
190 conserved in *D. santomea* and both contact- and non-contact-mediated attack patterns can be efficiently
191 evoked by their photoactivation. This rules out that the usual paucity of spontaneous attack in *D.*
192 *santomea* male pairs under naturalistic conditions derives from an evolved loss of function of (at least
193 these) aggression circuits, or broadly limiting factors such as energetic or muscular deficits. $P1^{dsx}$
194 experiments reveal that *D. santomea* aggression can be elevated to supernormal intensity and exhibit
195 persistence under optimal photoactivation conditions (~23-fold higher lunge rate observed after final
196 photostimulation compared to spontaneous interactions, Fig. 4I vs. 1C), but the direct effect of courtship
197 dominates and strongly suppresses attack while $P1^{dsx}$ is highly activated (as also in *D. melanogaster*) (*56*).
198 An opponent whose pheromone bouquet activates *D. santomea* $P1^{dsx}$, especially a non-aggressive one,
199 would therefore be expected to elicit courtship instead of attack as long as the activation perdures.
200

201 **A switch from cVA sexual attraction to aversion in *D. santomea* females**

202 *D. santomea* has an interesting natural history (Fig. 5A-C) (*110–112*). They are endemic to the
203 equatorial West African island of São Tomé, located 280 km from Gabon in the Gulf of Guinea. *D.*
204 *yakuba* also inhabits São Tomé, and the two sibling species largely segregate by elevation along the
205 elevation gradient from the volcanic island's warm, dry, and open perimeter (*D. yakuba's* range) to its
206 cool, humid, forested summit (*D. santomea's*). A sympatric zone is formed at their mid-elevation
207 boundary, where both species and rare F1 hybrids can be collected that adhere to Haldane's rule for
208 sterility in the heterogametic sex (i.e., males) (*113*). Since *D. santomea* and *D. yakuba* males court
209 females of both species promiscuously (*114*, *115*), male offspring sterility should pressure females
210 strongly to discriminate against heterospecific matings and maintain reproductive isolation (*116*). In flies
211 this challenge would normally be expected to be met by females detecting species-specific acoustic
212 features of male courtship song (*117*), but although *D. santomea* and *D. yakuba* songs are distinct (*61*,
213 *63*), *D. santomea* females are still able to distinguish males of each species even if they are muted by
214 wing amputation (*62*). These observations implicate additional species-identifying cues.

215 The cVA addition experiments above demonstrated that *D. santomea* males show increased
216 copulation latency and reduced copulation rates in the presence of high cVA (Fig. 3C,D), but we noticed

217 that the effects may not derive exclusively from alterations in the males' behavior. *D. santomea* females
218 exposed to cVA exhibited dramatically increased ovipositor extrusion (Fig. 5D, 5-S1), a sexual rejection
219 behavior typically seen in recently mated, unreceptive *Drosophila* females (*118–121*). Significant
220 rejection occurred at a lower cVA dose than was required to reduce male courtship (1 vs. 2 mg, Fig. 5D
221 vs. 3B), and measurements remained elevated even after normalization to the amount of male courtship
222 observed (Fig. 5E). Incorporating observations of wing spreading, a distinct female behavior signaling
223 sexual acceptance (*122*), into a combined index of *D. santomea* receptivity further captured the cVA-
224 dependent rejection response (Fig. 5F). Strikingly, Or67d OSN silencing via ectopic expression of the
225 inward rectifying potassium channel Kir2.1 (*123*) in *D. santomea* females paired with wildtype males
226 resulted in ~2-fold increased copulation rates compared to controls (Fig. 5G), indicating that cVA
227 sensation normally limits *D. santomea* female sexual responses. Unconditioned place preference tests
228 suggest that increased cVA aversion is likely innate (Fig. 5-S2).
229 The sexually appetitive effect of cVA on *D. melanogaster* females (*89*) is therefore reversed in *D.*
230 *santomea,* and this unexpected switch represents a third pheromone change in *D. santomea* (along with
231 attraction to 7-T and reduced cVA abundance in males). We hypothesize that the valence reversal may
232 help *D. santomea* females identify and avoid unwanted hybridization with high cVA-expressing *D.*
233 *yakuba* males, thereby maintaining reproductive isolation in São Tomé. This may have been preceded by
234 *D. santomea* male cVA reduction (making cVA-averse *D. santomea* females more sexually competitive),
235 or alternatively, was directly triggered by *D. yakuba* recolonization of São Tomé (*111*) and caused
236 compensatory male cVA reduction by sexual selection pressure (*124*) (Fig. 5H, Discussion). The latter
237 possibility raises a question of whether the increased intermale courtship that results from cVA reduction
238 is simply a costly but necessary accommodation by *D. santomea* males to appease conspecific females.
239 According to this view, same-sex sexual behavior (SSB) is inherently "non-reproductive" and may be
240 detrimental to fitness or, at best, a waste of energy (*64*). We next explored whether male-male courtship
241 might have any adaptive value in *D. santomea.*
242

243 **P1$^{dsx}$ activation or natural male-directed courtship induces a competitive mating advantage in *D.***
244 ***santomea* males**

245 In the original comparative screen and multiple experiments conducted thereafter, paired *D.*
246 *santomea* males were derived from the same stock and prepared for behavior assays identically, but
247 nevertheless exhibited a surprising degree of courtship bias between members of the pair. That is, it was
248 usually the case that just one male committed most of the total courtship observed (Fig. 6A, 6-S1), similar
249 to biases observed during intermale aggression in *D. melanogaster* (*125*). In pairs where fighting also

took place the two actions were most often attributable to the same fly (Fig. 6B), hinting that biased courtship and attack might both contribute to agonistic social dominance in *D. santomea.*

*D. santomea* males do not appear to be territorial (Fig. 6-S2), but we reasoned that dominance in male-directed courtship might facilitate its female-directed counterpart due to persistent social arousal (*126*), and therefore be a valuable action to the dominant fly. In *D. melanogaster*, pairs of males encountering one another for the first time ten minutes after P1/pC1 photostimulation will fight significantly more than controls (*56*). *D. santomea* female- and male-directed courtship uses the homologous neural circuit (Fig. 6C) and, when tested in a similar assay (called here a "sliding door" for the removable barrier separating the two flies), brief photostimulation of $P1^{dsx}$ neurons in *D. santomea* males also triggers persistent, intense aggression after the same ten-minute delay (Fig. 6D-I, 6-S3A-E). However, in mixed pairs between a photostimulated male and wildtype female, males switched to exclusive courtship during the interaction phase with significantly increased vigor and decreased latency compared to unstimulated controls (Fig. 6J-N, 6-S3F), indicating that persistent effects of $P1^{dsx}$ activation enhance later social interactions with both sexes, and highlighting *D. santomea* males' ability to discriminate sexes and adjust social behaviors accordingly even when highly aroused.

We recreated $P1^{dsx}$ circuit persistent activation in a naturalistic setting by taking wildtype males through two consecutive social encounters: first in a pair with one other male during which a courtship dominance relationship was allowed to form, and second in a trio with the same male and a newly added female (Fig. 6O-Q). Analogously to $P1^{dsx}$ photostimulation, *D. santomea* males that dominated courtship in the paired male setting showed significantly greater propensity to also do so toward females in the trio phase of the experiment (Fig. 6R,S). The effect appeared to strengthen in males that expressed higher amounts of male-directed courtship during the first phase (Fig. 6R, larger dots). Copulations were rare, but two of the three observed were obtained by previously dominant males (Fig. 6T) (the exception was by a male from a pair with very weak intermale dominance). Thus, male-directed courtship in *D. santomea* is sufficient to induce sexual priming, in which males who have recently courted (or otherwise experienced $P1^{dsx}$ activation) are better prepared to court and potentially also copulate with females that soon appear.

**Convergent social behaviors and pheromones in *D. persimilis* males**

Our screen also uncovered a second species highly prone to male-directed courtship, *D. persimilis* (Fig. 1B, 1-S1A). *D. santomea* and *D. persimilis* last shared a common ancestor ~50 million years ago and intermale courtship appears to be selectively derived in each species (Fig. 7A). *D. persimilis* and *D. santomea* both inhabit cool, high elevation, montane regions, *D. santomea* in West Africa and *D. persimilis* in Western North America, and both are members of a sibling species pair with which they

284 geographically overlap (*52*). Importantly, males of *D. persimilis* and *D. pseudoobscura* (the sibling
285 species) both court females interspecifically but females show strong discrimination against cross-
286 hybridization (*127–129*). Like *D. santomea, D. persimilis* male-directed courtship shares visual
287 resemblance with the female-directed form and is most often biased to just one male within each pair
288 (Fig. 7B-D, 7-S1A,C,D). *D. pseudoobscura* males instead show the more genus-typical social patterns of
289 male-directed aggression and female-directed courtship (Fig. 7E-G, 7-S1B-D) (*130*). Finally, *D.*
290 *persimilis* males have also converged on the two key pheromonal features of CHC monomorphism and
291 low cVA expected to reduce or eliminate major barriers to male-male courtship (Fig. 7H,I) (*67*, *131*).
292 Similar phylogenies and natural histories therefore correlate with convergent pheromones and male-male
293 sexual behaviors shared between these two distantly related flies.
294

## Discussion

Evolutionary changes in the expression and central processing of cuticular hydrocarbons (CHCs) have been shown to underlie phylogenetic variation in pheromonal control of male-female courtship in *Drosophila* (*22*, *132*). Two types have been described: a change in the sex-specificity of pheromone expression, from sexually dimorphic to monomorphic CHC patterns (*28*), and a switch in the behavioral valence of certain CHCs (e.g., 7-T) from male courtship-inhibitory in dimorphic *D. melanogaster* (*71–74*) to courtship-promoting in monomorphic species including *D. yakuba* (*32*) and, to a lesser extent, *D. simulans* (*27*, *30*, *71*). Here we identify a novel pheromonal valence switch in *D. santomea* females, from sexual receptivity-promoting (*89*) to receptivity-inhibiting, of cVA, a semi-volatile olfactory pheromone. Two additional pheromone changes in *D. santomea* males, a reduction in cVA abundance relative to other *melanogaster* subgroup species and a switch to monomorphism and sexual attraction to 7-T that is shared with *yakuba* clade species, can explain the amplification of *D. santomea* intermale courtship. The results illustrate how multiple changes in the behavioral valence or abundance of pheromones in both females (cVA valence) and males (7-T valence and cVA abundance) can collectively drive evolutionary variation in same-sex sexual behavior (SSB), as well as aggression. Our data also highlight potential social tensions between *D. santomea* and *D. yakuba* in their overlapping habitat in West Africa and the evolutionary impacts affecting both sibling species. A similar set of pheromonal events may also explain the difference in male-male social behaviors observed between *D. persimilis* and *D. pseudoobscura* in North America.

### A layered evolutionary path to elevated intermale courtship in *D. santomea*

*D. melanogaster* males (*49*, *109*) and males of most *Drosophila* species surveyed here exhibit primarily female-directed courtship and male-directed aggressive behavior. The sex-specificity of these social behaviors in dimorphic *D. melanogaster* is controlled in part by male-specific 7-T and cVA, which function similarly to suppress intermale courtship and promote aggression (*69*, *72*, *82*, *83*). However, *D. santomea* and other *yakuba* clade species are monomorphic for 7-T (*65–67*) and males show 7-T sexual attraction rather than aversion. This permits these species to pursue females and mate in the dark as dimorphic species can (but 7-T monomorphic species in which males show neutral 7-T sexual responses cannot) (*32*), and shifts the function of sex discrimination to other pheromones or sensory modalities. Despite high 7-T abundance and monomorphism, male-directed sexual behaviors in these species are usually minimal, except notably in *D. santomea*. The restricted specificity for elevated intermale courtship in *D. santomea* (and hence evolutionary recency) parallels a selective reduction in the abundance of cVA, an olfactory signal which in *D. melanogaster* suppresses male courtship (*71*, *86–90*) and is otherwise present at high levels on males of *melanogaster* subgroup species. That this correlation reflects causation is demonstrated by the fact that *D. santomea* courtship can be suppressed either by

329 addition of exogenous cVA or by direct photoactivation of olfactory sensory neurons (OSNs) expressing
330 the cVA receptor Or67d (*89*, *91–95*) . Thus, the high level of sexual behavior among *D. santomea* males
331 can be explained by two, presumably sequential evolutionary changes in distinct cuticular and olfactory
332 pheromone signaling pathways: a change in the behavioral valence of 7-T and a reduction in the
333 abundance of cVA. We note that, while our data indicate that 7-T can restore male courtship towards
334 hexane-washed dead *D. santomea* females and promote courtship of dead females of other species which
335 ordinarily do not express 7-T, we cannot exclude that other components of the female CHC bouquet
336 and/or non-CHC pheromones contribute to *D. santomea* male attraction. We also cannot exclude a limited
337 role for non-chemosensory signals (*30*).

338 A potential evolutionary explanation for the male cVA reduction was lacking until our unexpected
339 discovery of a second sexual valence switch (and third pheromonal change in total), this time in the
340 behavioral response to cVA by *D. santomea* females. cVA promotes mating receptivity in *D. melanogaster*
341 (*89*) but has the opposite effect in *D. santomea*: increasing cVA abundance promotes sexual rejection and
342 Or67d OSN silencing increases copulation rates ~2-fold. The switch may be related to interspecific sexual
343 dynamics between *D. santomea* and *D. yakuba* at their geographic boundary in São Tomé. *D. yakuba*
344 males court *D. santomea* females vigorously (*114*, *115*) and rare (sterile) F1 hybrid males can be collected
345 within the sympatric zone (*110–112*), so we speculate that the *D. santomea* female cVA valence switch
346 arose due to ongoing selection pressure to maintain reproductive isolation from *D. yakuba* (*116*). If the
347 model is correct, this would mean that *D. santomea* females use the high level of cVA on *D. yakuba* males
348 as a sex- and species-identifying cue to ward off unwanted advances from heterospecific suitors. Reduced
349 cVA abundance by *D. santomea* males may then have emerged by consequent sexual selection pressure
350 (*124*). However, two other evolutionary scenarios are also possible. In one, *D. santomea* males may have
351 initially reduced cVA abundance due to neutral drift or to pheromonally distinguish themselves from *D.*
352 *yakuba* males (*133*), which in turn may have pressured *D. santomea* females to develop cVA aversion by
353 sexual selection operating in the reverse direction. Alternatively, *D. santomea* female cVA aversion and
354 male cVA reduction may have evolved simultaneously, potentially in genetic linkage (*134*). In any of
355 these scenarios, the ultimate outcome would have been to maintain efficient intraspecific mating in *D.*
356 *santomea* but prevent hybridization with *D. yakuba*. The combination of reduced cVA and cuticular
357 pheromone monomorphism appears to be a generalizable mechanism for amplifying intermale courtship
358 because the same pattern is shared with *D. persimilis* compared to *D. pseudoobscura*.

359 Mechanistic explanations for the changes to cVA signaling in *D. santomea* females and males
360 remain to be elucidated. In *D. melanogaster*, cVA promotes female receptivity through activation of pCd
361 neurons (*135*). Whether behavioral inversion in *D. santomea* females is reflected in a physiological
362 inversion of the effect of cVA on pCd, from excitatory to inhibitory, is an interesting possibility. A

363 challenge also remains in resolving the genetic and biochemical nature of reduced cVA abundance in
364 males (e.g., decreased production vs. increased degradation), and determining whether the divergent *D.*
365 *santomea* and *D. persimilis* lineages achieved reductions by similar means. A biosynthetic logic for cVA
366 production in the ejaculatory bulb has been proposed (*136*) and one elongase identified (*137*), but
367 additional enzymes necessary to generate cVA from fatty acid precursors have not yet been identified.
368 *Cyp6a20* has been identified as a potential degradative enzyme for cVA which is expressed by non-
369 neuronal cells in Or67d-expressing sensillae (*44*, *47*), and may be another target of selection.
370

371 **Mechanisms for suppressing aggression in *D. santomea* males**

372 *D. santomea* males show little spontaneous attack. However, photoactivation of aggression-
373 promoting neural circuits in the central brain is sufficient to elicit multiple contact- or non-contact-
374 mediated agonistic actions (e.g., threat displays, lunging, tussling) with supernormal intensity, ruling out a
375 lack of vigor or selective atrophy of aggression circuits as explanations for the low level of spontaneous
376 aggressive behavior. Because *D. santomea* males can clearly discriminate conspecific sex, it can be
377 inferred that pheromones or behavioral cues from a *D. santomea* male are sufficient to signal "maleness,"
378 but are either insufficient to activate aggression circuits, or that coincident male-derived courtship-
379 promoting cues (e.g., 7-T) dominantly suppress attack through inhibitory influences on central circuits or
380 motor systems so long as the target male is present (*109*). A potentially relevant observation is that acute
381 inhibition of aggression by photoactivation of courtship circuits yields presumptive post-inhibitory
382 rebound fighting upon stimulation offset, which persists for minutes. This could explain why *D. santomea*
383 (and *D. melanogaster*) (*56*) males only attack each other during the light-off periods of our $P1^{dsx}$
384 photoactivation experiments when courtship subsides, and initiate aggression almost instantly minutes
385 after $P1^{dsx}$ neurons have been stimulated in the sliding door assay, when aggression circuits may still be in
386 the elevated rebound regime. Persistent neural effects must be flexible, however, because females are
387 instead met with vigorous and exclusive courtship following barrier removal.

388 In addition to the courtship-inhibiting effect discussed above, cVA also promotes aggression
389 among *D. melanogaster* males (*82–85*). At face value, this second signaling function predicts that reduced
390 cVA in *D. santomea* should have a corollary effect to decrease aggression, in which case cVA reduction
391 alone could have parsimoniously explained both the elevated courtship and reduced fighting observed in
392 *D. santomea* social interactions. We have so far been unable to verify this prediction, because various
393 experimental efforts to elevate cVA, including strong and direct photoactivation of Or67d OSNs, have
394 been ineffective at increasing *D. santomea* aggression (although effective at suppressing intermale
395 courtship). A possible explanation is suggested by the established hierarchical control of male-male social
396 behavior by 7-T and cVA in *D. melanogaster* (*72*). There, cVA can promote fighting but only if 7-T

signaling remains intact. In flies lacking 7-T or its receptor Gr32a, cVA has no effect to promote aggression or to inhibit the extensive male-male courtship unmasked by genetic disruption of 7-T signaling. Thus, suppression of intermale courtship by 7-T is likely a prerequisite for the aggression-promoting effect of cVA in *D. melanogaster*. By extension, since in *D. santomea* 7-T no longer suppresses courtship, according to this hierarchical model increasing cVA experimentally should be unable to promote fighting, as is observed. This hypothesis does not exclude the possibility that thus-far undetected evolutionary changes in aggression-promoting components of cVA central circuitry (*84*, *126*) may contribute to reduced fighting in *D. santomea* males as well.

**Recent speciation and intermale sexual behavior**

It seems unlikely to be a coincidence that the two cases of highly expressive and penetrant same-sex sexual behavior (SSB) discovered here in *Drosophila* are each observed in members of sibling species pairs, and particularly in species with the more restricted geographic range. The pattern suggests that recent speciation may predispose animals to elevated SSB expression (or, formally, high SSB may predispose to speciation), and in fact this correlation proved significant in a phylogenetic analysis of SSB incidence across all mammals, including the Hominidae (*138*). The findings here provide a general model that may explain at least some of these cases: where sympatry necessitates enforcement of reproductive isolation between interfertile species that produce unfit hybrid offspring (such as sterile F1 males) (*113*), the challenge of interspecies identification may draw upon sensory cues that, once altered, also result in modification of intraspecific social behaviors including SSB. If the condition of sympatry is removed, or additional species-identifying cues are enlisted, or compensatory intraspecific mechanisms evolve, then SSB may relax, unless it provides an adaptive value.

Such an adaptive value for SSB may have accrued in *D. santomea* for either of two reasons, not mutually exclusive. Males performing natural courtship during male-male encounters (or artificial courtship during direct $P1^{dsx}$ photostimulation) also initiate courtship more quickly and sustain it more vigorously toward a female if she appears within a few minutes. Males could therefore benefit from this sexual facilitation or "priming" effect. Alternatively, the strong bias observed in dyadic male-male courtship interactions, and the fact that the same male that courts is also the one more likely to attack, suggests that intermale courtship could have an adaptive function in mediating social dominance (*64*). Interestingly, evidence in mice suggests that most episodes of male SSB in that species reflect dominance mounting, a low-intensity form of aggressive behavior, rather than affiliative sexual behavior (*139*), and SSB as a dominance behavior has been proposed in other taxa (*140*, *141*).

The general relationship between SSB and aggression across animals appears more complex. The survey study in mammals (*138*) found a positive correlation between SSB and lethal male violence,

motivating the hypothesis that SSB may evolve to ease escalating intermale aggression. If this alternative model also pertains to *Drosophila*, then the sequence and causal role of evolutionary events identified here could be reinterpreted: rather than the key benefit of pheromone (especially cVA) changes being to avoid cross-species hybridization, it may instead have been to effectively replace intermale aggression with courtship, a form of social interaction carrying reduced risk of harm to individuals (*64*). In other words, *D. santomea* males may have evolved a social strategy in which the ultimate functions of aggression that improve fitness (e.g., securing resources, mates, etc.) can be achieved by increased male-male courtship instead, avoiding aggression's injurious costs but maintaining its agonistic or competitive intent (*142*). Resolving or harmonizing these alternatives, potentially by modeling or controlled selection experiments, should help to better understand the evolutionary origins of social behavior across the animal kingdom perhaps including in the human species.

443 **Main Figure Legends**

444

445 **Figure 1. Evolutionary variation in male-male social behavior within the genus *Drosophila***

446 **(A)** Ethograms from twenty-minute male-male interactions depicting aggressive and courtship actions
447 scored in three representative conspecific pairs per species across the melanogaster subgroup. Nodes are
448 bout counts of a given action type, with sizes representing frequency normalized to summed bouts scored
449 across all actions (expert annotation). Edges indicate action transitions, with weights representing the
450 fraction of bouts of a given action (arrow origin) for which a second action (arrow destination) occurred
451 within one second. Eleven total actions in each ethogram are arranged in four rows: first, three aggressive
452 threat actions (threat, pump, charge) (*102*); second, three aggressive contact-mediated actions (lunge,
453 hold, tussle) (*48*); third, three courtship actions utilizing the wings and typically directed toward females
454 (UWE, BWE, row) (*20*); fourth, two courtship actions involving locomotory maneuvers (circle,
455 copulation attempt). Nodes indicating aggressive actions are filled with blue shades and courtship actions
456 with reds. Species arrangement and divergence times according to compilation of available phylogenies
457 (*75*, *143*, *144*). Note emergence of male-directed courtship and reduction of aggression in *D. santomea*
458 (orange) and, to a lesser extent, its sympatric sister species *D. yakuba* (green). *D. erecta* ethogram gray
459 coloration indicates that very few social actions of any kind were observed. Abbreviations: UWE,
460 unilateral wing extension; BWE, bilateral wing extension; Cop. att., copulation attempt. See Table S2 for
461 wildtype strains used in figures throughout.

462 **(B)** Stacked barplots showing cumulative time spent by paired males in any aggressive (blue) or courtship
463 action (red) as a fraction of the twenty-minute total interaction. Additional Sophophora subgenus species
464 for which male-male interactions were scored for the same action set are included. Note unusually high
465 time dedication to male-directed courtship by *D. santomea. D. serrata* aggression scoring is inflated due
466 to unusually long holds.

467 **(C,D)** Expressivity and temporal dynamics of male-male aggression (C) and courtship (D) in *D.*
468 *melanogaster* (black), *D. simulans* (gray), *D. santomea* (orange), and *D. yakuba* (green). Bold traces
469 indicate the mean fraction of frames annotated as lunge (for aggression, C) or UWE (for courtship, D) by
470 automated classifiers in a 10-second sliding window. Envelopes represent standard error of the mean
471 (s.e.m.). Note high aggression in *D. melanogaster* male-male pairs and high courtship in *D. santomea*
472 throughout twenty-minute interactions (significance by Kolmogorov-Smirnov tests). See Supplemental
473 Table S4 for statistics related to figures throughout.

474 **(E-H)** Video stills of *D. melanogaster* (E,F) and *D. santomea* males (G,H) interacting with conspecific
475 female (E,G) or male targets (F,H). *D. melanogaster* court females (E, male shown in UWE) and attack

476 males (F, shown mid-lunge). *D. santomea* court both sexes using a similar set of motor patterns (G,H,
477 males shown in UWE for both) and rarely attack. Scale bars, 1 mm.
478 **(I,J)** Representative *D. santomea* courtship song traces showing "pulse" and "clack" emitted toward both
479 females (I) and males (J).
480 **(K)** Scheme for assessing social behavioral differences by *D. santomea* male tester flies paired
481 consecutively with a male then female conspecific target, or vice versa. Tester male experiences twenty
482 minutes with each sex.
483 **(L-O)** Aggression (L,N, measured as lunges per minute) and courtship (M,O, fraction of total interaction
484 time performing UWE) exhibited by *D. santomea* male testers towards female and male targets. (L,M)
485 Males presented first. (N,O) Females presented first. Data points derived from the same tester are paired
486 and distribution means shown as paired black dots. Note aggression towards males is never also observed
487 to females and significantly increased courtship rates to females, independent of the presentation order
488 (paired Mann-Whitney *U* tests).
489

**Figure 2. The abundant and monomorphic pheromone 7-tricosene is sexually attractive to *D. santomea* males**

**(A)** Mirrored gas chromatograms representing male (purple, top) and female (pink, bottom) *D. santomea* cuticular hydrocarbon (CHC) profiles. Individual measurements made on hexane extracts from ten pooled, age-matched adult flies (3 male, 2 female replicates). Peaks representing the internal standard (C18, 1), male-specific (Z)-11-octadecenyl acetate (cVA, 2), and monomorphic (Z)-7-tricosene (7-T, 3) are indicated.

**(B)** Fraction of time *D. santomea* males spend courting conspecific females or males in ambient light vs. dark during ten-minute interactions. Boxplots show full distribution range within whiskers (excluding statistically identified outliers) and second and third quartiles within boxes, with medians in bold. Individual data points (including outliers) overlayed as gray or, for males courting females that successfully copulated, red dots. Note slight but non-significant decreases in courtship toward both sexes in the dark (Mann-Whitney *U* tests), though a significant (binomial test) decrease in copulation rate with females.

**(C)** Fraction of time *D. santomea* males spend courting conspecific dead females or males with or without endogenous CHCs (removed by hexane washes) during ten-minute interactions. Significantly reduced courtship without CHCs for both target sexes (Mann-Whitney *U* tests).

**(D)** Similar to (C), with 10% 7-T add-back (or hexane solvent control) to conspecific dead females after CHC removal. 7-T treatment partially restores attractiveness to *D. santomea* male testers (lettered statistical groupings assigned by post-hoc Dunn's tests following significant Kruskal-Wallis). Cohen's *d* effect size for 10% 7-T addition (fourth) vs. no addition after CHC wash (second), 0.692 (95% CI -0.379-0.821, p=0.401). Cohen's *d* effect size for solvent addition (third) vs. no addition after CHC wash (second), 0.221 (95% CI 0.076-1.31, p=0.042). Cohen's *d* effect size for 10% 7-T addition (fourth) vs. solvent addition (third), 0.617 (95% CI 0.069-1.17, p=0.039).

**(E)** Fraction of time *D. santomea* males spend courting dead *D. melanogaster* females (endogenous 7-T low) perfumed with 10% 7-T or solvent control (hexane). 7-T addition elicits courtship from *D. santomea* males. Significance by Dunn's tests.

**(F)** Fraction of time *D. santomea* males spend courting conspecific (orange) or heterospecific males (*D. yakuba* green, all others black) during twenty-minute interactions. 7-T presence in each species from GC-MS and phylogeny shown below, statistical groupings by Dunn's tests above. Note correlation between 7-T presence and elevated *D. santomea* courtship.

**(G)** Summarized indications of 7-T monomorphism (*65*, *66*), evidence for 7-T as a sexual attractant (*32*, *71*, *72*), and binarized male-male courtship expression in *melanogaster* subgroup species arranged by phylogeny. "(–)" indicates dimorphic species for which 7-T is not expected to be sexually attractive but

524 has not yet been tested. Pheromone status of common ancestors at phylogeny branchpoints inferred by
525 parsimony.
526

527 **Figure 3. Selectively low cVA abundance on *D. santomea* males amplifies intermale courtship**
528 **(A)** cVA abundance on males of the *melanogaster* subgroup measured in single flies (5-8 per species) by
529 TD-GC-MS. Statistical groupings by Dunn's tests; "a.u." arbitrary units. Note low cVA level selectively
530 in *D. santomea* males. Data derived from (*67*) with permission from the authors.
531 **(B-D)** *D. santomea* sexual behavior during twenty-minute interactions with females in the presence of
532 increasing cVA on a piece of filter paper nearby. (B) Fraction of time spent courting. (C) Latency to first
533 courtship bout. (D) Latency to copulation. Pairwise statistical significance by Dunn's tests, binomial tests
534 for copulation rates. Note decreased courtship, increased latency, and decreased copulation rate at the
535 highest cVA abundance (2 mg).
536 **(E)** Preference index for *D. santomea* courtship towards 10% cVA vs. solvent control (acetone) perfumed
537 live target female or male conspecific flies during twenty-minute trio interactions. Index calculated as the
538 difference in time spent courting each target normalized by the sum. Significance between distributions
539 and between each distribution and a null median of zero (indicating no preference) determined by two-
540 and one-sample Mann-Whitney *U* tests, respectively. Note that *D. santomea* male testers exhibit clear
541 aversion to cVA-perfurmed targets of either sex. All three observed copulations occurred with the solvent
542 control female.
543 **(F)** Photomicrograph showing labeling pattern of $Or67d^{Gal4}$ in the antennal lobes (AL) of a *D. santomea*
544 male. Immunostaining for Gal4-dependent cytoplasmic tdTomato pseudocolored green with Bruchpilot
545 synaptic counterstain (using nc82 monoclonal antibody) in magenta. Uniglomerular labeling pattern in
546 each AL matches the expected size and position of cVA-sensitive DA1 (*145*). Scale bar, 25 µm. See Table
547 S3 for genotypes of transgenic strains used in figures throughout.
548 **(G)** Courtship rasters (red) for a single-housed *D. santomea* male carrying $Or67d^{Gal4}$ and Gal4-dependent
549 CsChrimson paired with a group-housed wildtype conspecific male target. Two representative sham trials
550 (above dash) and two photostimulation (PS) trials (below dash) are shown. Two-second PS blocks repeat
551 every ten seconds for a total of six activations after a one-minute baseline. PS frequencies increase in
552 pairs from 10 to 40 Hz within each trial and increase in intensity across trials. Note that PS immediately
553 interrupts spontaneous courtship by tester males in experimental but not sham trials.
554 **(H,I)** Quantification of (G) showing fraction of $Or67d^{Gal4}$ tester males courting males (H) or females (I)
555 during six-second windows surrounding PS blocks (H, purple; I, pink) or sham controls (black). Data
556 filtered for blocks where tester males showed spontaneous courtship within a half second of PS onset.
557 Data from all three frequencies were grouped since they gave similar results but separated by intensity:
558 120 (H) or 260 $\mu W/mm^2$ (I). Most tester males cease courtship by PS offset in experimental trials
559 (significant for both target sexes by Kolmogorov-Smirnov tests).

560 **(J)** Summary of courtship suppression effects in *Or67d*$^{Gal4}$ tester males as a function of PS intensity with
561 male (purple) and female (pink) targets. Baselines (horizontal dashed lines) calculated as the fraction of
562 spontaneous courtship bouts in sham trials lasting more than two seconds. Note strong effects with male
563 targets at low intensities but only at the strongest intensity with females.
564 **(K)** *D. santomea* male aggression during twenty-minute interactions between single-housed males in the
565 presence of increasing cVA on filter paper. Not significant by Kruskal-Wallis test.
566 **(L)** *D. santomea* male aggression towards males directly perfumed with 10% cVA or solvent control
567 (acetone) during twenty-minute trio interactions. Not significant by Mann-Whitney *U* test.
568 **(M)** Aggression in *D. santomea* males carrying *Or67d*$^{Gal4}$ and Gal4-dependent CsChrimson or genetic
569 controls during twelve-minute photoactivation trials. Pairs of group-housed males are exposed to six
570 thirty-second photostimulation (PS) blocks with fixed intensity and monotonically increasing frequency
571 (1-40 Hz), with a two-minute baseline and one-minute inter-block intervals. Measurements represent
572 cumulative lunge counts from all six PS blocks. Note insufficiency of *Or67d*$^{Gal4}$ activation to induce
573 attack (no significance between genotypes by Kruskal-Wallis test).
574 **(N-P)** Logic models for control of male social behaviors by 7-T and cVA in *D. melanogaster* (7-T
575 dimorphic, N), *D. yakuba* (7-T monomorphic, O), and *D. santomea* (7-T monomorphic with reduced cVA,
576 P). In *D. melanogaster* where 7-T inhibits intermale courtship, 7-T also gates the effect of cVA to promote
577 aggression (*72*). A switch in 7-T function from suppressing to stimulating courtship in monomorphic
578 species is predicted to reduce or eliminate the aggression-promoting effect of cVA without impacting its
579 courtship-suppressing effect, as evident in *D. santomea.* Intermale courtship promoted by 7-T in *D.*
580 *santomea* is further amplified due to reduced inhibition by cVA. Edge terminating in white box indicates a
581 permissive "gating" effect by 7-T on cVA-induced aggression, in addition to its direct effect.
582

583 **Figure 4. Central aggression circuits in *D. santomea* can evoke intense attack when photoactivated**
584 **(A)** Photomicrograph showing labeling pattern of *20E08*$^{Gal4}$ in the central brain of a *D. santomea* male.
585 Immunostaining for Gal4-dependent cytoplasmic tdTomato (green) with synaptic counterstain (nc82,
586 magenta). Close-up (A') shows AIP somata and axons (arrowhead) from boxed region. Scale bars, 50 µm
587 (A), 10 µm (A').
588 **(B)** Video still of bilateral wing elevation (threat) elicited by PS in a solitary *D. santomea* male carrying
589 *20E08*$^{Gal4}$ and Gal4-dependent CsChrimson. Scale bar, 1 mm.
590 **(C,D)** Quantification of PS effects in solitary *20E08*$^{Gal4}$ tester males (purple) and genetic controls (black)
591 exposed to two fifteen-second PS blocks with thirty-second baseline and inter-block interval. (C) Fraction
592 of flies showing threat (penetrance). (D) Mean fraction of frames with flies showing threat in a five-
593 second sliding window with s.e.m. envelopes (expressivity). Significant induction of threat during PS in
594 *20E08*$^{Gal4}$ by Mann-Whitney *U* tests.
595 **(E)** Photomicrograph showing *P1*$^{dsx}$ split-Gal4 (*71G01*$^{DBD}$*;dsx*$^{AD}$) labeling in the central brain of a *D.*
596 *santomea* male. Immunostaining for Gal4-dependent cytoplasmic tdTomato (green) with synaptic
597 counterstain (nc82, magenta). Close-ups show a characteristic region of P1$^{dsx}$ neuropil (lateral junction,
598 E') and somata and axons (E'') from boxed regions. Scale bars, 50 µm (F), 10 µm (F',F'').
599 **(F,G)** Courtship elicited in solitary (F) and aggression in paired (G) *D. santomea* males carrying *P1*$^{dsx}$
600 split-Gal4 and Gal4-dependent CsChrimson or a genetic control during twelve-minute photoactivation
601 trials. In both cases group-housed males are exposed to six thirty-second PS blocks with fixed intensity
602 and monotonically increasing frequency (1-40 Hz), with a two-minute baseline and one-minute inter-
603 block intervals (as in H). "PS–" represents the two-minute baseline period prior to first PS. "PS+"
604 cumulatively represents all six PS blocks (for courtship, G) or all five inter-block intervals (IBIs) and
605 period following final PS (for aggression, F). See behavior dynamics in (H) for justification of aggression
606 quantification during IBIs. Note significant PS induction for both actions (Dunn's tests).
607 **(H)** Fraction of flies showing attack (lunge, blue) and courtship (UWE, red) in same-genotype pairs of
608 *P1*$^{dsx}$ males during six PS blocks with fixed intensity and increasing frequencies. Note highly penetrant
609 attack mostly during light-off periods punctuated by time-locked courtship during high frequency PS
610 blocks. Video stills at right show aggressive tussling following 2 Hz PS (1) and simultaneous courtship by
611 both tester males during 10 Hz PS (2). Scale bars, 1 mm.
612 **(I,J)** Expressivity and temporal dynamics of attack (I) and courtship (J) elicited by PS in *P1*$^{dsx}$ male pairs
613 (I, blue; J, red) or a genetic control (black). Significant attack induction during inter-block intervals and
614 after final PS (I) or courtship during PS compared to control (J) by Mann-Whitney *U* tests.
615

616 **Figure 5. A switch from cVA sexual attraction to aversion in *D. santomea* females**
617 **(A)** Elevation map of equatorial Central and West Africa with the volcanic island of São Tomé in the Gulf
618 of Guinea boxed. Data from (*146*) and Terrain Tiles (Mapzen, accessed Aug. 24, 2025).
619 **(B)** Elevation map of São Tomé. Note the central summit of Pico de São Tomé.
620 **(C)** Latitudinal elevation profile of Pico de São Tomé showing *D. santomea* (orange) and *D. yakuba*
621 zones (green) separated by a hybrid zone where both pure species and F1 hybrid males are found (*112*).
622 **(D,E)** Behavioral dose-response curves of *D. santomea* female ovipositor extrusion (OE) to increasing
623 cVA on filter paper during conspecific male courtship. (D) Female OE as fraction of total observation
624 time. (E) Female OE normalized to male courtship (difference divided by sum of time spent by female in
625 OE and time spent by male in UWE). Red dots, females that copulated. The lowest cVA dose induces an
626 intermediate effect while both higher doses induce significant increases in OE expression (Dunn's tests).
627 **(F)** *D. santomea* female "receptivity index" as function of increasing cVA. For each female an index
628 value of 1, 0, or -1 is possible. Observations of female wing spreading (WS, an acceptance behavior) and
629 courtship-normalized OE (rejection, from E) were each binarized as present or absent (WS>0,
630 OE(norm)>-0.25) and overall index per dose is calculated as the difference between the two binary values
631 (WS-OE) normalized by the number of females scored. Note significantly decreased sexual acceptance
632 again at the two higher cVA doses (Dunn's tests).
633 **(G)** Cumulative copulation latencies and rates by *D. santomea* tester females carrying *Or67d*$^{Gal4}$ and
634 Gal4-dependent Kir2.1 (black) or genetic controls (grays) grouped with an equal number of wildtype
635 conspecific males for 45 minutes in large chambers. "BDP" refers to a Gal4 driver without labeling
636 evident in the central brain. 24 total females tested of each genotype (two trials each of 12 single-housed
637 males x 12 group-housed females), significance by Kolmogorov-Smirnov tests comparing latencies or
638 binomial tests comparing rates.
639 **(H)** Evolutionary model for the emergence of high intermale courtship and low intermale aggression in *D.*
640 *santomea,* incorporating three key pheromone changes inferred to occur prior to or following *D. santomea*
641 speciation in São Tomé. A common sexual attractant for *D. santomea* and *D. yakuba* males (7-T)
642 generates the behavioral potential for unfit hybridization in sympatry due to F1 hybrid male sterility
643 (*110*). *D. santomea* females evolve sexual aversion to cVA and *D. santomea* males reduce cVA, thereby
644 maintaining efficient intraspecific mating while also maintaining reproductive isolation from *D. yakuba*
645 (the two events cannot be definitively ordered). Reduced male cVA, together with monomorphic 7-T,
646 releases high intermale courtship. Reduced efficacy of cVA to promote aggression further suppresses
647 fighting. Placement of *D. yakuba* secondary colonization after allopatric *D. santomea* speciation (instead
648 of speciation in sympatry) from (*111*).
649

650 **Figure 6. P1$^{dsx}$ activation or natural male-directed courtship induces a competitive mating**
651 **advantage in *D. santomea* males**
652 **(A)** Spontaneous bias observed between flies in male-male *D. santomea* and *D. melanogaster* pairs for
653 attack and courtship. Indices derived from the same fly pair are connected as lines and distribution means
654 shown as paired orange (*D. santomea)* or black dots (*D. melanogaster*). Note high courtship bias in *D.*
655 *santomea.*
656 **(B)** Fraction of *D. santomea* male-male pairs with high attack bias where the same fly also showed
657 majority of courtship (left), or with high courtship bias where the same fly also showed majority of attack
658 (right). Significance compared to random chance (50%) by binomial tests.
659 **(C)** Courtship in the dark by single-housed *D. santomea* males carrying *P1$^{dsx}$* split-Gal4 and Gal4-
660 dependent Kir2.1 or a genetic control paired with group-housed wildtype conspecific female (left) or male
661 targets (right). Red dots, males that copulated (only observed in controls). Significant courtship reduction
662 in *P1$^{dsx}$* tester males toward both sexes by Mann-Whitney *U* tests.
663 **(D)** Scheme for assessing persistent behavioral effects of *D. santomea P1$^{dsx}$* split-Gal4 activation. After a
664 one-minute baseline, isolated *P1$^{dsx}$* tester males or genetic controls experience one-minute PS and a ten-
665 minute delay. Dividers ("sliding doors") are then removed to allow paired flies (either two same-genotype
666 males or a tester male and wildtype female) to interact spontaneously for an additional ten minutes.
667 **(E)** Behavior rasters for same-genotype *P1$^{dsx}$* male pairs (both experienced PS before the delay) during
668 the ten-minute interaction phase. Data from just one male per pair is shown and quantified in (F-I) for fair
669 comparison to interactions with females below. Blue, attack (lunge); red, courtship (UWE).
670 **(F-I)** Quantification of (E) showing expressivity and temporal dynamics and of male-male aggression
671 (F,H) and courtship (G,I) during the interaction phase. Note highly increased aggression and slightly
672 increased courtship in *P1$^{dsx}$* compared to genetic controls without PS (significance by Kolmogorov-
673 Smirnov (F,G) or Mann-Whitney *U* tests (H,I)).
674 **(J-N)** Behavior rasters (J), temporal dynamics, and expressivity of courtship (K,M,N) and aggression (L)
675 between *P1$^{dsx}$* males or genetic controls paired with wildtype females during the interaction phase. Note
676 highly increased courtship expression (M) and decreased courtship latency (N) in *P1$^{dsx}$* without any
677 incidence of attack.
678 **(O)** Scheme for determining a sexual priming effect of male-directed courtship. Two single-housed
679 wildtype *D. santomea* males are paired for ten minutes before a wildtype female is added for an additional
680 ten minutes (trio period). Male-directed courtship dominance is measured and identity of the dominant
681 courter ascertained in the paired period then compared to female-directed courtship dominance in the trio.
682 **(P,Q)** Video stills of a male courting another male first in the paired period (P) then courting a female in
683 the trio (Q). Scale bars, 1 mm.

**(R)** Quantification of the sexual priming effect (O-Q). Female-directed courtship dominance in trios (y-axis) plotted as a function of male-directed courtship dominance in pairs (x-axis). Points above the x-axis represent cases where the same male exhibited male-directed courtship dominance in pairs and female-directed courtship dominance in trios. Dot size represents total amount of male-directed courtship in pairs and data are filtered for pairs with at least twenty seconds of courtship during this phase (no matter the bias). Red dots, males that copulated. Gray box, males with high levels of courtship dominance during the paired period. Note enrichment of points above the x-axis in cases of high male-male courtship dominance.

**(S,T)** Categorization of effects on female-directed courtship dominance (S) and copulation advantage (T) from (R). (S) All but one male exhibiting male-directed courtship dominance in pairs (89%) also exhibited female-directed courtship dominance in trios (significant by binomial test). (T) Two out of three copulations observed were by the male exhibiting male-directed courtship dominance in pairs (circled red dots in R). The exception was from a “submissive” male in which courtship bias was very weak (uncircled red dot at bottom left in R).

**Figure 7. Convergent social behaviors and pheromones of *D. santomea* and *D. persimilis* males**

**(A)** Summarized indications of male-male courtship presence/absence in *Drosophila* species arranged by phylogeny. Note sibling species *D. persimilis* (purple) and *D. pseudoobscura* (blue) in the obscura group.

**(B,C)** Video stills of *D. persimilis* males promiscuously courting conspecific female (B) and male targets (C). Images selected to represent species-typical action selection. Scale bars, 1 mm.

**(D)** Action biases in *D. persimilis* male-male pairs. Male-directed courtship (red dots) is more common than attack (blue dots) and often shows strong bias to one fly (boxed region). Attack and courtship measurements from the same pair connected by thin lines. Circled "X" indicates mean value for the corresponding action.

**(E-G)** Video stills (E,F) and action biases (G) for *D. pseudoobscura* as for *D. per*. Note female-directed courtship (E) and biased male-directed attack (F,G). Scale bars, 1 mm.

**(H)** cVA abundance on males of the *melanogaster* subgroup and *D. persimilis* / *D. pseudoobscura* by TD-GC-MS (*67*). Statistical groupings by Dunn's tests; "a.u." arbitrary units. Note low cVA levels in *D. persimilis* and high in *D. pseudoobscura* as in *D. santomea* / *D. yakuba*.

**(I)** Summary of relevant pheromones (*67*, *76*, *131*) and social behaviors for the *melanogaster* subgroup (excluding *D. teissieri* and *D. orena*) and the *D. persimilis* / *D. pseudoobscura* sibling species pair. CHC monomorphism is common to multiple species but low cVA abundance and high male-male courtship are shared only between *D. santomea* (orange) and *D. persimilis* (purple). Information compiled from the current study and prior sources.

719 **Supplemental Figure Legends**

720

721 **Figure 1-S1. Additional behavior ethograms and locomotor analyses of *Drosophila* intermale social**
722 **interactions**

723 **(A)** Ethograms from twenty-minute interactions depicting aggressive and courtship actions scored in three
724 representative conspecific male-male pairs per species across various *Sophophora* and *Drosophila*. Nodes
725 are bout counts of a given action type, with sizes representing frequency normalized to summed bouts
726 scored across all actions (expert annotation). Edges indicate action transitions, with weights representing
727 the fraction of bouts of a given action (arrow origin) for which a second action (arrow destination)
728 occurred within one second. Nine total actions in each ethogram are arranged in five rows: first, two
729 aggressive threat actions (threat, pump) (*102*); second, two aggressive contact-mediated actions (lunge,
730 hold) (*48*); third, two additional contact-mediated aggressive actions (headbutt, barrage) (*147*); fourth,
731 two courtship actions utilizing the wings and typically directed toward females (UWE, BWE) (*20*); fifth,
732 copulation attempt. Nodes indicating aggressive actions are filled with blue shades and courtship actions
733 with reds, except for headbutt (white) and barrage (black). Species arrangement and divergence times
734 according to compilation of available phylogenies (*75*, *143*, *144*). Gray coloration indicates that very few
735 social actions of any kind were observed. Abbreviations: UWE, unilateral wing extension; BWE, bilateral
736 wing extension; Cop. att., copulation attempt. Barrage described previously in *D. pseudoobscura*
737 (*130*) but named here.

738 **(B-E)** Locomotor summaries for all fifteen species included in the behavioral screen. Per-frame
739 calculations of each fly's forward velocity (B), angular velocity (C), facing angle relative to the partner
740 (D), and inter-fly distance (E) are derived from automated tracking of both flies (*55*) in all recorded male-
741 male pairs. Distributions shown as violin plots with dotted means. *D. santomea,* orange; *D. yakuba*,
742 green.

743

744 **Figure 1-S2. Performance and usage of automated behavior classifiers for intermale social**
745 **interactions within the *melanogaster* subgroup and additional *D. santomea* strains**
746 **(A,B)** Automated behavior classifier performance for lunge (A) and unilateral wing extension (B). Three
747 twenty-minute representative recordings of male-male pairs for each species were manually scored for
748 both actions (expert annotation, same pairs as in Fig. 1A) and exposed to automated behavior classifiers
749 trained previously for *D. melanogaster* (*56*), implemented in JAABA (*54*). Manual (x-axis) vs. classifier-
750 generated annotations (y-axis) are compared in $\log_{10}$ scale, using either the number of bouts (lunge) or
751 their cumulative time duration (UWE). Solid lines, diagonals; dashed lines, linear fits. Adjusted $R^2$,
752 significance by F-tests for fits, and Pearson correlations (r) indicated at bottom right. *D. melanogaster*,
753 black; *D. santomea,* orange; *D. yakuba*, green; *D. simulans*, *D. mau*, *D. sec*, *D. erecta*, gray. Note near-
754 perfect overlap with the diagonal for lunge and strong correlation for UWE despite classifier false
755 positives in cases with few manual annotations (all subgroup species except *D. santomea* show very little
756 male-male courtship).
757 **(C,D)** Aggression (lunge, C) and courtship (UWE, D) measurements from automated classifiers in all
758 recorded male-male pairs for *melanogaster* subgroup species and additional *D. santomea* strains. *D.*
759 *santomea* 00 (also called STO.4) is the strain included in the behavioral screen and used throughout as
760 "wildtype" (National Drosophila Species Stock Center 14021.0271.00). Strains 146 (STO-CAGO 1482),
761 148 (STO.7), and 151 (STO.6) also derive from São Tomé from females collected between 1100 and 1500
762 m elevation (*111*). Boxplots show full distribution range within whiskers (excluding statistically identified
763 outliers) and second and third quartiles within boxes, with medians in bold. Individual data points
764 (including outliers) overlayed as gray dots. Lettered statistical groupings assigned by post-hoc Dunn's
765 tests following significant Kruskal-Wallis. Note low aggression and high courtship conserved in *D.*
766 *santomea* strains (orange), low aggression and courtship in the sibling species *D. yakuba* (green), and
767 high aggression and low courtship in *D. melanogaster* (black).
768 **(E,F)** Summaries of penetrance (x-axes) and expressivity (y-axes) for aggression (E) and courtship (F)
769 across subgroup species and *D. santomea* strains. Metrics derived from data in (C,D).
770

**Figure 1-S3. Intermale aggression and courtship in *melanogaster* subgroup species with host specializations**

**(A,B)** Aggression (A) and courtship (B) in *D. melanogaster*, *D. sechellia*, *D. santomea* (orange), and *D. erecta* male-male pairs competing over the standard apple juice substrate and other fruits based on reported specializations (*53*). Significance for each fruit/species combination by pairwise Mann-Whitney *U* tests to apple. Removing food source entirely significantly reduces aggression in *D. melanogaster* (*59*). Using morinda (also called noni) significantly increases aggression but not courtship in *D. sec*. *D. santomea* aggression and courtship depend only weakly if at all on food presence and source.

780 **Figure 1-S4. Male- and female-directed social behaviors by *D. melanogaster*, *D. simulans*, *D.***
781 ***santomea,* and *D. yakuba* males**
782 **(A,B)** Ethograms representing male-male (A) and male-female (B) social behaviors for *melanogaster*
783 subgroup species of interest. Phylogeny also includes *D. mauritiana* and *D. sechellia* from the *simulans*
784 clade, *D. teissieri* from the *yakuba* clade, and *D. erecta* without associated ethograms. Female-directed
785 ethograms represent expert annotation for three recordings of male-female pairs per species, with male
786 flies similarly prepared by single-housing and interactions taking place under identical conditions. Male-
787 directed ethograms reproduced from Fig. 1A for visual comparison to female-directed counterparts. Note
788 nearly exclusive male-directed aggressive actions (blue nodes) by *D. melanogaster* and *D. simulans* males
789 but prevalence of male-directed courtship actions (red nodes) by *D. santomea* and *D. yakuba* (though in
790 *D. yakuba* total male-direcetd actions are many fewer on average than *D. santomea)*, matching the actions
791 taken when paired with females.
792

**Figure 1-S5. Acoustic features of female- and male-directed courtship song by *D. santomea* males**

**(A,B)** Representative courtship song traces by *D. santomea* males toward a female (A, pink) or male conspecific target fly (B, purple). Key acoustic features are indicated including pulse, pulse train, inter-pulse interval (IPI), clack, clack train, and inter-clack interval (ICI) (*63*). Traces reproduced and enlarged from Fig. 1I,J.

**(C,D)** Video stills of song recording chambers (*60*) containing *D. santomea* males courting either a female (C) or male (D). Isolated waveforms of single clacks and pulse trios shown below, with asterisks indicating event peaks. Scale bars, 1 mm.

**(E-J)** Quantitative acoustic analyses of female- (pink) and male-directed *D. santomea* courtship songs (purple). Clacks (E-G) and pulses (H-J) were identified by expert annotation from three recordings with each sex (clack, 32-103 events per recording; pulse, 140-346 events per recording). Data shown as "hemiviolin" plots in which female- and male-directed distributions are vertically mirrored. Distribution means are semicircles on the appropriate side. Note general similarity between female- and male-directed song features (significant differences based on Mann-Whitney *U* tests despite small difference magnitudes are often because so many data points make up the underlying distributions). Analyses of absolute event abundances were omitted since annotations captured only a fraction of events in each recording.

811 **Figure 2-S1. GC-MS profiling of *D. santomea* male and female cuticular hydrocarbons (CHCs)**
812 **(A,B)** Absolute (A) and relative abundances (B) of 41 compounds identifiable as peaks in *D. santomea*
813 male (purple) and female hexane extracts (pink). Individual measurements are made on ten pooled, age-
814 matched adult flies (3 male, 2 female replicates). Calculation of absolute abundance uses known
815 concentration of the internal standard (octadecane/C18, not shown) and normalizes for number of flies
816 included in the extract. Relative abundances normalize to the summed absolute abundance of all
817 compounds excluding the standard. Male-specific (Z)-11-octadecenyl acetate (cVA, purple) and
818 monomorphic (Z)-7-tricosene (7-T, black) are indicated. Question marks in compound names indicate
819 uncertainty in chemical assignment. See Table S5 for retention times and diagnostic ions used to identify
820 and assign CHCs.
821

822 **Figure 2-S2. 7-T abundance in males and females of various *Drosophila* species**

823 **(A)** Absolute 7-T abundances on males (purple) and females (pink) *Drosophila* measured by GC-MS on
824 hexane extracts from ten pooled, age-matched adult flies (2-8 replicates each). Monomorphic species (*D.*
825 *santomea, D. yakuba*, *D. simulans*) show similar 7-T abundance between sexes while dimorphic species
826 show large differences (*D. erecta*, *D. melanogaster*). nd, not detected in either sex (*D. serrata*, *D.*
827 *ananassae*, *D. willistoni*).

828 **(B-D)** Fraction of time *D. santomea* males spend courting conspecific (B) or heterospecific dead females
829 (C,D) perfumed with 10% 7-T or solvent control (hexane). Species selected for having either low (*D.*
830 *erecta*) or undetectable (*D. ana*) endogenous 7-T levels (from GC-MS). *D. santomea* female targets as
831 positive controls. 7-T addition elicits courtship from *D. santomea* males in both heterospecific cases.
832 Significance by Dunn's tests.

833

834 **Figure 3-S1. Reduced cVA on *D. santomea* males compared to *D. yakuba* and *D. erecta***
835 **(A-C)** Mirrored gas chromatograms representing male (purple, top) and female (pink, bottom) cuticular
836 hydrocarbon (CHC) profiles of *D. santomea* (A), *D. yakuba* (B), and *D. erecta* (C). Individual
837 measurements made on hexane extracts from ten pooled, age-matched adult flies (2-3 replicates each).
838 Peaks representing male-specific (Z)-11-octadecenyl acetate (cVA) indicated. *D. santomea*
839 chromatograms reproduced from Fig. 2A for visual comparison.
840 **(D,E)** Absolute (D) and relative abundances (E) of cVA on *D. santomea* (orange), *D. yakuba* (green), and
841 *D. erecta* males. Calculation of absolute abundance uses known concentration of the internal standard
842 (C18) and normalizes for number of flies included in the extract. Relative abundances normalize to the
843 summed absolute abundance of all compounds detected excluding the standard. *D. santomea* males show
844 63% and 75% reduced cVA comparing absolute abundance means or 64% and 65% reductions comparing
845 relative abundance means to *D. yakuba* and *D. erecta*, respectively.
846

847 **Figure 3-S2. CRISPR-Cas9 HDR knock-in strategy used to generate *D. santomea Or67d*$^{Gal4}$**
848 **(A)** Schematic diagrams of the Gal4 transgene and selection marker assembled into an Atalanta vector
849 (pJAT32, addgene #204297) (*148*) and *Or67d* genomic target locus shown with upstream and downstream
850 sgRNA cleavage sites. Transgene (above) contains two cassettes: *T2A-Gal4-stop(hsp70)* oriented natively
851 to the genomic target, and downstream *ie1-mCherry-stop(p10)* fluorescent marker for successful
852 integration (*32*) with inverted orientation. One kilobase homology arms flank both ends. *Or67d* genomic
853 locus (below) is targeted using sgRNAs directing double-strand breaks to immediately (15 bp)
854 downstream of the translational start codon and 348 bp downstream of the stop, resulting in removal of
855 1152 of 1167 protein coding base pairs (99%). Co-injection of the assembled Atalanta vector and nls-
856 Cas9-nls protein into wildtype *D. santomea* eggs gives mosaic *ie1-mCherry*$^{pos}$ G0 progeny carrying *T2A-*
857 *Gal4* inserted in-frame with the five residual residues of *Or67d*. G1 progeny resulting from G0 crosses to
858 wildtype are re-screened for abdominal *ie1-mCherry* expression to ensure germline transmission. In this
859 strategy spatiotemporal patterns and magnitude of Gal4 expression are controlled entirely by *Or67d*
860 endogenous genomic regulation.
861 **(B)** Photomicrograph showing labeling pattern of *Or67d*$^{Gal4}$ in the whole brain of a *D. santomea* male
862 (same fly from which close-up of antennal lobes (ALs) is shown in Fig. 3F). Immunostaining for Gal4-
863 dependent cytoplasmic tdTomato pseudocolored green with Bruchpilot synaptic counterstain (using nc82
864 monoclonal antibody) in magenta. Uniglomerular labeling pattern in each AL (arrowheads) matches the
865 expected size and position of cVA-sensitive DA1 (*145*). Bifurcating OSN commissures (axon bundles)
866 from the antennae leading into ALs can also be seen. Scale bar, 50 µm.
867

868 **Figure 3-S3. Ineffectiveness of naturally varying cVA levels to promote aggression by *D. santomea***
869 **males**
870 **(A)** Absolute cVA abundance on *Drosophila* males measured by GC-MS on hexane extracts from ten
871 pooled, age-matched adult flies (2-8 replicates each). Calculation uses known concentration of the
872 internal standard (C18) and normalizes for number of flies included in the extract. *D. santomea* (orange),
873 *D. yakuba* (green), and *D. erecta* measurements reproduced from Fig. 3-S1 for visual comparison to
874 additional species. Means indicated above and phylogeny below.
875 **(B)** Spontaneous aggression (lunges per minute) exhibited by *D. santomea* males toward conspecific
876 (orange) or heterospecific males (*D. yakuba* green, all others black) in single-housed pairs during twenty-
877 minute interactions. Statistical groupings by Dunn's tests shown above and phylogeny below. Note
878 similarly low or even decreased attack levels toward males of all species.
879 **(C)** Correlation between cVA abundance measured by GC-MS and aggression elicited from *D. santomea*
880 males. Dashed line, linear fit. Adjusted $R^2$, significance by F-test for fit, and Pearson correlation (r)
881 indicated at bottom right. Note marginally significant correlation driven mostly by low attack rates toward
882 distant species (*D. serrata*, *D. ananassae*, *D. willistoni*) with many other pheromone changes in addition
883 to low cVA. Three of four species with higher cVA abundance than *D. santomea* elicit less attack than
884 observed among *D. santomea* males (*D. simulans* is the exception but the slight increase is non-
885 significant). Data derived from (A,B).
886

887 **Figure 3-S4. cVA abundances and social behavior changes by *melanogaster* subgroup males toward**
888 ***D. santomea* males**
889 **(A)** Relative fraction of time *D. yakuba* (green), *D. simulans*, and *D. melanogaster* males court
890 conspecific males (first distribution of each pair) vs. *D. santomea* males (second distribution, orange). All
891 measurements within each species normalized to the conspecific median and $\log_{10}$ transformed. Males of
892 all three *melanogaster* subgroup species show significantly increased courtship toward *D. santomea*
893 males by Mann-Whitney *U* tests, including *D. melanogaster* where 7-T (abundant on *D. santomea* males)
894 is male-specific and sexually aversive (*71–74*).
895 **(B)** Similar to (A) but showing paired relative distributions for aggression within and between males of
896 the three subgroup species. Note decreases in male-directed aggression by all three toward *D. santomea*
897 (significant for *D. yakuba* and *D. melanogaster* by Mann-Whitney *U* tests).
898 **(C)** Heatmap showing median fraction time spent courting by males in conspecific (diagonal) and
899 heterospecific male-male pairs (off-diagonal) among the four subgroup species. Rows ("courters") are
900 males whose courtship is measured (UWE). Columns ("courtees") are males targeted by courtship. Gray
901 entry where data not collected. Data derived from (A) and additional pairings. Horizontal dashed arrows
902 identify relevant comparisons between conspecific male- and *D. santomea* male-directed courtship for
903 visual aid.
904 **(D)** Similar heatmap showing median aggression (lunge rate) by male "attackers" (rows) and "attackees"
905 (columns). Data derived from (B) and additional pairings. Note consistently decreased aggression toward
906 *D. santomea* males.
907 **(E)** Summarized changes in courtship (first row) and aggression rates (second row) by heterospecific
908 males toward *D. santomea* compared to conspecific rates for each, derived from data in (A,B). Percent
909 increases in first row (courtship) and percent decreases in second (aggression).
910

**Figure 4-S1. Induction of time-locked wing threat by photoactivation of AIP neurons in solitary *D. santomea* males**

**(A)** Optogenetic photoactivation scheme for solitary *D. santomea* males carrying *20E08*$^{Gal4}$ and Gal4-dependent CsChrimson. Group-housed *20E08*$^{Gal4}$ tester males or genetic controls are exposed to two fifteen-second photostimulation (PS) blocks with a thirty-second baseline and inter-block interval.

**(B)** Manually scored wing threat rasters (purple) for solitary *20E08*$^{Gal4}$ males during the two-minute trial. Note threat induction time-locked to PS in most flies. Genetic controls showed no threat.

**(C,D)** Locomotor dynamics in *20E08*$^{Gal4}$ males (browns) and genetic controls (black). Per-frame calculations of each fly's forward velocity (C) and angular velocity (D) are derived from automated tracking (*55*). Data is smoothed by averaging within a five-second sliding window (precluding analysis of sub-second locomotor dynamics such as "turn" and "charge") (*102*). Envelopes represent s.e.m.

923 **Figure 4-S2. Induction of time-locked courtship by photoactivation of *P1$^{dsx}$* neurons in solitary *D.***
924 ***santomea* males**
925 **(A)** Optogenetic photoactivation scheme for solitary group-housed *D. santomea* males carrying *P1$^{dsx}$*
926 split-Gal4 (*71G01$^{DBD}$;dsx$^{AD}$*) and Gal4-dependent CsChrimson. *P1$^{dsx}$* tester males or a genetic control are
927 exposed to six thirty-second photostimulation (PS) blocks with fixed intensity and monotonically
928 increasing frequency as indicated, with a two-minute baseline and one-minute inter-block intervals.
929 **(B)** Courtship rasters (red) for *P1$^{dsx}$* tester males during the twelve-minute trial. Note early but sporadic
930 courtship bouts that time-lock to PS blocks and increase in penetrance starting at 5 and 10 Hz.
931 **(C,D)** Penetrance (C) and expressivity (D) of courtship (UWE) elicited by *P1$^{dsx}$* PS. Significant courtship
932 expression during PS blocks compared to the genetic control in (D) by Mann-Whitney *U* tests.
933

934 **Figure 4-S3. Induction of courtship and attack by photoactivation of *P1$^{dsx}$* neurons in same-**
935 **genotype pairs of *D. santomea* males**
936 **(A)** Optogenetic photoactivation scheme for same-genotype pairs of group-housed *D. santomea* males
937 carrying *P1$^{dsx}$* split-Gal4 and Gal4-dependent CsChrimson. *P1$^{dsx}$* tester males or a genetic control are
938 exposed to six thirty-second photostimulation (PS) blocks with fixed intensity and monotonically
939 increasing frequency as indicated, with a two-minute baseline and one-minute inter-block intervals.
940 **(B,C)** Behavior rasters for *P1$^{dsx}$* male pairs (B) and genetic controls (C) during the twelve-minute trial.
941 Blue, attack (lunge); red, courtship (UWE). Note early induction of attack which increases in penetrance
942 and expressivity as the trial continues. Attacks interrupted by time-locked courtship during later PS blocks
943 (>5 Hz). Genetic controls show little courtship or attack.
944 **(D,E)** Locomotor dynamics in *P1$^{dsx}$* males (browns) and genetic controls (black). Per-frame calculations
945 of each fly's forward velocity (D) and angular velocity (E) derived from automated tracking (*55*). Data
946 smoothed by averaging within a ten-second sliding window. Envelopes represent s.e.m. PS time-locked
947 locomotor arrest similar to observed previously in *D. melanogaster* (*56*).
948

949 **Figure 4-S4. Photoactivation effects of *D. santomea P1$^{dsx}$* neurons in mixed-genotype male pairs**
950 **(A)** Expressivity and temporal dynamics of attack (lunge) elicited by PS in mixed-genotype pairs between
951 a *P1$^{dsx}$* split-Gal4 tester male carrying Gal4-dependent CsChrimson (or genetic control) and group-housed
952 wildtype *D. santomea* target male. Traces show the mean fraction of frames containing lunge in a ten-
953 second sliding window with s.e.m. envelopes for *P1$^{dsx}$* (blue) and control (black). PS block frequency,
954 intensity, and timing indicated above for the twelve-minute trial. Note significant attack induction (Mann-
955 Whitney *U* tests) in *P1$^{dsx}$* starting after 5 Hz.
956 **(B)** Attack elicited during inter-bout intervals and after final PS in same-genotype *P1$^{dsx}$* male pairs (blue,
957 data from Fig. 4I) vs. mixed-genotype pairs between a *P1$^{dsx}$* tester and group-housed wildtype male
958 (orange, from A). Period means connected with solid lines and data from individual flies shown as thin
959 lines. Note significant right shift in mixed pairs (Mann-Whitney *U* tests) indicating higher PS frequencies
960 required to induce intense attack.
961 **(C)** Action latencies for courtship and attack exhibited by *P1$^{dsx}$* tester males in same- and mixed-genotype
962 pairs under identical PS trial structures. Data points derived from the same fly pair (or tester fly for mixed
963 pairs) are connected as lines and distribution means shown as paired dots. Attack and courtship latencies
964 are similar on average in same-genotype pairs whereas attack is significantly delayed in mixed pairs.
965 Significance by paired or unpaired Mann-Whitney *U* tests (for within- or between-genotype group
966 comparisons, respectively).
967 **(D)** Fraction of flies showing attack (lunge, blue) and courtship (UWE, red) in *P1$^{dsx}$* mixed-genotype
968 pairs. Note overlap of actions during middle phase of the trials (boxed).
969 **(E)** Relative frequencies of *P1$^{dsx}$* same- and mixed-genotype pairs showing courtship (red) or attack (blue)
970 first. Significance between distributions and between each distribution and a null probability of 50%
971 (random chance) determined by binomial tests. Note courtship precedence in mixed pairs.
972

973 **Figure 5-S1. cVA promotes *D. santomea* female sexual rejection during courtship by conspecific**
974 **males**
975 **(A)** Rasters of *D. santomea* female and male sexual behaviors during dyadic courtship interactions with
976 increasing cVA on a nearby piece of filter paper. For each pair, male courtship (UWE, red) is shown
977 above and female rejection (ovipositor extrusion, orange) or acceptance (wing spreading, cyan) below.
978 Timing of copulations indicated with asterisks. cVA doses indicated at top. Note increased rejection and
979 decreased copulation rates at 1 and 2 mg cVA.
980

**Figure 5-S2. Unconditioned place preference tests with cVA in *D. melanogaster* and *D. san***

**(A)** Video still illustrating the y-maze arena. Four group-housed *D. melanogaster* males are introduced into the central bowl at the bottom and odors (10% cVA in acetone or acetone control) into ports at the head of each arm. Vacuum pressure continuously pulls air down the arms through an outlet. Flies can walk freely within the bowl and arms during ten-minute trials and odors are replaced into the same port (to avoid contamination) before each trial. Scale bar, 10 mm.

**(B)** Cumulative position trace representing movement of all four flies throughout the duration of the trial. Position density in each of multiple trials is used to calculate the odor preference index.

**(C-H)** Video stills and cumulative position traces as in (A,B) for *D. santomea* males (C,D), *D. melanogaster* females (E,F), and *D. santomea* females (G,H). Scale bars, 10 mm.

**(I)** Odor preference indices by species and sex. Index calculated as the difference in fly occupancy between the two arms normalized by the sum. Small gray dots represent single trials with 2-4 flies each (8-14 trials and 26-44 flies per species/sex). Distributions represented as violins with means shown as large black dots. Note significantly reduced attraction (or increased aversion) to 10% cVA in both *D. santomea* males and females (orange) compared to *D. melanogaster* (black). Significance by Mann-Whitney *U* tests.

998 **Figure 6-S1. Aggression and courtship biases in *melanogaster* subgroup male-male pairs**
999 **(A-D)** Behavior rasters for three twenty-minute conspecific male-male pairs each of wildtype *D.*
1000 *melanogaster* (A), *D. simulans* (B), *D. yakuba* (C), and *D. santomea* (D) (same pairs as in Fig. 1A).
1001 Annotations of six aggressive interactions by manual scoring (blues) are shown above the horizontal
1002 dashed lines and five courtship actions (reds) beneath. Actions split by identity of the male to which they
1003 are attributed with the one exhibiting the greater total number of actions assigned as "Male 1." *D.*
1004 *melanogaster* and *D. simulans* males fight with some characteristic bias between flies, *D. yakuba* males
1005 are mostly passive but can either fight or court, and *D. santomea* males show frequent and elaborate
1006 courtship often with strong bias.
1007 **(E)** Spontaneous action biases observed between flies in male-male pairs. Male-directed courtship (red
1008 dots) and attack (blue) are plotted as a function of their bout abundance (x-axis) and bias indices (y-axis).
1009 Measurements from the same pair connected by thin lines. Cases where the same fly is dominant for both
1010 actions show connections confined to the sector above the x-axis. Circled "X" indicates mean value for
1011 the corresponding action by color. Boxed regions indicate pairs with high attack expression and wide
1012 range of biases in *D. melanogaster* or high courtship expression and consistently strong bias in *D.*
1013 *santomea,* for visual aid.
1014

1015 **Figure 6-S2. Weak supporting evidence for territoriality in paired *D. santomea* males**
1016 **(A)** Video still of a pair of single-housed, wildtype *D. santomea* males in a large behavior chamber (40
1017 mm wide x 50 mm long x 60 mm tall) containing an apple juice-based "food patch" (25 mm diameter)
1018 and neutral surround used to test territoriality. (A') Close-up of intermale courtship from boxed region.
1019 Scale bars, 10 mm (A), 1 mm (A').
1020 **(B-D)** Heatmaps representing cumulative spatial patterns of all fly positions (B), attack (lunge) positions
1021 (C), and courtship (UWE) positions (D) for 17 *D. santomea* male-male pairs recorded during ten-minute
1022 interactions. Normalization in (B) to all frames, in (C) to attack frames only, and in (D) to courtship
1023 frames only. Note little sign of increased density on or around the food patch in any case, unlike
1024 previously observed for *D. melanogaster* aggression in similar assays (*59*).
1025 **(E)** Quantification of (B-D) showing the fraction of time spent on the food patch in total, during attack,
1026 and during courtship for each individual *D. santomea* male. Normalizations as in heatmaps above. None
1027 are significantly different from having a null median of 25% (random chance, calculated as surface area
1028 of the food patch relative to the full arena) by one-sample Mann-Whitney *U* tests. Attack frames show
1029 near-significant deviation from chance, but in the opposite direction from that expected for territoriality
1030 (enrichment off the food patch).
1031 **(F)** "Territoriality index" for *D. santomea* males calculated as the difference in time spent on the food
1032 patch between flies normalized by the sum. First distribution represents all pairs, second filtered for pairs
1033 where one of the flies showed attack dominance, and third filtered for pairs where one of the flies showed
1034 courtship dominance. None are significantly different from having a null median of zero (no territorial
1035 advantage) by one-sample Mann-Whitney *U* tests.
1036

1037 **Figure 6-S3. Additional behavior characterizations for the sliding door assay**

1038 **(A)** Optogenetic photoactivation scheme for isolated *D. santomea* males carrying $P1^{dsx}$ split-Gal4
1039 ($71G01^{DBD}$;$dsx^{AD}$) and Gal4-dependent CsChrimson during the first phase of the delayed encounter
1040 ("sliding door") assay. After a one-minute baseline, two group-housed $P1^{dsx}$ tester males on either side of
1041 a removable divider are exposed to a one-minute photostimulation (PS) block. PS is followed by a ten-
1042 minute delay before doors are opened and flies allowed to interact. Delay phase shown as split into one-
1043 and nine-minute subphases to reflect cessation of detailed courtship annotations one minute after PS
1044 offset (videos were visually scanned after this point and very little UWE was observed).

1045 **(B)** Manually scored courtship rasters (UWE, red) for isolated $P1^{dsx}$ tester males during the first three
1046 minutes of the trial.

1047 **(C,D)** Expressivity (C) and penetrance (D) of courtship elicited by PS. (C) Traces show the mean fraction
1048 of frames containing UWE in a ten-second sliding window with s.e.m. envelopes for $P1^{dsx}$ (red) and a
1049 genetic control (black, no courtship observed). (D) Fraction of flies showing courtship. Note extremely
1050 high penetrance and expressivity of induced courtship time-locked to PS in $P1^{dsx}$.

1051 **(E,F)** Fraction of flies showing courtship (red) and attack (blue) during the ten-minute interaction phase
1052 after doors open. (E) $P1^{dsx}$ in same-genotype male pairs (both experienced PS). (F) $P1^{dsx}$ males with
1053 wildtype females. Switching target sex produces a dramatic shift from predominant aggression to
1054 exclusive courtship.

1055

1056 **Figure 7-S1. Aggression and courtship by *D. persimilis* and *D. pseudoobscura* males**
1057 **(A,B)** Behavior rasters for three twenty-minute conspecific male-male pairs each of wildtype *D.*
1058 *persimilis* (A) and *D. pseudoobscura* (B). Annotations of seven aggressive interactions by manual scoring
1059 (blues and black) are shown above the horizontal dashed lines and five courtship actions (reds) beneath.
1060 Actions split by identity of the male to which they are attributed with the one exhibiting the greater total
1061 number of actions assigned as "Male 1." *D. persimilis* males court frequently including making
1062 copulation attempts (e.g., Pair 3). *D. pseudoobscura* also show some courtship but attack more intensely
1063 and often.
1064 **(C,D)** Ethograms representing male- (C) and female-directed social behaviors (D) by *D. persimilis* and *D.*
1065 *pseudoobscura* males. Male-female ethograms represent expert annotation for three recordings of male-
1066 female pairs per species, with male flies similarly prepared by single-housing and interactions taking
1067 place under identical conditions. Male-directed ethograms reproduced from Fig. 1-S1A for visual
1068 comparison to female-directed counterparts. Note similarity between interactions with males and females
1069 in *D. per*.
1070 **(E)** Spontaneous bias observed between flies in male-male *D. persimilis* and *D. pseudoobscura* pairs for
1071 attack and courtship. Indices derived from the same fly pair are connected as lines and distribution means
1072 shown as paired purple (*D. per*) or blue dots (*D. pse*). Both species show strong behavioral biases.
1073

1074 **Materials and Methods**

1075

1076 **Fly stocks**

1077 All species, stocks, and crosses were reared at 24-25C and 50% humidity on a 12hr:12hr light
1078 cycle with standard Caltech fly media. Details about the flies used in each experiment (species, strain,
1079 sex, genetic background, and experimental and control genotypes) are listed in Supplemental Tables 2 and
1080 3. Supplemental Table 2 provides identifiers for the 18 wildtype strains and lists their usage by figure.
1081 Supplemental Table 3 provides similar information for *D. santomea* transgenic lines. All wildtype strains
1082 were obtained from the National Drosophila Species Stock Center (Cornell College of Agriculture and
1083 Life Science, Ithaca, NY) except *D. melanogaster* Canton-S (Anderson lab, Caltech) and three additional
1084 *D. santomea* strains (David Stern lab, Janelia Research Campus).

1085

1086 **Generation of transgenic and knock-in alleles in *D. santomea***

1087 Transgenic *D. santomea* driver and hemidriver lines using enhancer fragments to regulate Gal4
1088 expression were made using phiC31 recombination (*106*) into existing attP landing sites (*107*). White-
1089 mutant *D. santomea* attP sites 2251 (2R) and 2253 (3R) (*107*) were targeted using Gal4 (pBPGUw),
1090 Gal4DBD (pBPZpGAL4DBDUw), or p65AD (pBPp65ADZpUw) vectors carrying an attB recognition
1091 site and mini-white selection marker (*149*, *150*). When available, ready-made constructs with desired
1092 enhancer sequences were obtained from Janelia. Otherwise enhancer sequences were obtained from (*149*),
1093 synthesized by Twist Bioscience (South San Francisco, CA) with flanking attL1/L2 recognition sites, and
1094 cloned upstream of transcriptional control cassettes in the backbone vectors using Gateway LR reactions
1095 (Thermo Fisher Scientific, Waltham, MA). Assembled constructs were verified by sequencing and
1096 restriction digest, maxi-prepped using endotoxin-free kits, and cleaned using ethanol precipitation before
1097 sending for injection. Rainbow Transgenic Flies, Inc. (Camarillo, CA) generated injection mixes
1098 containing the construct and phiC31 integrase mRNA (and sometimes also integrase plasmid to increase
1099 efficiency) and performed injections into *D. santomea* eggs in batches of 200-250 per desired
1100 transformant. Viable G0 (injected) flies were collected and crossed to a white-mutant strain (*2041/w-*
1101 *[3.2]*) (*107*) before screening for yellow-eyed (transgene heterozygous) flies in the G1 progeny to confirm
1102 germline transmission. Heterozygotes were crossed together to generate transgene homozygotes as stable
1103 lines used for experiments.

1104 Knock-in driver lines were generated using CRISPR/Cas9-mediated homology-directed repair
1105 (HDR) (*104*). Donor construct assembly and sgRNA selection for *D. santomea dsx-p65AD* were
1106 performed previously (*105*) but transformants positive for the selection marker (*MHC-DsRed*) had not
1107 been obtained. The same reagents were re-injected into *D. santomea 146/STO-CAGO 1482* (David Stern,

1108 Janelia) in a mixture with nls-Cas9-nls protein (PNA Bio, Thousand Oaks, CA) and one transformant with
1109 germline transmission of abdominal mCherry was successfully recovered. Crosses among G1 progeny
1110 yielded sporadic G2 flies with the expected *dsx* genital phenotype, verifying the genomic insertion.
1111 *D. santomea Or67d*$^{Gal4}$ was generated using the Atalanta strategy (*148*). A backbone vector with
1112 two U6 promoters (for expression of two sgRNAs) and an "empty payload" (pJAT32) was selected as the
1113 Gateway acceptor. Two donor sequences were synthesized by Twist Bioscience and cloned into the
1114 acceptor in a simultaneous double-Gateway reaction. The first (flanked by attL3/L4) is a *T2A-Gal4-*
1115 *stop(hsp70)* cassette (*Gal4-stop(hsp70)* from pBPGUw) designed to be inserted downstream from but as
1116 close as possible to the *D. santomea Or67d (3L:LOC120447699)* translational start codon. Placement of
1117 the adjacent homology arm ensures that insertion occurs in-frame with the residual 15 coding base pairs
1118 so that Gal4 is properly translated. The second (flanked by attL5/L6) is an *ie1-mCherry-stop(p10)*
1119 selection marker (*32*) with inverted orientation relative to Gal4. Both donors also contain a 1 kb
1120 homology arm and U6-tRNA-sgRNA-tRNA array which, following LR recombination, is positioned
1121 downstream of U6. Candidate sgRNAs were designed in Geneious Prime (Auckland, NZ) and a pair was
1122 selected which excises 99% of *Or67d* coding sequence, resulting in a null allele (upstream
1123 *AATGGCAAAAGTTGAGCCCG*, downstream *ACTGCTGGTTTCCAAAGGAG*). Successful Gateway
1124 products were verified by restriction digest and tiled sequencing. Injection into *D. santomea 146/STO-*
1125 *CAGO 1482* was performed by Rainbow Transgenic Flies using nls-Cas9-nls protein as the enzyme
1126 source and G1 progeny were screened for germline-transmitting abdominal mCherry. Multiple
1127 independent insertion lines were recovered and homozygosed, one of which was used throughout after
1128 anatomical verification of uniglomerular labeling in the antennal lobes of the size and position expected
1129 for Or67d OSNs (*145*). Note that in this strategy Gal4 expression is controlled exclusively by the *Or67d*
1130 native genomic regulatory context rather than an exogenous promoter.
1131
1132 **Spontaneous behavior experiments with video recording**
1133 Experimental crosses were seeded with 10-12 virgin females and 5-6 males and flipped every 3-4
1134 days. Experimental flies were collected mostly as virgins on the day of eclosion and reared either in
1135 isolation (single-housed, 1 individual per vial) or in same-sex groups (group-housed, 10-20 individuals
1136 per vial) for 5-6 days until testing. Group-housed (but not single-housed) flies were flipped into fresh
1137 vials 1-2 days before testing. For experiments requiring unambiguous determination of individual identity
1138 (e.g., in mixed-genotype or mixed-species male-male pairs), a small distal portion of one fly's wing was
1139 clipped using a razor blade under light anesthesia. Whenever possible, the "target" fly (individual whose
1140 behavior was not being measured) was selected for wing clipping. Otherwise clips were balanced between
1141 the two interacting species or genotypes. Females were collected and group-housed as were males (mostly

1142 as virgins on the day of eclosion, 10-20 individuals per vial) and age-matched to the males they were
1143 tested with as courtship targets. As this was usually a period of 5-6 days, it is likely that even the few
1144 females that were not virgins upon collection had by the time of the experiment shed residual male
1145 pheromones potentially transferred during prior copulation (e.g., cVA). Group-housed females were also
1146 flipped 1-2 days before testing. Housing for each experiment arranged by figure can be found in
1147 Supplemental Tables 2 and 3 ("single" or "group" under the "Housing" heading).

1148 Behavior experiments took place in the morning between 9:00AM (ZT0) and 1:00PM (ZT4) in a
1149 temperature and humidity-controlled room (24C, 50% humidity) with ambient white lighting. Single,
1150 pairs, or trios of flies interacted in 8-well acrylic circular chambers (~2.0 $cm^2$ surface area, ~2.4 $cm^3$
1151 volume) designed and described previously (*56*, *151*). Walls of the chambers were coated with Fluon (Tar
1152 Heel Ants, Raleigh, NC) and lids with a siliconizing fluid (Thermo Fisher) to discourage flies from
1153 climbing. Chamber floors were covered with a thin layer of freshly prepared "food" (2.5% (w/v) sucrose,
1154 2.25% (w/v) agarose in Tropicana apple juice) and illuminated with an 855 nm backlight (Smart Vision
1155 Lights, Muskegon, MI). Experiments testing alternative foods replaced the apple with other juices
1156 acquired commercially (morinda, fig) or from botanical gardens (marula, pandanus), or with water as a
1157 "no food" condition (sucrose was also omitted in this case). Flies were introduced one at a time into
1158 chambers by gentle aspiration through a small hole in the lid. Interactions were video recorded from
1159 above using a Point Grey Flea3 camera running at 30 Hz with a 780 nm long pass IR filter (Midwest
1160 Optical Systems, Palatine, IL). Experiments performed in 8-well chambers are listed as "small" under the
1161 "Chamber" heading in Supplemental Tables 2 and 3.

1162 For copulation tests of Or67d OSN-silenced *D. santomea* females and territoriality assays of
1163 wildtype *D. santomea* males, "large" chambers consisting of a central food patch (apple juice agarose)
1164 and a neutral surround (bare acrylic) were used. Chambers measure 20 $cm^2$ surface area and 120 $cm^3$
1165 volume, and the circular food patch ~4.9 $cm^2$ (25% surface area). Flies (12 females and 12 males for
1166 copulation tests, 2 males for territoriality tests) were gently aspirated into chambers and video recorded
1167 using identical lighting and camera settings as for small chambers described above.
1168

1169 **Optogenetic photoactivation experiments**

1170 Flies were collected on the day of eclosion into vials containing food supplemented with 400 μM
1171 all *trans*-Retinal (Millipore Sigma, Burlington, MA) and reared in the dark for 5-6 days, with one flip into
1172 fresh supplemented vials 1-2 days before testing. Photoactivated flies were usually group-housed (10-20
1173 males per vial), except in male Or67d OSN courtship suppression experiments which were single-housed
1174 to encourage spontaneous courtship prior to stimulation. Group-housed males paired together during
1175 behavior assays came from different vials.

1176 Experiments took place in the small chambers using an 8-LED array setup reported previously
1177 (*56*, *151*). LEDs delivered flashing 685 nm red light in photostimulation (PS) blocks with 10 ms pulse
1178 width, frequencies ranging from 1-40 Hz, and intensities 10-260 $\mu W/mm^2$, calibrated with a photodiode
1179 power sensor (S130VC, Thorlabs, Newton, NJ) placed at the location of the behavior chambers. Exact PS
1180 conditions (timing, frequency, intensity) for each experiment are shown in Figures and described in
1181 Figure Legends.
1182 "Sliding door" experiments testing persistent behavioral responses after PS were performed in 8-
1183 well chambers fitted with vertical slits to allow metal barriers to divide each chamber in half. Barriers
1184 remained in place during the isolation/PS phase of the experiment, which upon completion of the delay
1185 were manually removed during a ~30 second period while video recordings were paused. Once the
1186 barriers were removed recordings resumed for the interaction phase.
1187
1188 **Behavior annotations and analysis**
1189 Annotations of aggressive (A) and courtship behaviors (C) in male-male pairs from each species
1190 for the primary screen were performed manually using action definitions from (*55*) (threat (A), charge
1191 (A), lunge (A), hold (A), tussle (A), unilateral wing extension (C), circle (C), copulation attempt (C)),
1192 (*102*) (pump (A)), (*20*) (bilateral wing extension (C), row (C)), and (*147*) (headbutt (A)). One additional
1193 action observed exclusively in *D. pseudoobscura* males, "barrage," is defined as follows: *the attacking fly*
1194 *pushes into and quickly chases the opponent while both wings are fully extended and vibrating rapidly as*
1195 *if in flight.* This action appears to have been described once before without being named (*130*). Ethograms
1196 were constructed from calculations of action frequencies and transition matrices using a 1-second cutoff.
1197 For most experiments, video recordings were analyzed in an automated fashion by first tracking
1198 the absolute and relative positions of flies in the chamber at every frame (Caltech FlyTracker,
1199 https://kristinbranson.github.io/FlyTracker/) (*55*) and using the tracking information as input to automated
1200 behavior classifiers developed previously for *D. melanogaster* social interactions (*56*), implemented in
1201 JAABA (https://jaaba.sourceforge.net/) (*54*). Two classifiers were used extensively after satisfactory
1202 performance evaluation for species within the melanogaster subgroup: "lunge" for consummatory,
1203 contact-mediated male aggression, and "unilateral wing extension" for male courtship. Recordings
1204 analyzed in this way are listed as "automated" under the "Behavioral analysis" heading in Supplemental
1205 Tables 2 and 3. Manually annotated recordings, including ones analyzed for the female sexual behaviors
1206 ovipositor extrusion (*120*, *121*) and wing spreading (*122*), are instead labeled "manual." For experiments
1207 involving a male-female pair, analysis ended at the point of copulation (if it occurred) and the latency to
1208 copulation was used for normalization procedures rather than total interaction time.
1209

1210 **Courtship song recordings and analysis**

1211 Flies (*D. santomea* wildtype strain 14021-0271.00) were raised in standard laboratory conditions
1212 at 23C and 12:12 light cycle. Sexually naïve individuals were isolated within 3 hours of eclosion and
1213 single-housed for 5-7 days prior to behavioral analysis. Synchronized audio and video song recordings
1214 were made within 4 hours of lights-on in the morning using the Song Torrent system (*60*). Individual flies
1215 arranged in male-male or male-female pairs were loaded onto opposite sides of a divider in recording
1216 chambers and introduced to each other simultaneously at the beginning of 30-minute recordings.

1217 Videos of 16 male-male and 16 male-female pairs of *D. santomea* flies were visually scanned and
1218 3 pairs of each type with ample courtship were selected for audio analysis. Song traces were visualized
1219 and annotated in Tempo (*63*) until dozens to hundreds of both "pulse" and "clack" events had been
1220 recorded for each courting male (instead of to saturation). The exact amplitude and position of each
1221 event's peak was determined by obtaining the maximum signal intensity within a 20 ms time window
1222 centered on the annotation point. Events were assigned to being part of a "train" when their separation
1223 from another event of the same type was less than 200 ms for pulse and 400 ms for clack.

1224

1225 **Pheromone applications**

1226 (Z)-11-octadecenyl acetate (cVA) and (Z)-7-tricosene (7-T) were acquired commercially from Pherobank
1227 B.V. (Wijk bij Duurstede, NL) as neat liquid formulations (i.e., without a solvent). For behavioral
1228 experiments with cVA on filter paper, 0.5-2 µl neat formulation was applied just prior to introduction of
1229 flies into the chamber. For direct treatment of live flies, cVA neat formulation was diluted to a 10%
1230 working solution in acetone (179124, Millipore Sigma), from which 0.2 µl was pipetted onto the
1231 abdomen of target flies under anesthesia 1-2 hours prior to behavioral testing, as previously (*89*). Flies
1232 that did not rouse were discarded. For direct treatment of dead flies, 0.2 µl of 10% cVA (acetone) or 7-T
1233 (hexane) working solutions was directly pipetted onto the abdomen of flies freshly killed by freezing at -
1234 80C and glued to the chamber floor using melted agarose of the same "food" composition.

1235

1236 **Odor place preference tests**

1237 The olfactory "y-maze" was constructed by laser cutting multiple layers of 1/8th inch 3143
1238 infrared (IR)-transmitting acrylic (ACRY31430.125PM, ePlastics, San Diego, CA) to shape. The bottom
1239 floor layer was finely wet sanded for texture. Chambers at the end of each arm meant for odor reservoirs
1240 and a center port for the vacuum line were blocked off with fine mesh. Top layers consisted of a ceiling of
1241 static dissipating acrylic (8774K11, McMaster-Carr, Santa Fe Springs, CA) with a rim of IR acrylic to
1242 block ambient light, and a final roof layer with small holes above the chambers to allow air to be drawn
1243 into and down the arena by the vacuum line. The layers were supported and sealed with three threaded

rods and bolts. Acrylic layers were periodically cleaned with 1% SDS, water, and isopropanol. The arena was illuminated from below using a custom-built IR 810 nm LED lighting board and diffused with semi-opaque white acrylic. Videos were collected with a machine vision camera (BFS-U3-04S2M-C: 0.4 MP, Teledyne FLIR) running at 45 Hz and a Pentax 12mm 1:1.2 TV lens (FL-HC1212B-VG, Ricoh).

Flies were collected on the day of eclosion, separated by sex, and single- or group-housed for one week until testing. For each trial, 5 µl odor (10% cVA in acetone or acetone control) was first loaded at the top of each arm of the y-maze then 2-4 cold anesthetized males or females were aspirated into the central bowl and the lid quickly fastened. Ten-minute recordings initiated once the flies had roused. Cumulative position traces were obtained by first median filtering on a subset of frames to construct a background image. OpenCV (4.6.0) was used to perform thresholding on background-subtracted frames. The resulting "blob detection" indicated animal position per frame, and positions across the entire trial were plotted using Matplotlib (3.4.3). Normalized occupancy in the left vs. right arm was calculated from cumulative position traces using cutoffs including the two arms but excluding the central bowl.

**Gas chromatography – mass spectrometry (GC-MS)**

Flies were collected on the day of eclosion, separated by sex, and group-housed in sets of 10 for one week until analysis. Flies were anesthetized and transferred to 2 ml glass screw top vials (Thermo Fisher) containing 100 µl hexane (139386, Millipore Sigma) with 10 ng/µl octadecane (C18) internal standard (O652, Millipore Sigma). Hexane extraction was allowed to proceed for 15 minutes at room temperature, after which extracts were transferred to glass inserts (Ibis Scientific, Clark County, NV) positioned in new screw top vials for either immediate analysis or storage at -80C.

An AOC-2i autoinjector (Shimadzu, Kyoto, Japan) was used to inject 2 µl of each sample into a Shimadzu QP-2020 GC-MS system (Shimadzu, Kyoto, Japan) equipped with a ZB-5MS fused silica capillary column (30 m x 0.25 mmID, df=0.25) (Phenomenex, Torrance, CA) and helium as the carrier gas. The injection port was maintained at a temperature of 310C and was operated in splitless mode, with a column flow rate of 2.15 ml/min. The temperature program consisted of a 40C hold for 1 minute, followed by a 20C/min ramp to 250C, a 5C/min ramp to 320C, and a 320C hold for 7.5 minutes. The transfer line to the mass spectrometer was held at 320C and the ion source temperature at 230C. Electron ionization was performed at 70 eV and MS scans were collected at 2 Hz, spanning 40-650 m/z. Identification of cuticular hydrocarbon (CHC) and ester compounds was determined by retention index, diagnostic ions, and comparison to previous GC-MS results from *Drosophila* (*65*, *66*, *152*, *153*). GC-MS spectra were integrated in python using the pyteomics package (v4.4.0).

**Immunostaining and imaging**

Whole brains were dissected in ice-cold phosphate-buffered saline (PBS) and fixed in 4% paraformaldehyde for 20 minutes at room temperature (RT). Samples were washed three times in 0.5% PBST (PBS containing 0.5% (v/v) Triton X-100) for 10 minutes at RT, then permeabilized in 2% PBST for 30 minutes at RT. Samples were blocked in 0.5% PBST with 5% normal goat serum (NGS) for 1 hour at RT or overnight at 4C. Samples were incubated with primary antibodies in blocking solution for 48-72 hours at 4C (rabbit anti-DsRed 1:1000, mouse anti-Bruchpilot 1:50) followed by three 10-minute washes in 0.5% PBST. Samples were incubated in secondary antibodies (anti-rabbit IgG AF568 and anti-mouse IgG AF633, 1:1000) in blocking solution for 36-48 hours at 4C, then again washed three times in 0.5% PBST for 10 minutes at RT before mounting.

Samples were mounted in VectaShield antifade medium (Vector Laboratories, Newark, CA) and imaged on an Olympus Fluoview FV3000 confocal microscope (Tokyo, JP) with inverted 30X/1.05 or 60X/1.30 oil immersion objectives. Image stacks were acquired at 1024 x 1024 $px^2$ spatial resolution with 1.0-1.5 µm z-step intervals. Images (referred to as "photomicrographs") are maximum intensity projections (MIPs) of image stacks generated in Fiji. Fiji was also used to pseudocolor, overlay, adjust brightness and contrast, and add scale bars to images.

**Quantification and statistical analysis**

Fly positional tracking, automated social behavior annotations, and song analyses were performed using software implemented in MATLAB (MathWorks, Natick, MA). Odor place preference and GC-MS experiments were analyzed in python using Jupyter Notebooks (https://jupyter.org/). The tabulated outputs of these analyses were saved and exported as text files for final analyses in R (R Project for Statistical Computing) using RStudio (Posit PBC, Boston, MA). Custom scripts in R were used to calculate raw data derivations reported in figures, produce plots visualizing them, and perform statistical tests. Illustrator 2025 (Adobe, San Jose, CA) was used to adjust aesthetic features of plots and assemble figures.

Measurement distributions are often shown as boxplots highlighting the median and overlayed data points. Outliers are identified in the standard way (> Q3+1.5*QR or < Q1-1.5*QR) and visually excluded from whiskers, but are retained in all quantifications (including statistical tests) and still shown as dots. Violin plots show full distribution ranges as vertically mirrored kernel density plots with mean highlighted. Statistical tests consisted mostly of non-parametric comparisons between pairs of or multiple distributions and were implemented in R. Mann-Whitney *U* tests (R base *stats* package: *wilcox.test* function) were used to compare pairs of distributions (two-sample) or an empirical distribution to a null median (one-sample), and could be paired or unpaired depending on whether the comparison involved the same individual or interacting pair. Two-sample Kolmogorov–Smirnov tests (*stats: ks.test*) were used to

compare pairs of time-evolving distributions or cumulative distributions. Kruskal-Wallis tests (*stats: kruskal.test*) and post-hoc Dunn's tests (*FSA: dunnTest*) were used to compare multiple distributions and assign lettered groupings. Binomial tests (*stats: binom.test*) were used to compare pairs of frequencies for binary outcomes (two-sample) or an empirical frequency to a null probability (one-sample). Linear fits and Pearson correlations were calculated using the *lm* and *cor* functions (*stats*), respectively. Benjamini-Hochberg multiple test correction was used to adjust p-values whenever appropriate (*stats: p.adjust: method='BH'*). Standardized effect sizes were calculated using Cohen's *d* (*effsize: cohen.d*). Tests shown in each figure can be referenced in Supplemental Table 4 for details including sample sizes, sample units, test used, whether correction was applied, adjusted p-value, and effect size. Significance levels are reported in Figures as *<0.05, **<0.01, and ***<0.001.

**Acknowledgments**

We thank the Anderson lab (Caltech) for help throughout the project, including experimental suggestions and conceptual advice. Liliana Chavarria, Gina Mancuso, Celine Chiu (Caltech) for administrative help. Arnold Sanchez (Caltech) for fly stock maintenance. Heather Dionne, Jeremy Hasseman, Elizabeth Kim, Katie Schretter, and Hiroshi Shiozaki (Janelia Research Campus) for constructs, reagents, and fly stocks. Rory Coleman (NYU) and Vanessa Ruta (Rockefeller) for constructs, fly stocks, information related to unpublished results, and comments on the manuscript. Hong Yu and Garrett Kuiken (Rainbow Transgenic Flies) for embryo injections. Kathy Musial, Gary Roberson (Huntington Botanical Gardens), and David Orr (Waimea Botanical Garden) for access to fruits for host specialization experiments. Ryan York (Arcadia Science) for help with behavioral and evolutionary analyses. Peter Andolfatto (Columbia) for access to an assembled and annotated *D. santomea* reference genome. Markus Knaden (MPI Chemical Ecology) for permission to reanalyze published TD-GC-MS data.

**Funding**

This work was supported by a Jane Coffin Childs Memorial Fund Postdoctoral Fellowship, Della Martin Foundation Postdoctoral Fellowship, and Caltech Center for Evolutionary Science grant to YO. NIH NIDA 5R37DA031389 grant and Howard Hughes Medical Institute funding to DJA.

**Author Contributions**

Conceptualization: YO, DJA
Formal Analysis: YO, DJA
Funding Acquisition: YO, DJA
Investigation: YO, THN, HS, ELB
Methodology: ELB, YD, DLS
Resources: HS, MAK, YD, DLS, JP
Software: THN, HS
Visualization: YO, DJA
Writing – Original Draft Preparation: YO
Writing – Review & Editing: YO, THN, HS, ELB, MAK, YD, DLS, JP, DJA

**Competing Interests**

The authors declare no competing interests.

**Data and Materials Availability**

All data are available in the main manuscript or the supplementary materials. Raw source data, analytical code, constructs and associated maps, and fly stocks will be made publicly available upon submission of the manuscript in accordance with current Caltech and HHMI policies.

**References**

1. T. Clutton-Brock, Social evolution in mammals. *Science* **373**, eabc9699 (2021).

2. C. B. Stanford, The Social Behavior of Chimpanzees and Bonobos: Empirical Evidence and Shifting Assumptions. *Curr Anthropol* **39**, 399–420 (1998).

3. E. O. Wilson, The Sociogenesis of Insect Colonies. *Science* **228**, 1489–1495 (1985).

4. R. D. Alexander, The Evolution of Social Behavior. *Annu Rev Ecol Syst* **5**, 325–383 (1974).

5. S. A. West, G. A. Cooper, M. B. Ghoul, A. S. Griffin, Ten recent insights for our understanding of cooperation. *Nat Ecol Evol* **5**, 419–430 (2021).

6. N. Tinbergen, A. C. Perdeck, On the Stimulus Situation Releasing the Begging Response in the Newly Hatched Herring Gull Chick (Larus Argentatus Argentatus Pont.). *Behaviour* **3**, 1–39 (1951).

7. A. Butenandt, R. Beckmann, E. Hecker, Über den Sexuallockstoff des Seidenspinners, I. Der biologische Test und die Isolierung des reinen Sexuallockstoffes Bombykol. *Hoppe-Seylers Z für Physiol Chem* **324**, 71–83 (1961).

8. D. W. Pfaff, Luteinizing Hormone-Releasing Factor Potentiates Lordosis Behavior in Hypophysectomized Ovariectomized Female Rats. *Science* **182**, 1148–1149 (1973).

9. M. de Bono, C. I. Bargmann, Natural Variation in a Neuropeptide Y Receptor Homolog Modifies Social Behavior and Food Response in C. elegans. *Cell* **94**, 679–689 (1998).

10. L. Keller, K. G. Ross, Selfish genes: a green beard in the red fire ant. *Nature* **394**, 573–575 (1998).

11. C. F. Yang, M. C. Chiang, D. C. Gray, M. Prabhakaran, M. Alvarado, S. A. Juntti, E. K. Unger, J. A. Wells, N. M. Shah, Sexually Dimorphic Neurons in the Ventromedial Hypothalamus Govern Mating in Both Sexes and Aggression in Males. *Cell* **153**, 896–909 (2013).

12. H. Lee, D.-W. Kim, R. Remedios, T. E. Anthony, A. Chang, L. Madisen, H. Zeng, D. J. Anderson, Scalable control of mounting and attack by Esr1+ neurons in the ventromedial hypothalamus. *Nature* **509**, 627–632 (2014).

13. Z. Wu, A. E. Autry, J. F. Bergan, M. Watabe-Uchida, C. G. Dulac, Galanin neurons in the medial preoptic area govern parental behaviour. *Nature* **509**, 325–330 (2014).

14. H. Chang, S. Cassau, J. Krieger, X. Guo, M. Knaden, L. Kang, B. S. Hansson, A chemical defense deters cannibalism in migratory locusts. *Science* **380**, 537–543 (2023).

15. N. Niepoth, J. R. Merritt, M. Uminski, E. Lei, V. S. Esquibies, I. B. Bando, K. Hernandez, C. Gebhardt, S. A. Wacker, S. Lutzu, A. Poudel, K. K. Soma, S. Rudolph, A. Bendesky, Evolution of a novel adrenal cell type that promotes parental care. *Nature* **629**, 1082–1090 (2024).

16. P. M. O'Grady, R. DeSalle, Phylogeny of the Genus Drosophila. *Genetics* **209**, 1–25 (2018).

17. A. H. Sturtevant, Experiments on sex recognition and the problem of sexual selection in Drosophila. *J Anim Behav* **5**, 351–366 (1915).

18. H. T. Spieth, Courtship Behavior in Drosophila. *Annu Rev Entomol* **19**, 385–405 (1974).

19. A. W. Ewing, Functional Aspects of Drosophila Courtship. *Biol Rev* **58**, 275–292 (1983).

20. M. Cobb, K. Connolly, B. Burnet, Courtship Behaviour in the Melanogaster Species Sub-Group of Drosophila. *Behaviour* **95**, 203–230 (1985).

21. R. J. Greenspan, J.-F. Ferveur, Courtship in Drosophila. *Annu Rev Genet* **34**, 205–232 (2000).

22. R. R. H. Anholt, P. O'Grady, M. F. Wolfner, S. T. Harbison, Evolution of Reproductive Behavior. *Genetics* **214**, 49–73 (2020).

23. M. Bastock, A. Manning, The Courtship of Drosophila melanogaster. *Behaviour* **8**, 85–110 (1955).

24. J. C. Hall, The Mating of a Fly. *Science* **264**, 1702–1714 (1994).

25. D. Yamamoto, M. Koganezawa, Genes and circuits of courtship behaviour in Drosophila males. *Nat Rev Neurosci* **14**, 681–692 (2013).

26. D. A. Wheeler, C. P. Kyriacou, M. L. Greenacre, Q. Yu, J. E. Rutila, M. Rosbash, J. C. Hall, Molecular Transfer of a Species-specific Behavior from Drosophila simulans to Drosophila melanogaster. *Science* **251**, 1082–1085 (1991).

27. J. Coyne, A. Crittenden, K. Mah, Genetics of a pheromonal difference contributing to reproductive isolation in Drosophila. *Science* **265**, 1461–1464 (1994).

28. T. R. Shirangi, H. D. Dufour, T. M. Williams, S. B. Carroll, Rapid Evolution of Sex Pheromone-Producing Enzyme Expression in Drosophila. *PLOS Biol* **7**, e1000168 (2009).

29. Y. Ding, A. Berrocal, T. Morita, K. D. Longden, D. L. Stern, Natural courtship song variation caused by an intronic retroelement in an ion channel gene. *Nature* **536**, 329–332 (2016).

30. L. F. Seeholzer, M. Seppo, D. L. Stern, V. Ruta, Evolution of a central neural circuit underlies Drosophila mate preferences. *Nature* **559**, 564–569 (2018).

31. O. M. Ahmed, A. Avila-Herrera, K. M. Tun, P. H. Serpa, J. Peng, S. Parthasarathy, J.-M. Knapp, D. L. Stern, G. W. Davis, K. S. Pollard, N. M. Shah, Evolution of Mechanisms that Control Mating in Drosophila Males. *Cell Reports* **27**, 2527-2536.e4 (2019).

32. R. T. Coleman, I. Morantte, G. T. Koreman, M. L. Cheng, Y. Ding, V. Ruta, A modular circuit coordinates the diversification of courtship strategies. *Nature* **635**, 142–150 (2024).

33. R. Tanaka, Y. Hara, K. Sato, S. Kohatsu, H. Murakami, T. Higuchi, T. Awasaki, S. Kondo, A. Toyoda, A. Kamikouchi, D. Yamamoto, Cross-species implementation of an innate courtship behavior by manipulation of the sex-determinant gene. *Science* **389**, 747–752 (2025).

34. T. Dobzhansky, Species of Drosophila. *Science* **177**, 664–669 (1972).

35. J. A. Coyne, H. A. Orr, Patterns of Speciation in Drosophila. *Evolution* **43**, 362–381 (1989).

36. N. Jourjine, H. E. Hoekstra, Expanding evolutionary neuroscience: insights from comparing variation in behavior. *Neuron* **109**, 1084–1099 (2021).

37. C. T. Miller, D. Gire, K. Hoke, A. C. Huk, D. Kelley, D. A. Leopold, M. C. Smear, F. Theunissen, M. Yartsev, C. M. Niell, Natural behavior is the language of the brain. *Curr Biol* **32**, R482–R493 (2022).

38. G. L. Hunt, M. W. Hunt, Female-Female Pairing in Western Gulls (Larus occidentalis) in Southern California. *Science* **196**, 1466–1467 (1977).

39. D. W. Mock, Siblicidal Aggression and Resource Monopolization in Birds. *Science* **225**, 731–733 (1984).

40. M. E. Jacobs, Influence of Light on Mating of Drosophila Melanogaster. *Ecology* **41**, 182–188 (1960).

41. M. A. Dow, F. von Schilcher, Aggression and mating success in Drosophila melanogaster. *Nature* **254**, 511–512 (1975).

42. K. H. Skrzipek, B. Kröner, H. Hager, Aggression bei Drosophila melanogaster— Laboruntersuchungen. *Z für Tierpsychol* **49**, 87–103 (1979).

43. A. A. Hoffmann, A laboratory study of male territoriality in the sibling species Drosophila melanogaster and D. simulans. *Anim Behav* **35**, 807–818 (1987).

44. H. A. Dierick, R. J. Greenspan, Molecular analysis of flies selected for aggressive behavior. *Nat Genet* **38**, 1023–1031 (2006).

45. A. C. Edwards, S. M. Rollmann, T. J. Morgan, T. F. C. Mackay, Quantitative Genomics of Aggressive Behavior in Drosophila melanogaster. *PLOS Genet* **2**, e154 (2006).

46. S. C. Hoyer, A. Eckart, A. Herrel, T. Zars, S. A. Fischer, S. L. Hardie, M. Heisenberg, Octopamine in Male Aggression of Drosophila. *Curr Biol* **18**, 159–167 (2008).

47. L. Wang, H. Dankert, P. Perona, D. J. Anderson, A common genetic target for environmental and heritable influences on aggressiveness in Drosophila. *PNAS* **105**, 5657–5663 (2008).

48. S. Chen, A. Y. Lee, N. M. Bowens, R. Huber, E. A. Kravitz, Fighting fruit flies: A model system for the study of aggression. *PNAS* **99**, 5664–5668 (2002).

49. H. Dankert, L. Wang, E. D. Hoopfer, D. J. Anderson, P. Perona, Automated monitoring and analysis of social behavior in Drosophila. *Nat Methods* **6**, 297–303 (2009).

50. E. D. Hoopfer, Neural control of aggression in Drosophila. *Curr Opin Neurobiol* **38**, 109–118 (2016).

51. J. R. David, F. Lemeunier, L. Tsacas, A. Yassin, The Historical Discovery of the Nine Species in the Drosophila melanogaster Species Subgroup. *Genetics* **177**, 1969–1973 (2007).

52. S. Leigh, M. G. Ritchie, A history of studies of reproductive isolation between Drosophila pseudoobscura and D. persimilis. *Fly* **19**, 2439111 (2025).

53. T. O. Auer, M. P. Shahandeh, R. Benton, Drosophila sechellia: A Genetic Model for Behavioral Evolution and Neuroecology. *Annu Rev Genet* **55**, 1–28 (2021).

54. M. Kabra, A. A. Robie, M. Rivera-Alba, S. Branson, K. Branson, JAABA: interactive machine learning for automatic annotation of animal behavior. *Nat Methods* **10**, 64–67 (2013).

55. E. Eyjolfsdottir, S. Branson, X. P. Burgos-Artizzu, E. D. Hoopfer, J. Schor, D. J. Anderson, P. Perona, Detecting Social Actions of Fruit Flies. *ECCV*, 772–787 (2014).

56. E. D. Hoopfer, Y. Jung, H. K. Inagaki, G. M. Rubin, D. J. Anderson, P1 interneurons promote a persistent internal state that enhances inter-male aggression in Drosophila. *eLife* **4**, e11346 (2015).

57. J. Linz, A. Baschwitz, A. Strutz, H. K. M. Dweck, S. Sachse, B. S. Hansson, M. C. Stensmyr, Host plant-driven sensory specialization in Drosophila erecta. *Proc Royal Soc B* **280**, 20130626 (2013).

58. S. J. Certel, M. G. Savella, D. C. F. Schlegel, E. A. Kravitz, Modulation of Drosophila male behavioral choice. *PNAS* **104**, 4706–4711 (2007).

59. R. S. Lim, E. Eyjólfsdóttir, E. Shin, P. Perona, D. J. Anderson, How Food Controls Aggression in Drosophila. *PLOS One* **9**, e105626 (2014).

60. S. Sawtelle, L. Narayan, Y. Ding, E. Kim, E. L. Behrman, J. L. Lillvis, T. Kawase, D. L. Stern, Song Torrent: A modular, open-source 96-chamber audio and video recording apparatus with optogenetic activation and inactivation capabilities for Drosophila. *bioRxiv*, doi: 10.1101/2024.01.09.574712 (2024).

61. E. T. Watson, E. Rodewald, J. A. Coyne, The courtship song of Drosophila santomea and a comparison to its sister species D. yakuba (Diptera: Drosophilidae). *Eur J Entomol* **104**, 145–148 (2007).

62. J. E. Blyth, D. Lachaise, M. G. Ritchie, Divergence in Multiple Courtship Song Traits between Drosophila santomea and D. yakuba. *Ethology* **114**, 728–736 (2008).

63. Y. Ding, J. L. Lillvis, J. Cande, G. J. Berman, B. J. Arthur, X. Long, M. Xu, B. J. Dickson, D. L. Stern, Neural Evolution of Context-Dependent Fly Song. *Curr Biol* **29**, 1089-1099.e7 (2019).

64. N. W. Bailey, M. Zuk, Same-sex sexual behavior and evolution. *Trends Ecol Evol* **24**, 439–446 (2009).

65. J. Jallon, J. R. David, Variations in Cuticular Hydrocarbons Among the Eight Species of the Drosophila melanogaster Subgroup. *Evolution* **41**, 294–302 (1987).

66. F. Mas, J.-M. Jallon, Sexual Isolation and Cuticular Hydrocarbon Differences between Drosophila santomea and Drosophila yakuba. *J Chem Ecol* **31**, 2747–2752 (2005).

67. M. A. Khallaf, R. Cui, J. Weißflog, M. Erdogmus, A. Svatoš, H. K. M. Dweck, D. R. Valenzano, B. S. Hansson, M. Knaden, Large-scale characterization of sex pheromone communication systems in Drosophila. *Nat Commun* **12**, 4165 (2021).

68. F. Lacaille, M. Hiroi, R. Twele, T. Inoshita, D. Umemoto, G. Manière, F. Marion-Poll, M. Ozaki, W. Francke, M. Cobb, C. Everaerts, T. Tanimura, J.-F. Ferveur, An Inhibitory Sex Pheromone Tastes Bitter for Drosophila Males. *PLOS One* **2**, e661 (2007).

69. T. Miyamoto, H. Amrein, Suppression of male courtship by a Drosophila pheromone receptor. *Nat Neurosci* **11**, 874–876 (2008).

1493 70. A. Llopart, S. Elwyn, D. Lachaise, J. A. Coyne, Genetics of a Difference in Pigmentation between Drosophila
1494 yakuba and Drosophila santomea. *Evolution* **56**, 2262–2277 (2002).

1495 71. J.-C. Billeter, J. Atallah, J. J. Krupp, J. G. Millar, J. D. Levine, Specialized cells tag sexual and species identity
1496 in Drosophila melanogaster. *Nature* **461**, 987–991 (2009).

1497 72. L. Wang, X. Han, J. Mehren, M. Hiroi, J.-C. Billeter, T. Miyamoto, H. Amrein, J. D. Levine, D. J. Anderson,
1498 Hierarchical chemosensory regulation of male-male social interactions in Drosophila. *Nat Neurosci* **14**, 757–762
1499 (2011).

1500 73. R. Thistle, P. Cameron, A. Ghorayshi, L. Dennison, K. Scott, Contact Chemoreceptors Mediate Male-Male
1501 Repulsion and Male-Female Attraction during Drosophila Courtship. *Cell* **149**, 1140–1151 (2012).

1502 74. P. Fan, D. S. Manoli, O. M. Ahmed, Y. Chen, N. Agarwal, S. Kwong, A. G. Cai, J. Neitz, A. Renslo, B. S.
1503 Baker, N. M. Shah, Genetic and Neural Mechanisms that Inhibit Drosophila from Mating with Other Species. *Cell*
1504 **154**, 89–102 (2013).

1505 75. D. A. Turissini, D. R. Matute, Fine scale mapping of genomic introgressions within the Drosophila yakuba
1506 clade. *PLOS Genet* **13**, e1006971 (2017).

1507 76. M. Cobb, J.-M. Jallon, Pheromones, mate recognition and courtship stimulation in the Drosophila melanogaster
1508 species sub-group. *Anim Behav* **39**, 1058–1067 (1990).

1509 77. F. M. Butterworth, Lipids of Drosophila: A Newly Detected Lipid in the Male. *Science* **163**, 1356–1357 (1969).

1510 78. G. Brieger, F. M. Butterworth, Drosophila melanogaster: Identity of Male Lipid in Reproductive System.
1511 *Science* **167**, 1262–1262 (1970).

1512 79. R. J. Bartelt, A. M. Schaner, L. L. Jackson, cis-Vaccenyl acetate as an aggregation pheromone in Drosophila
1513 melanogaster. *J Chem Ecol* **11**, 1747–1756 (1985).

1514 80. P. Xu, R. Atkinson, D. N. M. Jones, D. P. Smith, Drosophila OBP LUSH Is Required for Activity of
1515 Pheromone-Sensitive Neurons. *Neuron* **45**, 193–200 (2005).

1516 81. S. Lebreton, V. Grabe, A. B. Omondi, R. Ignell, P. G. Becher, B. S. Hansson, S. Sachse, P. Witzgall, Love
1517 makes smell blind: mating suppresses pheromone attraction in Drosophila females via Or65a olfactory neurons. *Sci*
1518 *Rep* **4**, 7119 (2014).

1519 82. L. Wang, D. J. Anderson, Identification of an aggression-promoting pheromone and its receptor neurons in
1520 Drosophila. *Nature* **463**, 227–231 (2010).

1521 83. W. Liu, X. Liang, J. Gong, Z. Yang, Y.-H. Zhang, J.-X. Zhang, Y. Rao, Social regulation of aggression by
1522 pheromonal activation of Or65a olfactory neurons in Drosophila. *Nat Neurosci* **14**, 896–902 (2011).

1523 84. I. Taisz, E. Donà, D. Münch, S. N. Bailey, B. J. Morris, K. I. Meechan, K. M. Stevens, I. Varela-Martínez, M.
1524 Gkantia, P. Schlegel, C. Ribeiro, G. S. X. E. Jefferis, D. S. Galili, Generating parallel representations of position and
1525 identity in the olfactory system. *Cell* **186**, 2556-2573.e22 (2023).

1526 85. C. Gao, M. Ma, J. Chen, X. Ji, Q. Peng, Y. Pan, Social experience shapes fighting strategies in Drosophila. *eLife*
1527 **13**, RP104212 (2025).

1528 86. J.-M. Jallon, C. Antony, O. Benamar, Un anti-aphrodisiaque produit par les mâles Drosophila melanogaster et
1529 transféré aux femelles lors de la copulation. *C R Acad Sc Paris* **292**, 1147–1149 (1981).

1530 87. S. D. Mane, L. Tompkins, R. C. Richmond, Male Esterase 6 Catalyzes the Synthesis of a Sex Pheromone in
1531 Drosophila melanogaster Females. *Science* **222**, 419–421 (1983).

1532 88. S. Zawistowski, R. C. Richmond, Inhibition of courtship and mating of Drosophila melanogaster by the male-
1533 produced lipid, cis-vaccenyl acetate. *J Insect Physiol* **32**, 189–192 (1986).

1534 89. A. Kurtovic, A. Widmer, B. J. Dickson, A single class of olfactory neurons mediates behavioural responses to a
1535 Drosophila sex pheromone. *Nature* **446**, 542–546 (2007).

1536 90. A. Ejima, B. P. C. Smith, C. Lucas, W. van der G. van Naters, C. J. Miller, J. R. Carlson, J. D. Levine, L. C.
1537 Griffith, Generalization of Courtship Learning in Drosophila Is Mediated by cis-Vaccenyl Acetate. *Curr Biol* **17**,
1538 599–605 (2007).

1539 91. T. S. Ha, D. P. Smith, A Pheromone Receptor Mediates 11-cis-Vaccenyl Acetate-Induced Responses in
1540 Drosophila. *J Neurosci* **26**, 8727–8733 (2006).

1541 92. R. Benton, K. S. Vannice, L. B. Vosshall, An essential role for a CD36-related receptor in pheromone detection
1542 in Drosophila. *Nature* **450**, 289–293 (2007).

1543 93. W. van der G. van Naters, J. R. Carlson, Receptors and Neurons for Fly Odors in Drosophila. *Curr Biol* **17**, 606–
1544 612 (2007).

1545 94. M. L. Schlief, R. I. Wilson, Olfactory processing and behavior downstream from highly selective receptor
1546 neurons. *Nat Neurosci* **10**, 623–630 (2007).

1547 95. S. R. Datta, M. L. Vasconcelos, V. Ruta, S. Luo, A. Wong, E. Demir, J. Flores, K. Balonze, B. J. Dickson, R.
1548 Axel, The Drosophila pheromone cVA activates a sexually dimorphic neural circuit. *Nature* **452**, 473–477 (2008).

1549 96. T. H. Sten, R. Li, F. Hollunder, S. Eleazer, V. Ruta, Male-male interactions shape mate selection in Drosophila.
1550 *Cell* **188**, 1486-1503.e25 (2025).

1551 97. M. Koganezawa, K. Kimura, D. Yamamoto, The Neural Circuitry that Functions as a Switch for Courtship
1552 versus Aggression in Drosophila Males. *Curr Biol* **26**, 1395–1403 (2016).

1553 98. K. Ishii, M. Wohl, A. DeSouza, K. Asahina, Sex-determining genes distinctly regulate courtship capability and
1554 target preference via sexually dimorphic neurons. *eLife* **9**, e52701 (2020).

1555 99. M. Wohl, K. Ishii, K. Asahina, Layered roles of fruitless isoforms in specification and function of male
1556 aggression-promoting neurons in Drosophila. *eLife* **9**, e52702 (2020).

1557 100. H. Chiu, E. D. Hoopfer, M. L. Coughlan, H. J. Pavlou, S. F. Goodwin, D. J. Anderson, A circuit logic for
1558 sexually shared and dimorphic aggressive behaviors in Drosophila. *Cell* **184**, 507-520.e16 (2021).

1559 101. C. Han, Q. Peng, M. Sun, X. Jiang, X. Su, J. Chen, M. Ma, H. Zhu, X. Ji, Y. Pan, The doublesex gene regulates
1560 dimorphic sexual and aggressive behaviors in Drosophila. *PNAS* **119**, e2201513119 (2022).

1561 102. B. J. Duistermars, B. D. Pfeiffer, E. D. Hoopfer, D. J. Anderson, A Brain Module for Scalable Control of
1562 Complex, Multi-motor Threat Displays. *Neuron* **100**, 1474-1490.e4 (2018).

1563 103. L. Tao, D. Ayambem, V. J. Barranca, V. Bhandawat, Neurons Underlying Aggression-Like Actions That Are
1564 Shared by Both Males and Females in Drosophila. *J Neurosci* **44**, e0142242024 (2024).

1565 104. F. Port, H.-M. Chen, T. Lee, S. L. Bullock, Optimized CRISPR/Cas tools for efficient germline and somatic
1566 genome engineering in Drosophila. *PNAS* **111**, E2967–E2976 (2014).

1567 105. D. Ye, J. T. Walsh, I. P. Junker, Y. Ding, Changes in the cellular makeup of motor patterning circuits drive
1568 courtship song evolution in Drosophila. *Curr Biol* **34**, 2319-2329.e6 (2024).

1569 106. A. C. Groth, M. Fish, R. Nusse, M. P. Calos, Construction of Transgenic Drosophila by Using the Site-Specific
1570 Integrase From Phage φC31. *Genetics* **166**, 1775–1782 (2004).

1571 107. D. L. Stern, J. Crocker, Y. Ding, N. Frankel, G. Kappes, E. Kim, R. Kuzmickas, A. Lemire, J. D. Mast, S.
1572 Picard, Genetic and Transgenic Reagents for Drosophila simulans, D. mauritiana, D. yakuba, D. santomea, and D.
1573 virilis. *G3* **7**, 1339–1347 (2017).

1574 108. N. C. Klapoetke, Y. Murata, S. S. Kim, S. R. Pulver, A. Birdsey-Benson, Y. K. Cho, T. K. Morimoto, A. S.
1575 Chuong, E. J. Carpenter, Z. Tian, J. Wang, Y. Xie, Z. Yan, Y. Zhang, B. Y. Chow, B. Surek, M. Melkonian, V.
1576 Jayaraman, M. Constantine-Paton, G. K.-S. Wong, E. S. Boyden, Independent optical excitation of distinct neural
1577 populations. *Nat Methods* **11**, 338–346 (2014).

1578 109. D. J. Anderson, Circuit modules linking internal states and social behaviour in flies and mice. *Nat Rev Neurosci*
1579 **17**, 692–704 (2016).

110. D. Lachaise, M. Harry, M. Solignac, F. Lemeunier, V. Bnassi, M.-L. Cariou, Evolutionary novelties in islands: Drosophila santomea, a new melanogaster sister species from São Tomé. *Proc Royal Soc B* **267**, 1487–1495 (2000).

111. M. -L. Cariou, J. -F. Silvain, V. Daubin, J. -L. D. Lage, D. Lachaise, Divergence between Drosophila santomea and allopatric or sympatric populations of D. yakuba using paralogous amylase genes and migration scenarios along the Cameroon volcanic line. *Mol Ecol* **10**, 649–660 (2001).

112. A. Llopart, D. Lachaise, J. A. Coyne, An anomalous hybrid zone in Drosophila. *Evolution* **59**, 2602–2607 (2005).

113. J. B. S. Haldane, Sex ratio and unisexual sterility in hybrid animals. *J Genet* **12**, 101–109 (1922).

114. J. A. Coyne, S. Y. Kim, A. S. Chang, D. Lachaise, S. Elwyn, Sexual isolation between two sibling species with overlapping ranges: Drosophila santomea and Drosophila yakuba. *Evolution* **56**, 2424–2434 (2002).

115. J. A. Coyne, S. Elwyn, E. Rolán-Alvarez, Impact of experimental design on Drosophila sexual isolation studies: Direct effects and comparison to field hybridization data. *Evolution* **59**, 2588–2601 (2005).

116. J. A. Coyne, H. A. Orr, *Speciation* (Sinauer Associates, Inc., 2004).

117. C. A. Baker, J. Clemens, M. Murthy, Acoustic Pattern Recognition and Courtship Songs: Insights from Insects. *Annu Rev Neurosci* **42**, 1–19 (2019).

118. K. Connolly, R. Cook, Rejection Responses By Female Drosophila Melanogaster : Their Ontogeny, Causality and Effects Upon the Behaviour of the Courting Male. *Behaviour* **44**, 142–165 (1973).

119. K. Kimura, C. Sato, M. Koganezawa, D. Yamamoto, Drosophila Ovipositor Extension in Mating Behavior and Egg Deposition Involves Distinct Sets of Brain Interneurons. *PLOS One* **10**, e0126445 (2015).

120. C. Mezzera, M. Brotas, M. Gaspar, H. J. Pavlou, S. F. Goodwin, M. L. Vasconcelos, Ovipositor Extrusion Promotes the Transition from Courtship to Copulation and Signals Female Acceptance in Drosophila melanogaster. *Curr Biol* **30**, 3736-3748.e5 (2020).

121. F. Wang, K. Wang, N. Forknall, R. Parekh, B. J. Dickson, Circuit and Behavioral Mechanisms of Sexual Rejection by Drosophila Females. *Curr Biol* **30**, 3749-3760.e3 (2020).

122. M. Li, D. S. Chen, I. P. Junker, F. I. Szorenyi, G. H. Chen, A. J. Berger, A. A. Comeault, D. R. Matute, Y. Ding, Ancestral neural circuits potentiate the origin of a female sexual behavior in Drosophila. *Nat Commun* **15**, 9210 (2024).

123. R. A. Baines, J. P. Uhler, A. Thompson, S. T. Sweeney, M. Bate, Altered electrical properties in Drosophila neurons developing without synaptic transmission. *J Neurosci* **21**, 1523–31 (2001).

124. M. E. N. Majerus, The genetics and evolution of female choice. *Trends Ecol Evol* **1**, 1–7 (1986).

125. A. Yurkovic, O. Wang, A. C. Basu, E. A. Kravitz, Learning and memory associated with aggression in Drosophila melanogaster. *PNAS* **103**, 17519–17524 (2006).

126. Y. Jung, A. Kennedy, H. Chiu, F. Mohammad, A. Claridge-Chang, D. J. Anderson, Neurons that Function within an Integrator to Promote a Persistent Behavioral State in Drosophila. *Neuron* **105**, 322-333.e5 (2020).

127. D. E. Lancefield, A genetic study of crosses of two races or physiological species of Drosophila obscura. *Z für Indukt Abstamm- Vererbungslehre* **52**, 287–317 (1929).

128. E. Mayr, Th. Dobzhansky, Experiments on Sexual Isolation in Drosophila IV. Modification of the Degree of Isolation Between Drosophila Pseudoobscura and Drosophila Persimilis and Sexual Preferences in Drosophila Prosoltans. *PNAS* **31**, 75–82 (1945).

129. M. A. Noor, Speciation driven by natural selection in Drosophila. *Nature* **375**, 674–675 (1995).

130. L. Partridge, A. Hoffmann, J. S. Jones, Male size and mating success in Drosophila melanogaster and D. pseudoobscura under field conditions. *Anim Behav* **35**, 468–476 (1987).

131. M. A. F. Noor, J. A. Coyne, Genetics of a difference in cuticular hydrocarbons between Drosophila pseudoobscura and D. persimilis. *Genet Res* **68**, 117–123 (1996).

132. R. J. V. Roberts, S. Pop, L. L. Prieto-Godino, Evolution of central neural circuits: state of the art and perspectives. *Nat Rev Neurosci* **23**, 725–743 (2022).

133. B. R. Grant, P. R. Grant, Songs of Darwin's finches diverge when a new species enters the community. *PNAS* **107**, 20156–20163 (2010).

134. S. Enge, C. Mérot, R. Mozūraitis, V. Apšegaitė, L. Bernatchez, G. A. Martens, S. Radžiutė, H. Pavia, E. L. Berdan, A supergene in seaweed flies modulates male traits and female perception. *Proc Royal Soc B* **290**, 20231494 (2023).

135. C. Zhou, Y. Pan, C. C. Robinett, G. W. Meissner, B. S. Baker, Central Brain Neurons Expressing doublesex Regulate Female Receptivity in Drosophila. *Neuron* **83**, 149–163 (2014).

136. J.-M. Jallon, A few chemical words exchanged by Drosophila during courtship and mating. *Behav Genet* **14**, 441–478 (1984).

137. T. Chertemps, L. Duportets, C. Labeur, C. Wicker-Thomas, A new elongase selectively expressed in Drosophila male reproductive system. *Biochem Biophys Res Commun* **333**, 1066–1072 (2005).

138. J. M. Gómez, A. Gónzalez-Megías, M. Verdú, The evolution of same-sex sexual behaviour in mammals. *Nat Commun* **14**, 5719 (2023).

139. T. Karigo, A. Kennedy, B. Yang, M. Liu, D. Tai, I. A. Wahle, D. J. Anderson, Distinct hypothalamic control of same- and opposite-sex mounting behaviour in mice. *Nature* **589**, 258–263 (2021).

140. F. A. Issa, D. H. Edwards, Ritualized Submission and the Reduction of Aggression in an Invertebrate. *Curr Biol* **16**, 2217–2221 (2006).

141. S. M. Lane, A. E. Haughan, D. Evans, T. Tregenza, C. M. House, Same-sex sexual behaviour as a dominance display. *Anim Behav* **114**, 113–118 (2016).

142. J. M. Smith, G. R. Price, The Logic of Animal Conflict. *Nature* **246**, 15–18 (1973).

143. T. Gregg, M. Hahn, Drosophila 25 species phylogeny, *figshare* (2017). https://doi.org/10.6084/m9.figshare.5450602.v1.

144. D. E. Miller, C. Staber, J. Zeitlinger, R. S. Hawley, Highly Contiguous Genome Assemblies of 15 Drosophila Species Generated Using Nanopore Sequencing. *G3* **8**, 3131–3141 (2018).

145. A. Depetris-Chauvin, D. Galagovsky, I. W. Keesey, B. S. Hansson, S. Sachse, M. Knaden, Evolution at multiple processing levels underlies odor-guided behavior in the genus Drosophila. *Curr Biol* **33**, 4771-4785.e7 (2023).

146. D. Runfola, A. Anderson, H. Baier, M. Crittenden, E. Dowker, S. Fuhrig, S. Goodman, G. Grimsley, R. Layko, G. Melville, M. Mulder, R. Oberman, J. Panganiban, A. Peck, L. Seitz, S. Shea, H. Slevin, R. Youngerman, L. Hobbs, geoBoundaries: A global database of political administrative boundaries. *PLOS One* **15**, e0231866 (2020).

147. S. P. Nilsen, Y.-B. Chan, R. Huber, E. A. Kravitz, Gender-selective patterns of aggressive behavior in Drosophila melanogaster. *PNAS* **101**, 12342–12347 (2004).

148. D. L. Stern, E. Kim, E. L. Behrman, The Janelia Atalanta plasmids provide a simple and efficient CRISPR/Cas9-mediated homology directed repair platform for Drosophila. *bioRxiv*, 2023.06.17.545412 (2024).

149. B. D. Pfeiffer, A. Jenett, A. S. Hammonds, T.-T. B. Ngo, S. Misra, C. Murphy, A. Scully, J. W. Carlson, K. H. Wan, T. R. Laverty, C. Mungall, R. Svirskas, J. T. Kadonaga, C. Q. Doe, M. B. Eisen, S. E. Celniker, G. M. Rubin, Tools for neuroanatomy and neurogenetics in Drosophila. *PNAS* **105**, 9715–9720 (2008).

150. B. D. Pfeiffer, T.-T. B. Ngo, K. L. Hibbard, C. Murphy, A. Jenett, J. W. Truman, G. M. Rubin, Refinement of Tools for Targeted Gene Expression in Drosophila. *Genetics* **186**, 735–755 (2010).

151. H. K. Inagaki, Y. Jung, E. D. Hoopfer, A. M. Wong, N. Mishra, J. Y. Lin, R. Y. Tsien, D. J. Anderson, Optogenetic control of Drosophila using a red-shifted channelrhodopsin reveals experience-dependent influences on courtship. *Nat Methods* **11**, 325–332 (2014).

1668 152. J. Y. Yew, K. Dreisewerd, H. Luftmann, J. Müthing, G. Pohlentz, E. A. Kravitz, A New Male Sex Pheromone
1669 and Novel Cuticular Cues for Chemical Communication in Drosophila. *Curr Biol* **19**, 1245–1254 (2009).

1670 153. L. M. Dembeck, K. Böröczky, W. Huang, C. Schal, R. R. H. Anholt, T. F. C. Mackay, Genetic architecture of
1671 natural variation in cuticular hydrocarbon composition in Drosophila melanogaster. *eLife* **4**, e09861 (2015).

1672

**Table S1. Key reagents and resources**

| Reagent | Source | Identifier | RRID or CAS |
|---|---|---|---|
| *D. san BDPG4U-Gal4@2253* (mw) | This study | | |
| *D. san 20E08-Gal4@2253* (mw) | This study | | |
| *D. san Or67d-Gal4* (ie1-mCherry) | This study | | |
| *D. san 71G01-Gal4DBD@2251* (mw) | This study | | |
| *D. san dsx-p65AD* (MHC-DsRed) | This study | | |
| *D. san UAS-nlsTdT@2253* (mw) | 10.1101/2025.05.06.652433 | | |
| *D. san UAS-GCaMP7s-2A-tdT@2283* (mw) (introgressed 10 generations from *D. yak*) | Hiroshi Shiozaki, David Stern | | |
| *D. san UAS-CsChrimson-tdT@2252* (mw) | Yun Ding, David Stern | | |
| *D. san UAS-CsChrimson-tdT@2253* (mw) | Yun Ding, David Stern | | |
| *D. san UAS-EGFP-Kir2.1@2174* (mw) | 10.1016/j.cub.2019.02.019 | | |
| pBPGUw | Addgene | 17575 | Addgene_17575 |
| pBPZpGAL4DBDUw | Addgene | 26233 | Addgene_26233 |
| pBPp65ADZpUw | Addgene | 26234 | Addgene_26234 |
| pJAT32 | Addgene | 204297 | Addgene_204297 |
| Gateway LR Clonase II Enzyme mix | Thermo Fisher Scientific | 11791020 | |
| NucleoBond Xtra Maxi EF | Takara Bio | 740424 | |
| Cas9 with dual NLS | PNA Bio | CP01 | |
| anti-DsRed (rabbit) | Takara Bio | 632496 | AB_10013483 |
| anti-Bruchpilot (mouse) | Developmental Studies Hybridoma Bank | nc82 | AB_2314866 |
| Goat anti-rabbit IgG (H+L) Alexa Fluor 568 | Thermo Fisher Scientific | A-11011 | AB_143157 |
| Goat anti-mouse IgG (H+L) Alexa Fluor 633 | Thermo Fisher Scientific | A-21050 | AB_2535718 |
| Normal Goat Serum | Jackson ImmunoResearch Labs | 005-000-121 | AB_2336990 |
| Triton X-100 | Millipore Sigma | X100 | 9036-19-5 |

| | | | |
|---|---|---|---|
| Paraformaldehyde, 16% solution, EM grade | Electron Microscopy Sciences | 15710 | 30525-89-4 |
| VectaShield Antifade Mounting Medium | Vector Laboratories | H-1000 | AB_2336789 |
| all *trans* -Retinal | Millipore Sigma | R2500 | 116-31-4 |
| Hydrocarbon Soluble Siliconizing Fluid | Thermo Fisher Scientific | TS-42800 | 474-02-4 |
| Fluon (PTFE-30) | Tar Heel Ants | | 9002-84-0 |
| (Z)-7-Tricosene (7-T) | Pherobank B.V. | 12457 | 52078-57-6 |
| (Z)-11-octadecenyl acetate (cVA) | Pherobank B.V. | 10421 | 6186-98-7 |
| Octadecane (C18) | Millipore Sigma | O652 | 593-45-3 |
| Hexane | Millipore Sigma | 139386 | 110-54-3 |
| Acetone | Millipore Sigma | 179124 | 67-64-1 |
| Tropicana apple juice | Amazon | B007SNJDXM | |
| Virgin noni juice | Amazon | B082S4Q6C7 | |
| Caramelized fig syrup | Amazon | B0DHY7K9RP | |
| Marula (*Sclerocarya birrea* ) | Waimea Botanical Garden (O'ahu, HI) | | |
| Pandanus (*Pandanus furcatus* ) | Huntington Botanical Gardens (San Marino, CA) | | |
| *D. san* genome assembly (Prin_Dsan_1.1) | NCBI RefSeq | GCF_016746245.2 | |
| Geneious Prime | Biomatters | | SCR_010519 |
| Caltech FlyTracker | 10.1007/978-3-319-10605-2_50 | | SCR_027431 |
| JAABA | 10.1038/nmeth.2281 | | SCR_027430 |
| Tempo | 10.1016/j.cub.2019.02.019 | | SCR_027432 |
| Fiji | GitHub | | SCR_002285 |
| MATLAB | MathWorks | | SCR_001622 |
| Jupyter Notebook | GitHub | | SCR_018315 |
| R | R Project for Statistical Computing | | SCR_001905 |
| RStudio | Posit PBC | | SCR_000432 |
| Illustrator 2025 | Adobe | | SCR_010279 |

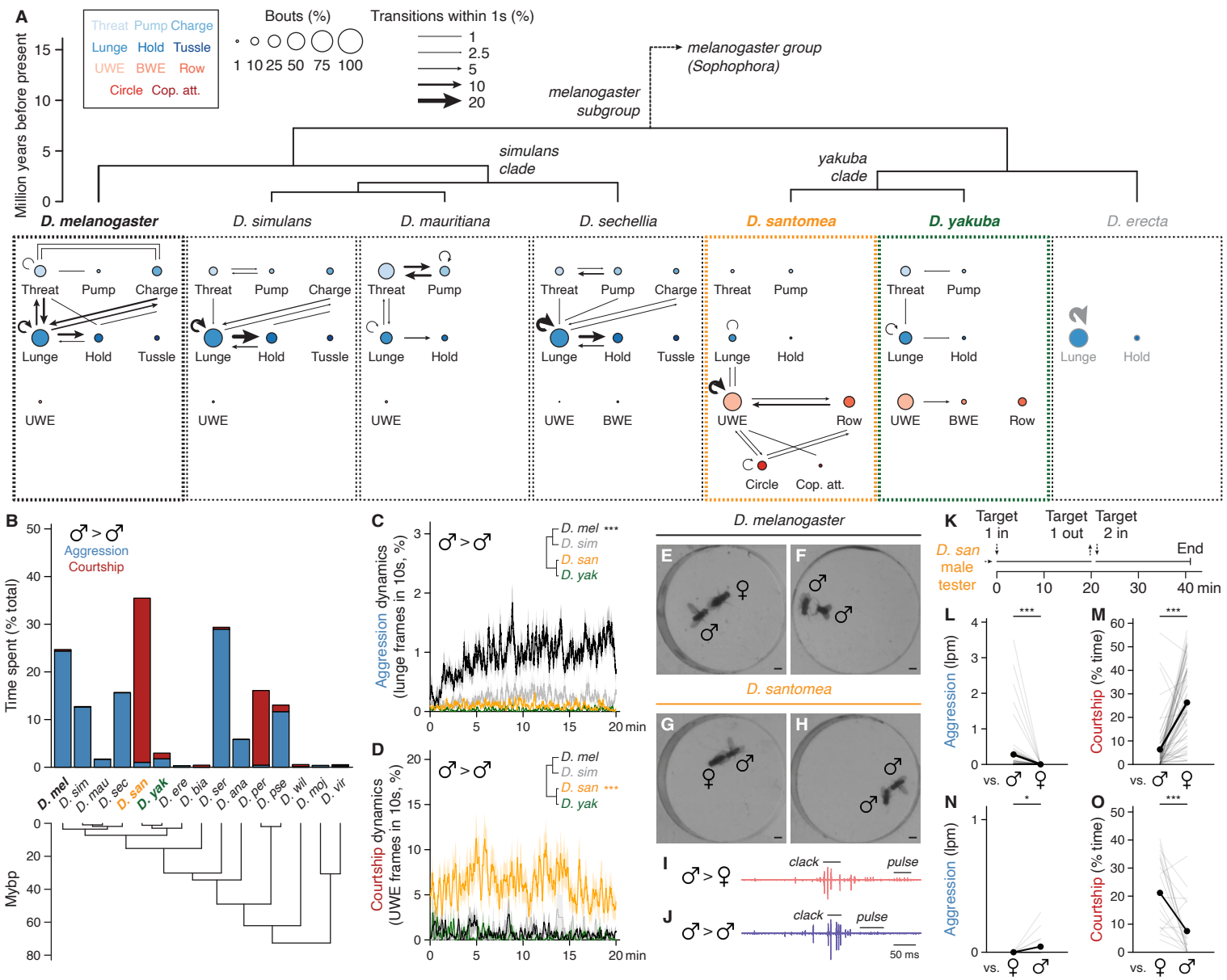
A
Threat Pump Charge
Lunge Hold Tussle
UWE BWE Row
Circle Cop. att.
Bouts (%)
1 10 25 50 75 100
Transitions within 1s (%)
1
2.5
5
10
20
Million years before present
melanogaster group (Sophophora)
melanogaster subgroup
simulans clade
yakuba clade
D. melanogaster
D. simulans
D. mauritiana
D. sechellia
D. santomea
D. yakuba
D. erecta
B
♂ > ♂
Aggression
Courtship
Time spent (% total)
D. mel
D. sim
D. mau
D. sec
D. san
D. yak
D. ere
D. bia
D. ser
D. ana
D. per
D. pse
D. wil
D. moj
D. vir
Mybp
C
Aggression dynamics (lunge frames in 10s, %)
D. mel ***
D. sim
D. san
D. yak
D
Courtship dynamics (UWE frames in 10s, %)
D. melanogaster
D. santomea
E
F
G
H
I
J
clack
pulse
50 ms
K
Target 1 in
Target 1 out
Target 2 in
D. san male tester
End
0 10 20 30 40 min
L
M
N
O
Aggression (lpm)
Courtship (% time)
vs. ♂ ♀
vs. ♀ ♂

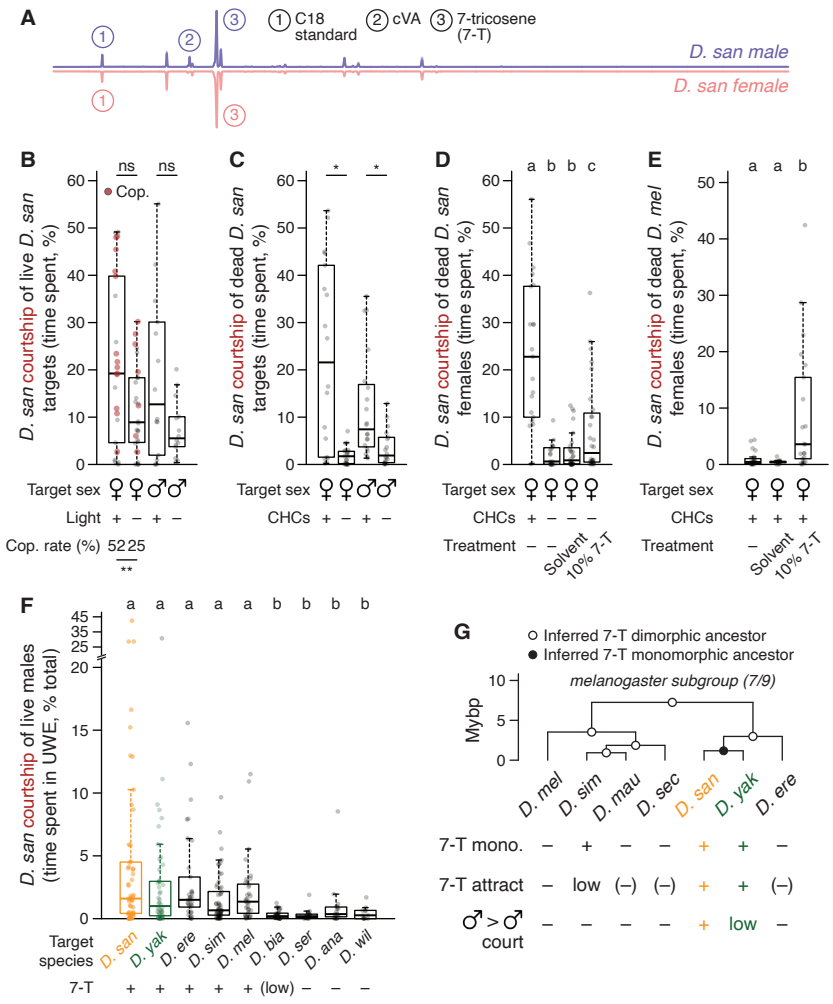
A
1 C18 standard
2 cVA
3 7-tricosene (7-T)
D. san male
D. san female
B
D. san courtship of live D. san targets (time spent, %)
Cop.
ns
Target sex
Light
Cop. rate (%) 52 25
**
C
D. san courtship of dead D. san targets (time spent, %)
CHCs
D
D. san courtship of dead D. san females (time spent, %)
Treatment
Solvent
10% 7-T
E
D. san courtship of dead D. mel females (time spent, %)
F
D. san courtship of live males (time spent in UWE, % total)
Target species
D. san
D. yak
D. ere
D. sim
D. mel
D. bia
D. ser
D. ana
D. wil
7-T
(low)
G
Inferred 7-T dimorphic ancestor
Inferred 7-T monomorphic ancestor
melanogaster subgroup (7/9)
Mybp
D. mel
D. sim
D. mau
D. sec
D. san
D. yak
D. ere
7-T mono.
7-T attract
♂>♂ court
low

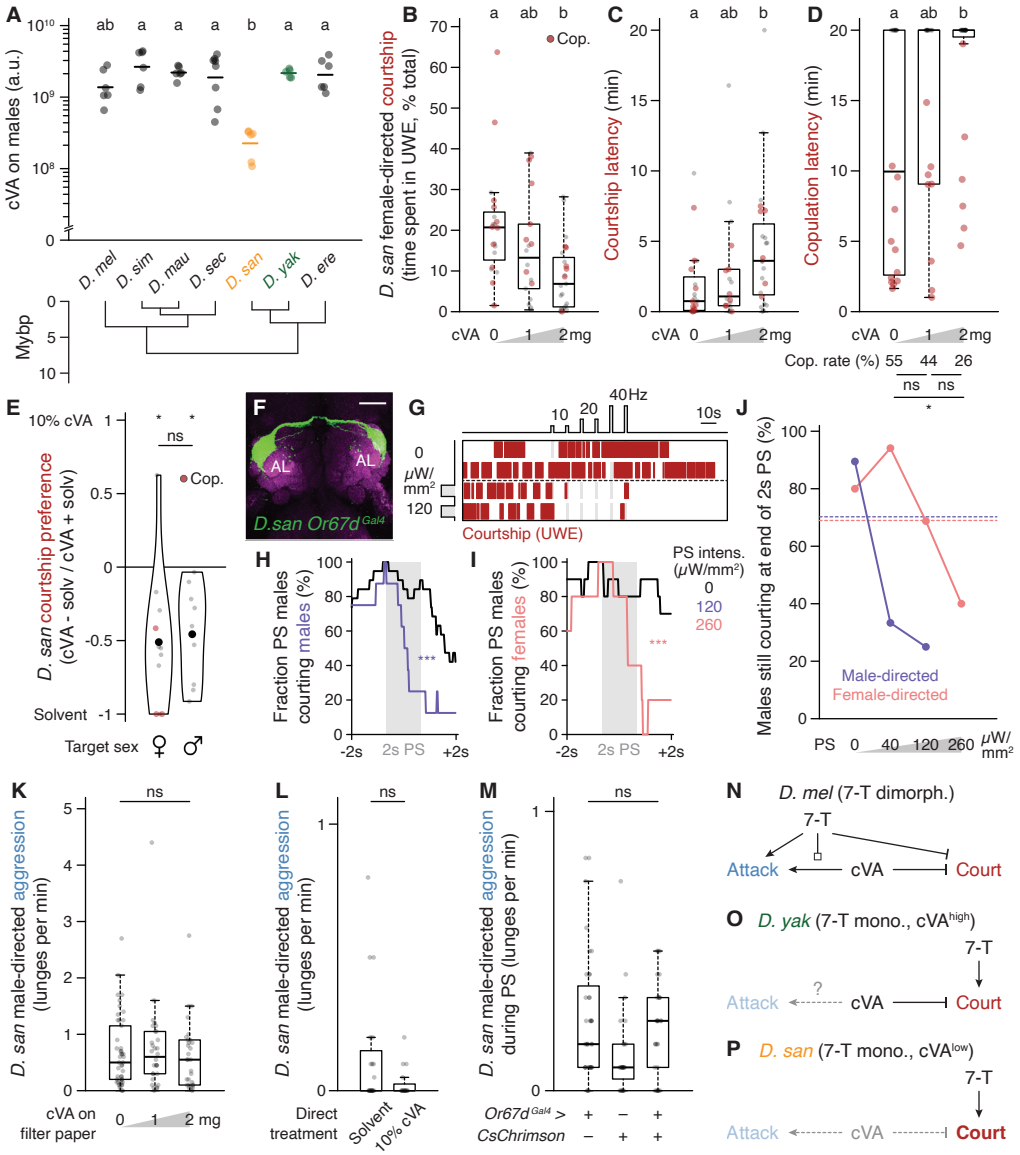
A
cVA on males (a.u.)
D. mel
D. sim
D. mau
D. sec
D. san
D. yak
D. ere
Mybp
B
D. san female-directed courtship (time spent in UWE, % total)
Cop.
cVA 0 1 2mg
C
Courtship latency (min)
D
Copulation latency (min)
Cop. rate (%) 55 44 26
ns ns
E
10% cVA
Solvent
D. san courtship preference (cVA - solv / cVA + solv)
Target sex ♀ ♂
F
AL
D.san Or67d Gal4
G
40Hz
10s
μW/mm²
Courtship (UWE)
H
Fraction PS males courting males (%)
-2s 2s PS +2s
I
Fraction PS males courting females (%)
PS intens. (μW/mm²)
0
120
260
J
Males still courting at end of 2s PS (%)
Male-directed
Female-directed
PS 0 40 120 260 μW/mm²
K
D. san male-directed aggression (lunges per min)
cVA on filter paper 0 1 2 mg
L
Direct treatment Solvent 10% cVA
M
D. san male-directed aggression during PS (lunges per min)
Or67d Gal4 >
CsChrimson
N
D. mel (7-T dimorph.)
7-T
Attack
cVA
Court
O
D. yak (7-T mono., cVA high)
P
D. san (7-T mono., cVA low)

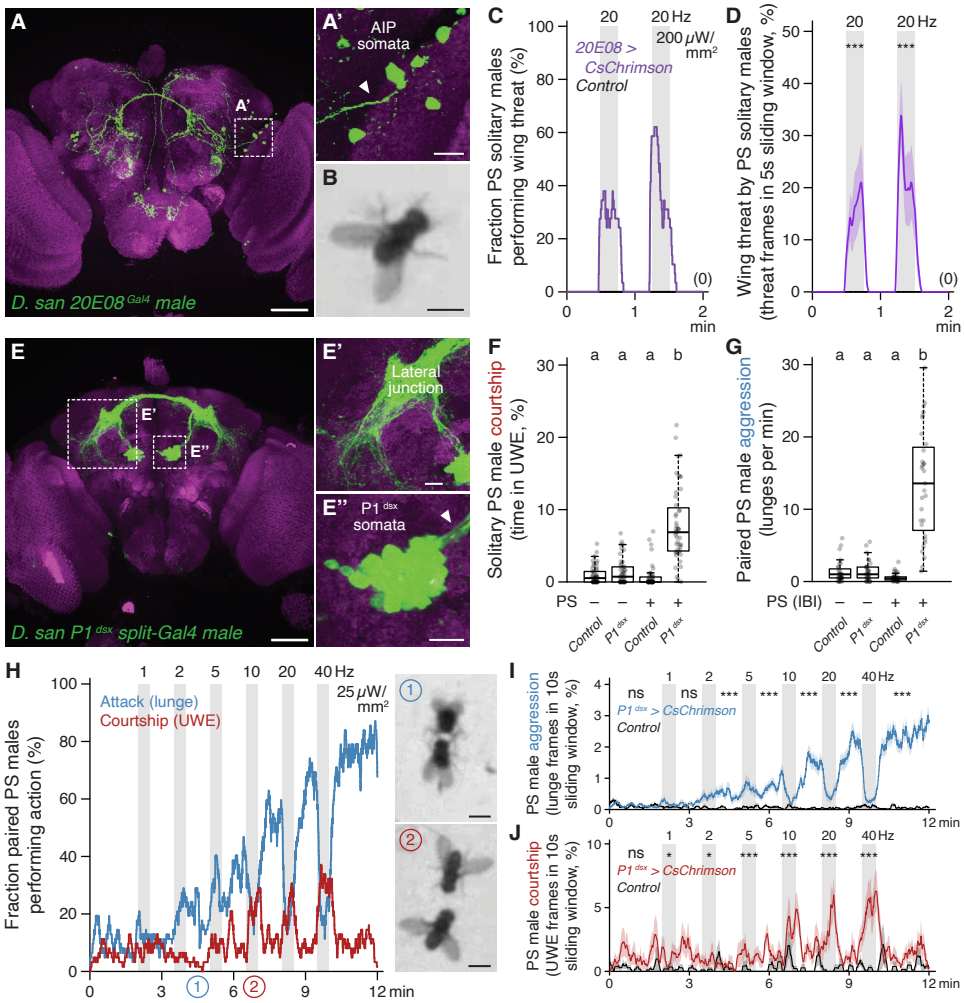
A
A'
AIP somata
B
D. san 20E08 Gal4 male
C
20
20 Hz
200 μW/mm²
20E08 > CsChrimson
Control
Fraction PS solitary males performing wing threat (%)
(0)
min
D
Wing threat by PS solitary males (threat frames in 5s sliding window, %)
E
E'
E''
Lateral junction
P1 dsx somata
D. san P1 dsx split-Gal4 male
F
Solitary PS male courtship (time in UWE, %)
a a a b
PS
Control
P1 dsx
G
Paired PS male aggression (lunges per min)
PS (IBI)
H
1 2 5 10 20 40 Hz
25 μW/mm²
Attack (lunge)
Courtship (UWE)
Fraction paired PS males performing action (%)
12 min
I
PS male aggression (lunge frames in 10s sliding window, %)
ns
***
P1 dsx > CsChrimson
Control
J
PS male courtship (UWE frames in 10s sliding window, %)

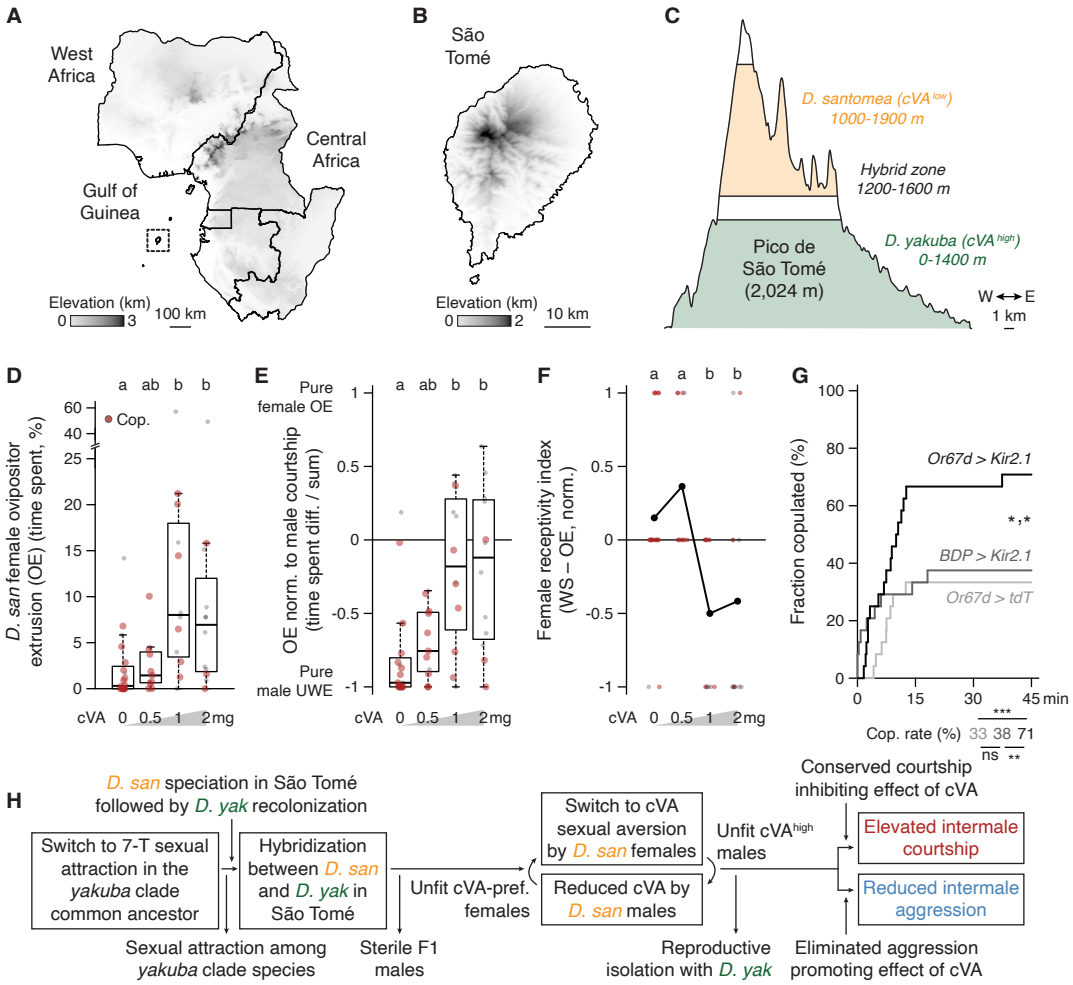
A
West Africa
Central Africa
Gulf of Guinea
Elevation (km)
0 3
100 km
B
São Tomé
Elevation (km)
0 2
10 km
C
D. santomea (cVA low)
1000-1900 m
Hybrid zone
1200-1600 m
D. yakuba (cVA high)
0-1400 m
Pico de São Tomé (2,024 m)
W E
1 km
D
D. san female ovipositor extrusion (OE) (time spent, %)
Cop.
a ab b b
cVA 0 0.5 1 2 mg
E
Pure female OE
Pure male UWE
OE norm. to male courtship (time spent diff. / sum)
a ab b b
cVA 0 0.5 1 2 mg
F
Female receptivity index (WS – OE, norm.)
a a b b
cVA 0 0.5 1 2 mg
G
Fraction copulated (%)
Or67d > Kir2.1
BDP > Kir2.1
Or67d > tdT
*,*
0 15 30 45 min
***
Cop. rate (%) 33 38 71
ns **
H
D. san speciation in São Tomé followed by D. yak recolonization
Switch to 7-T sexual attraction in the yakuba clade common ancestor
Hybridization between D. san and D. yak in São Tomé
Sexual attraction among yakuba clade species
Sterile F1 males
Unfit cVA-pref. females
Switch to cVA sexual aversion by D. san females
Reduced cVA by D. san males
Unfit cVA high males
Reproductive isolation with D. yak
Conserved courtship inhibiting effect of cVA
Elevated intermale courtship
Reduced intermale aggression
Eliminated aggression promoting effect of cVA

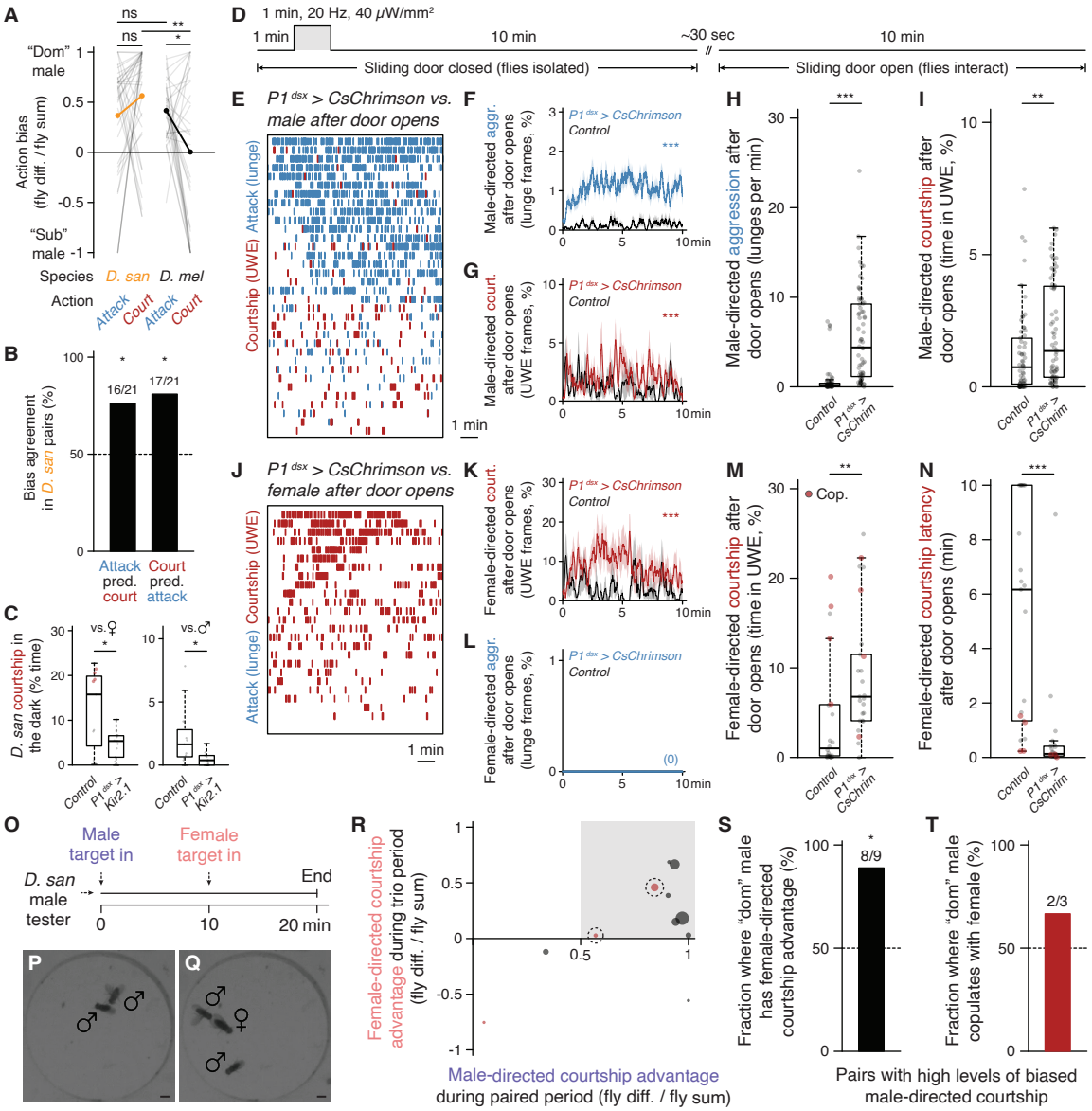
A
ns
ns
**
*
"Dom" male
"Sub" male
Action bias (fly diff. / fly sum)
Species D. san D. mel
Action Attack Court Attack Court
B
16/21
17/21
Bias agreement in D. san pairs (%)
Attack pred. court
Court pred. attack
C
vs.♀
vs.♂
D. san courtship in the dark (% time)
Control
P1dsx > Kir2.1
D
1 min, 20 Hz, 40 μW/mm²
1 min
10 min
~30 sec
10 min
Sliding door closed (flies isolated)
Sliding door open (flies interact)
E
P1dsx > CsChrimson vs. male after door opens
Courtship (UWE) Attack (lunge)
1 min
F
Male-directed aggr. after door opens (lunge frames, %)
P1dsx > CsChrimson
Control
G
Male-directed court. after door opens (UWE frames, %)
H
Male-directed aggression after door opens (lunges per min)
I
Male-directed courtship after door opens (time in UWE, %)
J
P1dsx > CsChrimson vs. female after door opens
Courtship (UWE) Attack (lunge)
K
Female-directed court. after door opens (UWE frames, %)
L
Female-directed aggr. after door opens (lunge frames, %)
(0)
M
Cop.
Female-directed courtship after door opens (time in UWE, %)
N
Female-directed courtship latency after door opens (min)
O
Male target in
Female target in
D. san male tester
End
0
10
20 min
P
Q
R
Female-directed courtship advantage during trio period (fly diff. / fly sum)
Male-directed courtship advantage during paired period (fly diff. / fly sum)
S
Fraction where "dom" male has female-directed courtship advantage (%)
8/9
T
Fraction where "dom" male copulates with female (%)
2/3
Pairs with high levels of biased male-directed courtship

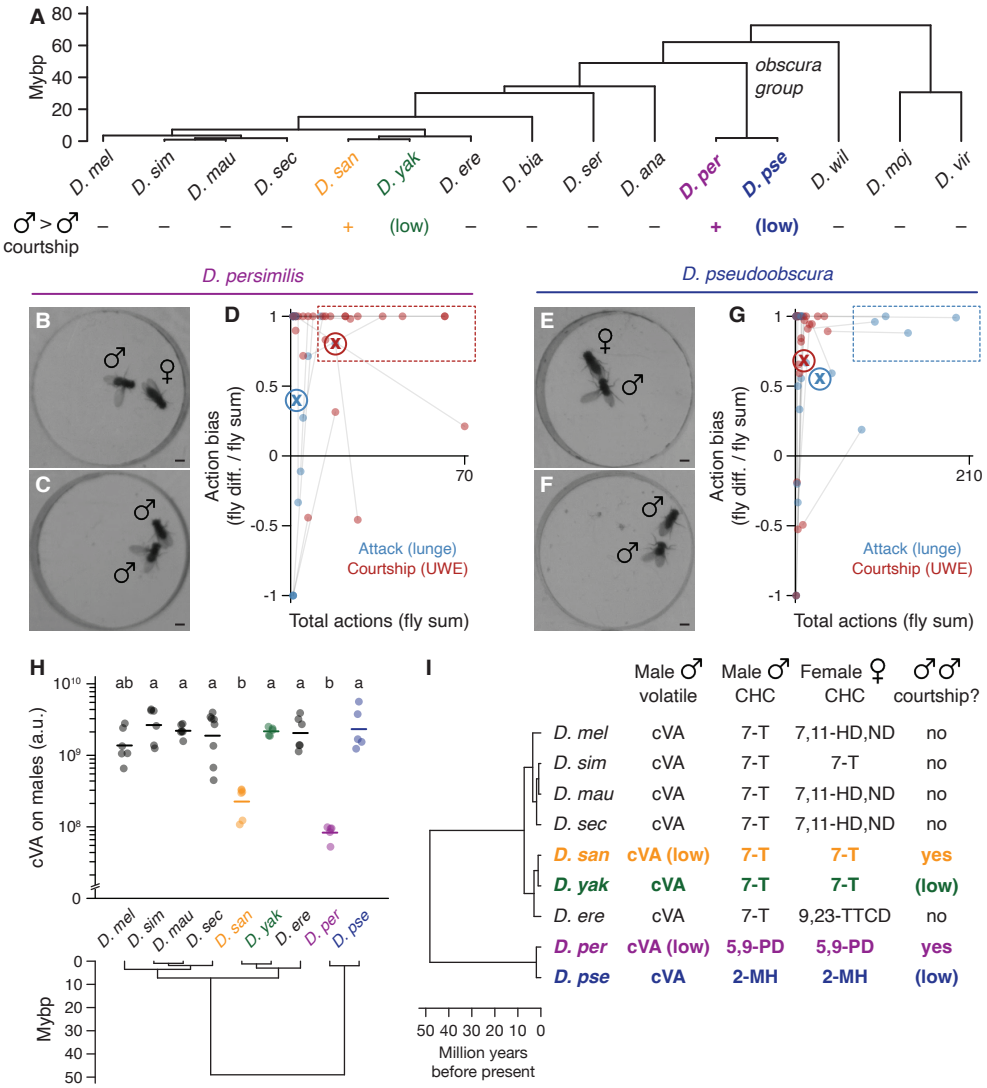
A
Mybp
80
60
40
20
0
obscura group
D. mel
D. sim
D. mau
D. sec
D. san
D. yak
D. ere
D. bia
D. ser
D. ana
D. per
D. pse
D. wil
D. moj
D. vir
♂ > ♂ courtship
– – – – + (low) – – – – + (low) – – –
D. persimilis
D. pseudoobscura
B
C
D
E
F
G
Action bias (fly diff. / fly sum)
Total actions (fly sum)
Attack (lunge)
Courtship (UWE)
70
210
H
cVA on males (a.u.)
ab a a a b a a b a
D. mel
D. sim
D. mau
D. sec
D. san
D. yak
D. ere
D. per
D. pse
Mybp
I
Male ♂ volatile
Male ♂ CHC
Female ♀ CHC
♂♂ courtship?
D. mel cVA 7-T 7,11-HD,ND no
D. sim cVA 7-T 7-T no
D. mau cVA 7-T 7,11-HD,ND no
D. sec cVA 7-T 7,11-HD,ND no
D. san cVA (low) 7-T 7-T yes
D. yak cVA 7-T 7-T (low)
D. ere cVA 7-T 9,23-TTCD no
D. per cVA (low) 5,9-PD 5,9-PD yes
D. pse cVA 2-MH 2-MH (low)
50 40 30 20 10 0
Million years before present

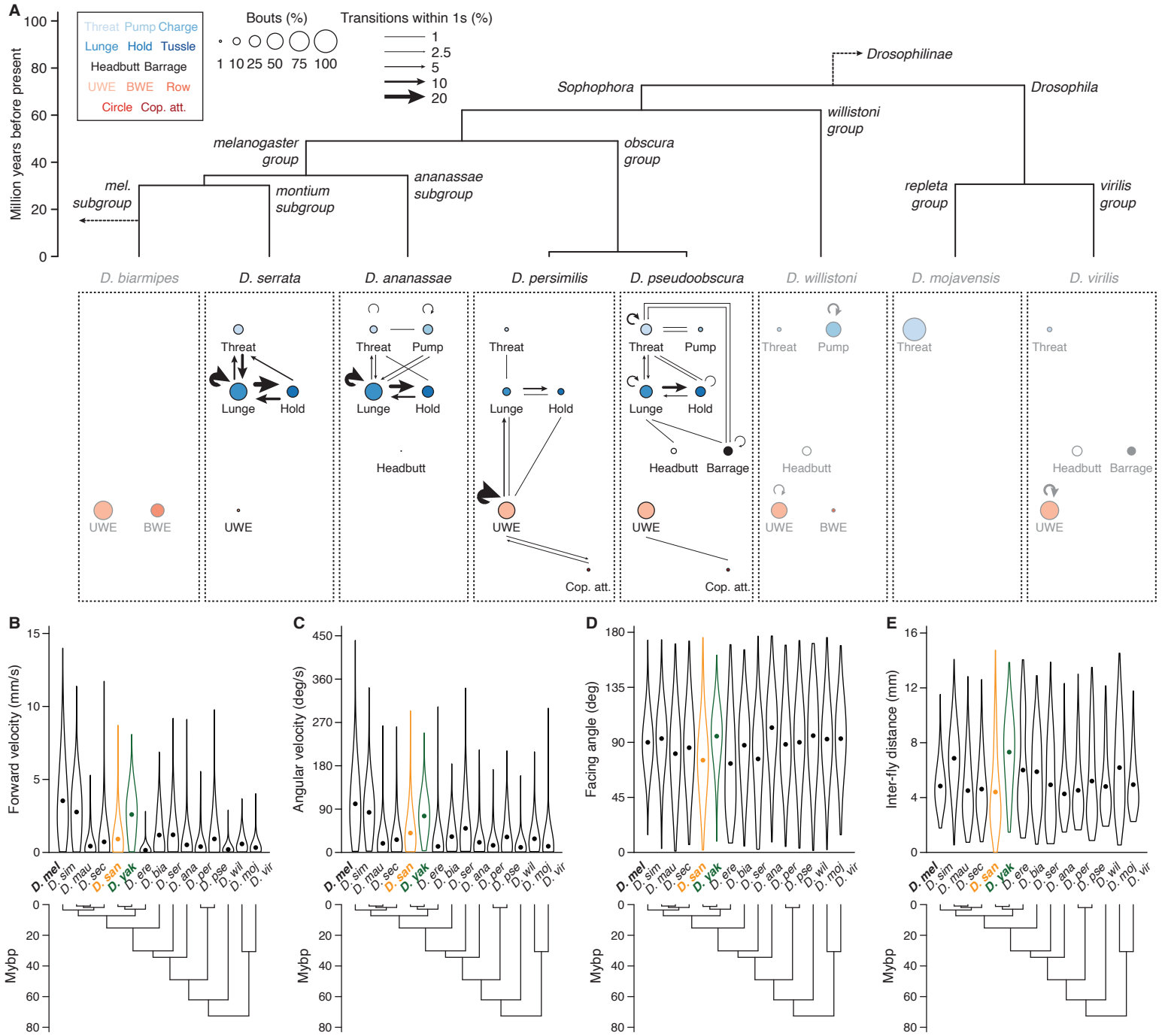
A
Million years before present
Threat Pump Charge
Lunge Hold Tussle
Headbutt Barrage
UWE BWE Row
Circle Cop. att.
Bouts (%)
1 10 25 50 75 100
Transitions within 1s (%)
1
2.5
5
10
20
Drosophilinae
Sophophora
Drosophila
willistoni group
melanogaster group
obscura group
mel. subgroup
montium subgroup
ananassae subgroup
repleta group
virilis group
D. biarmipes
D. serrata
D. ananassae
D. persimilis
D. pseudoobscura
D. willistoni
D. mojavensis
D. virilis
Threat
Pump
Lunge
Hold
Headbutt
Barrage
UWE
BWE
Cop. att.
B
Forward velocity (mm/s)
C
Angular velocity (deg/s)
D
Facing angle (deg)
E
Inter-fly distance (mm)
D. mel
D. sim
D. mau
D. sec
D. san
D. yak
D. ere
D. bia
D. ser
D. ana
D. per
D. pse
D. wil
D. moj
D. vir
Mybp

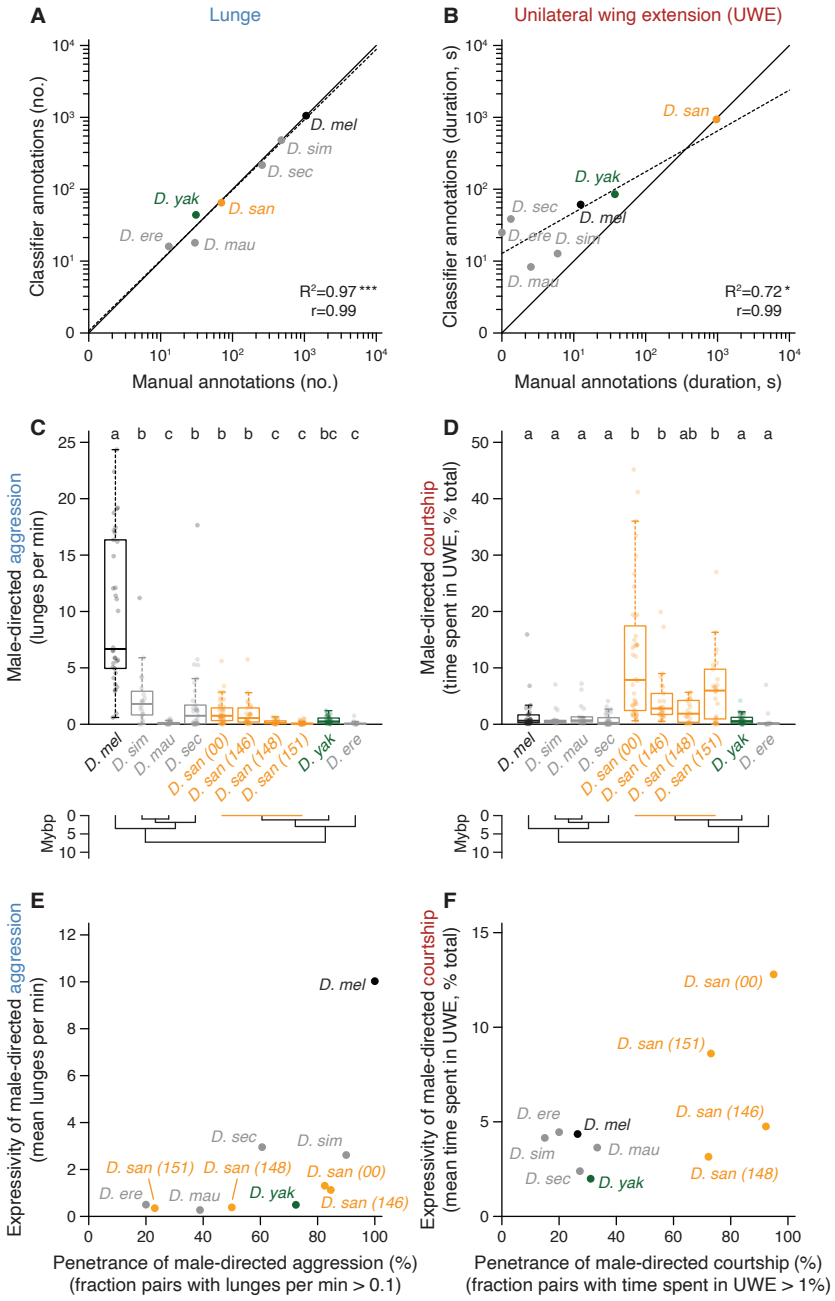
A
Lunge
Classifier annotations (no.)
Manual annotations (no.)
D. mel
D. sim
D. sec
D. yak
D. san
D. ere
D. mau
R²=0.97 ***
r=0.99
B
Unilateral wing extension (UWE)
Classifier annotations (duration, s)
Manual annotations (duration, s)
D. san
D. yak
D. sec
D. mel
D. ere
D. sim
D. mau
R²=0.72 *
r=0.99
C
Male-directed aggression (lunges per min)
a b c b b b c c bc c
D. mel
D. sim
D. mau
D. sec
D. san (00)
D. san (146)
D. san (148)
D. san (151)
D. yak
D. ere
Mybp
D
Male-directed courtship (time spent in UWE, % total)
a a a a b b ab b a a
E
Expressivity of male-directed aggression (mean lunges per min)
Penetrance of male-directed aggression (%) (fraction pairs with lunges per min > 0.1)
F
Expressivity of male-directed courtship (mean time spent in UWE, % total)
Penetrance of male-directed courtship (%) (fraction pairs with time spent in UWE > 1%)

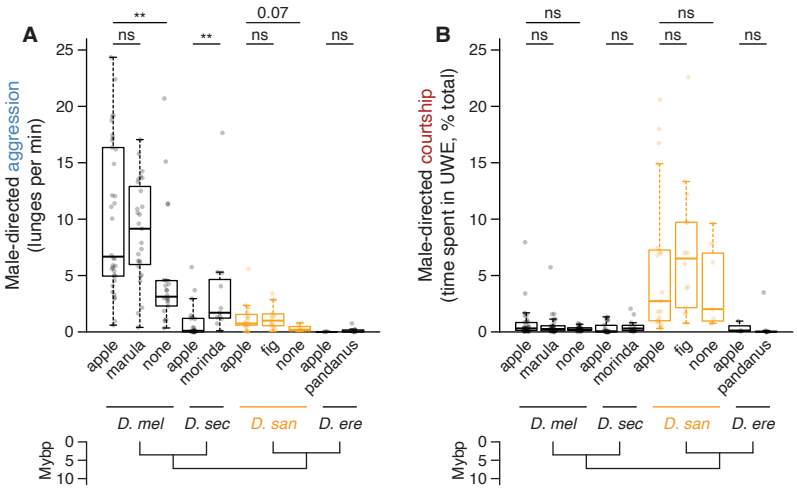
A
B
Male-directed aggression
(lunges per min)
Male-directed courtship
(time spent in UWE, % total)
**
ns
0.07
apple
marula
none
morinda
fig
pandanus
D. mel
D. sec
D. san
D. ere
Mybp

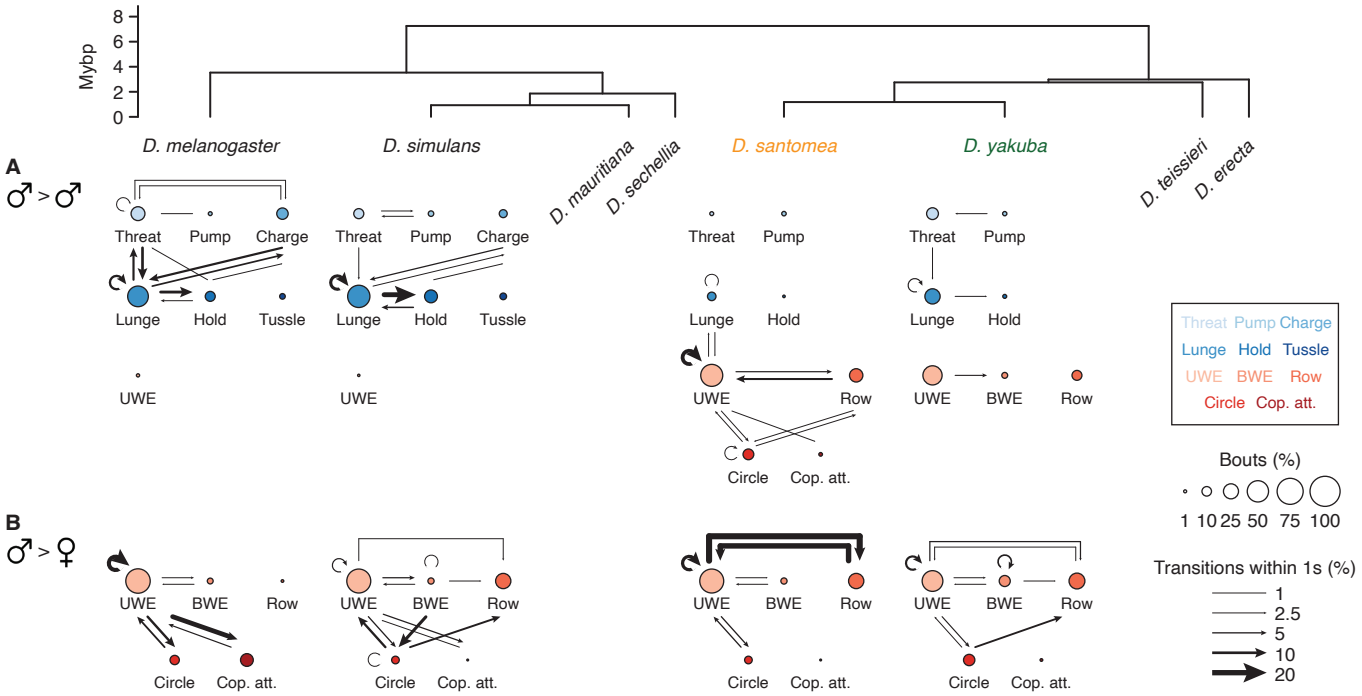
Mybp
8
6
4
2
0
D. melanogaster
D. simulans
D. mauritiana
D. sechellia
D. santomea
D. yakuba
D. teissieri
D. erecta
A
♂ > ♂
Threat
Pump
Charge
Lunge
Hold
Tussle
UWE
BWE
Row
Circle
Cop. att.
Threat Pump Charge
Lunge Hold Tussle
UWE BWE Row
Circle Cop. att.
Bouts (%)
1 10 25 50 75 100
B
♂ > ♀
Transitions within 1s (%)
1
2.5
5
10
20

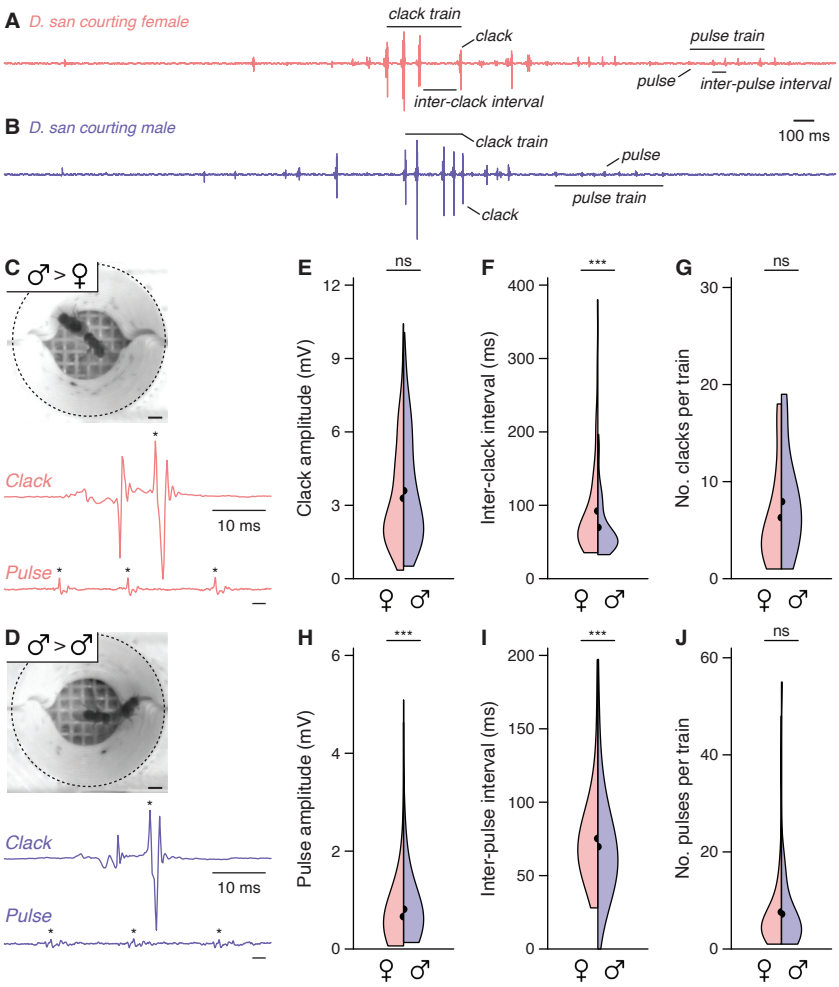
A D. san courting female
clack train
clack
pulse train
pulse
inter-pulse interval
inter-clack interval
B D. san courting male
clack train
pulse
pulse train
clack
100 ms
C ♂ > ♀
Clack
Pulse
10 ms
D ♂ > ♂
Clack
Pulse
10 ms
E
ns
Clack amplitude (mV)
F
***
Inter-clack interval (ms)
G
ns
No. clacks per train
H
***
Pulse amplitude (mV)
I
***
Inter-pulse interval (ms)
J
ns
No. pulses per train
♀ ♂

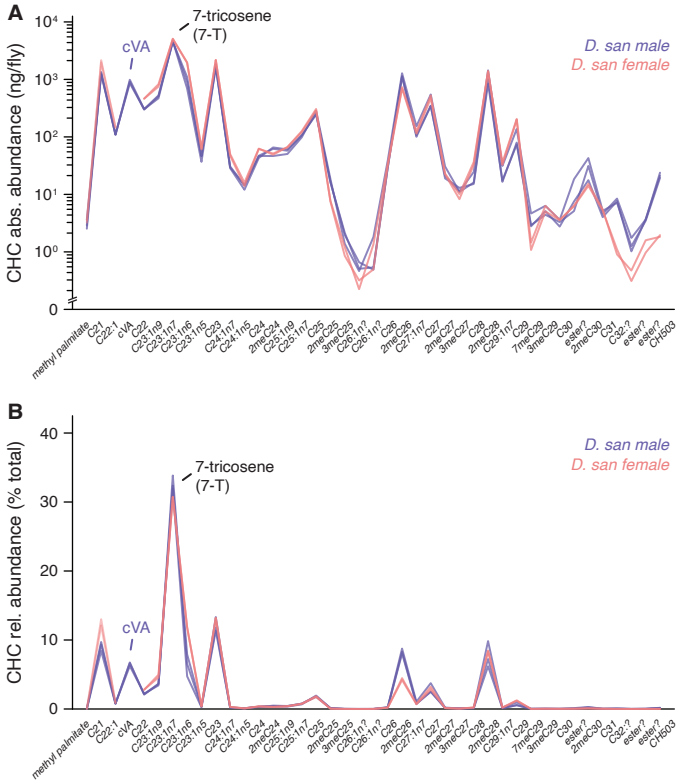
A
CHC abs. abundance (ng/fly)
7-tricosene
(7-T)
cVA
D. san male
D. san female
B
CHC rel. abundance (% total)
7-tricosene
(7-T)
cVA
D. san male
D. san female

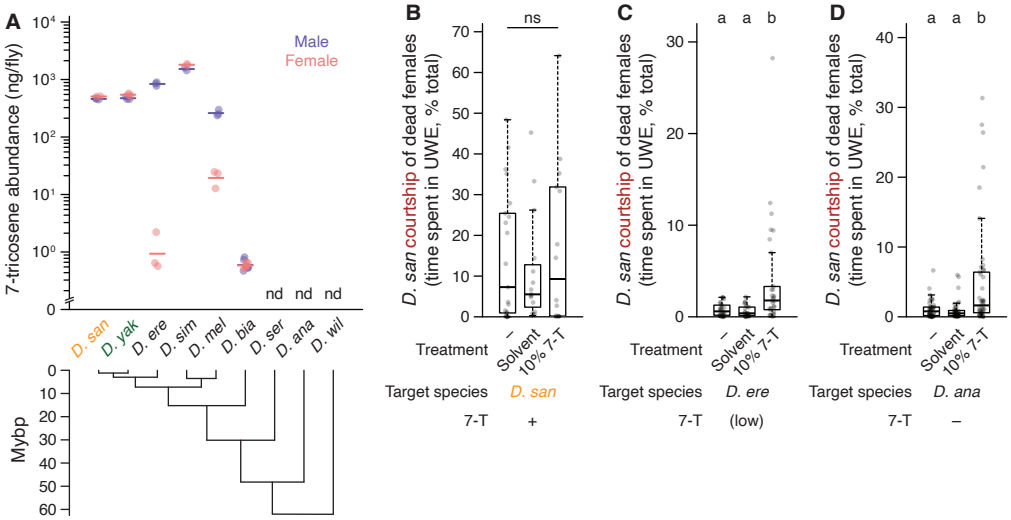
A
7-tricosene abundance (ng/fly)
Male
Female
nd nd nd
D. san
D. yak
D. ere
D. sim
D. mel
D. bia
D. ser
D. ana
D. wil
Mybp
B
D. san courtship of dead females (time spent in UWE, % total)
ns
Treatment
–
Solvent
10% 7-T
Target species
D. san
7-T
+
C
a a b
Target species
D. ere
7-T
(low)
D
a a b
Target species
D. ana
7-T
–

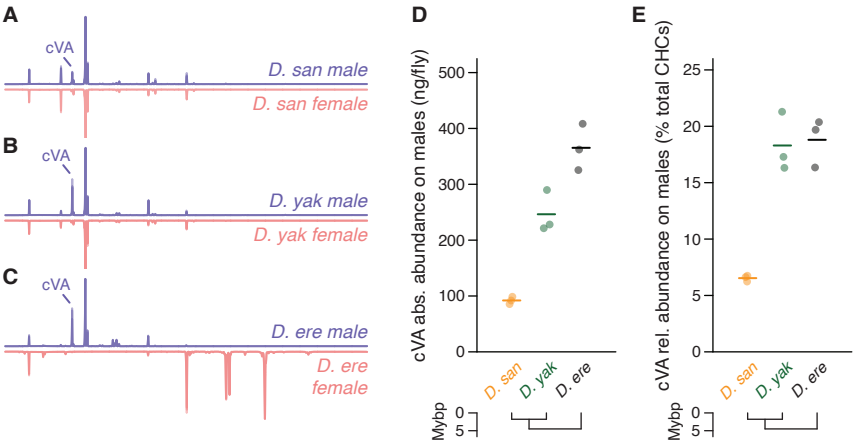
A
cVA
D. san male
D. san female
B
cVA
D. yak male
D. yak female
C
cVA
D. ere male
D. ere female
D
cVA abs. abundance on males (ng/fly)
500
400
300
200
100
0
D. san
D. yak
D. ere
Mybp
0
5
E
cVA rel. abundance on males (% total CHCs)
25
20
15
10
5
0
D. san
D. yak
D. ere
Mybp
0
5

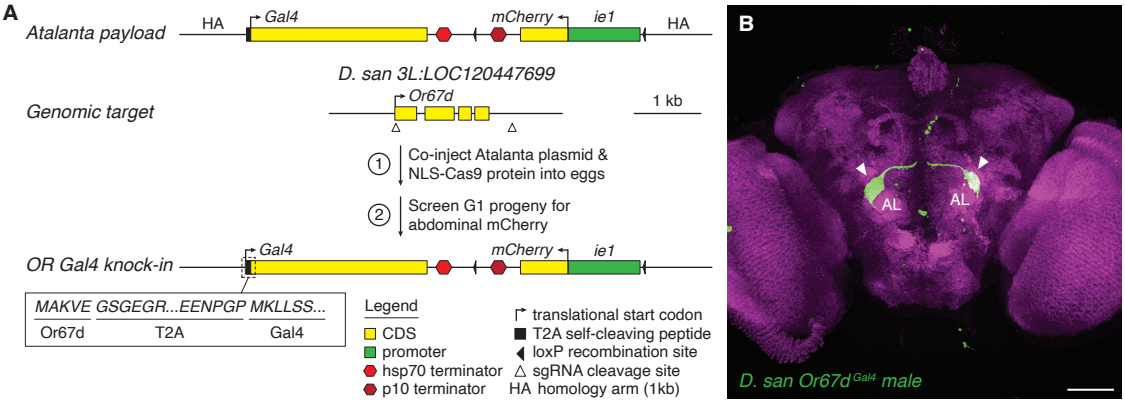
A
Atalanta payload
HA
Gal4
mCherry
ie1
HA
D. san 3L:LOC120447699
Genomic target
Or67d
1 kb
1
Co-inject Atalanta plasmid &
NLS-Cas9 protein into eggs
2
Screen G1 progeny for
abdominal mCherry
OR Gal4 knock-in
Gal4
mCherry
ie1
MAKVE GSGEGR...EENPGP MKLLSS...
Or67d
T2A
Gal4
Legend
CDS
promoter
hsp70 terminator
p10 terminator
translational start codon
T2A self-cleaving peptide
loxP recombination site
sgRNA cleavage site
HA homology arm (1kb)
B
AL
AL
D. san Or67d Gal4 male

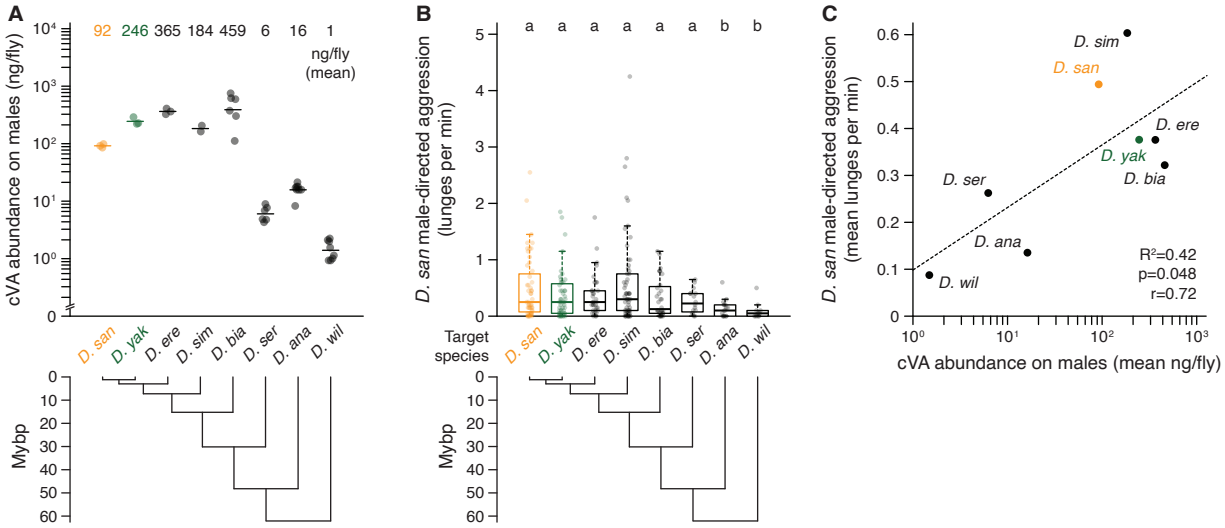
A
cVA abundance on males (ng/fly)
92 246 365 184 459 6 16 1
ng/fly (mean)
D. san
D. yak
D. ere
D. sim
D. bia
D. ser
D. ana
D. wil
Mybp
B
D. san male-directed aggression (lunges per min)
a a a a a a b b
Target species
C
D. san male-directed aggression (mean lunges per min)
cVA abundance on males (mean ng/fly)
R²=0.42
p=0.048
r=0.72

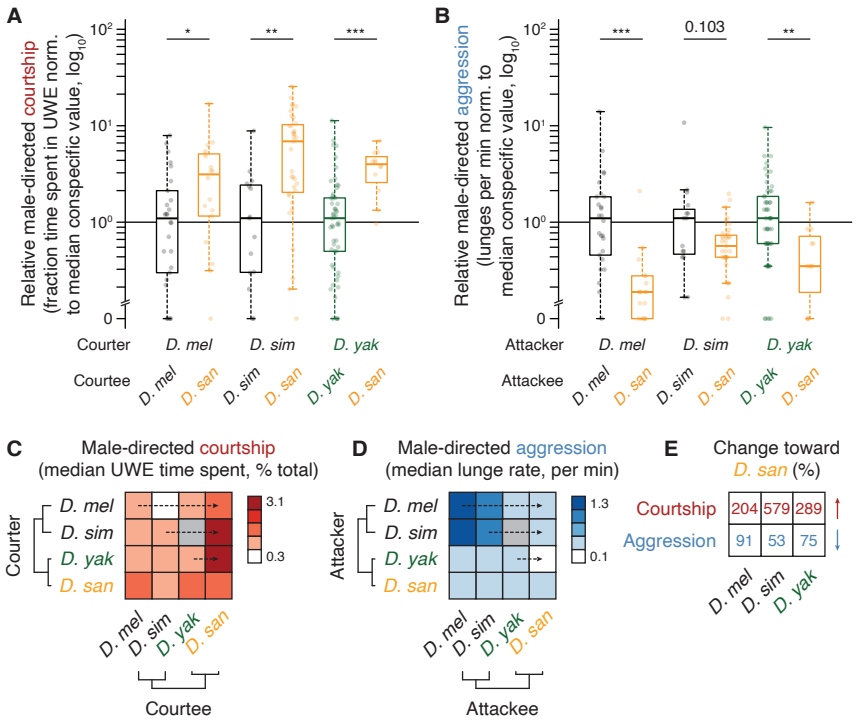
A
Relative male-directed courtship
(fraction time spent in UWE norm.
to median conspecific value, log10)
Courter
Courtee
D. mel
D. sim
D. yak
D. san
B
Relative male-directed aggression
(lunges per min norm. to
median conspecific value, log10)
Attacker
Attackee
0.103
C
Male-directed courtship
(median UWE time spent, % total)
3.1
0.3
Courter
Courtee
D
Male-directed aggression
(median lunge rate, per min)
1.3
0.1
Attacker
Attackee
E
Change toward
D. san (%)
Courtship
Aggression
204
579
289
91
53
75

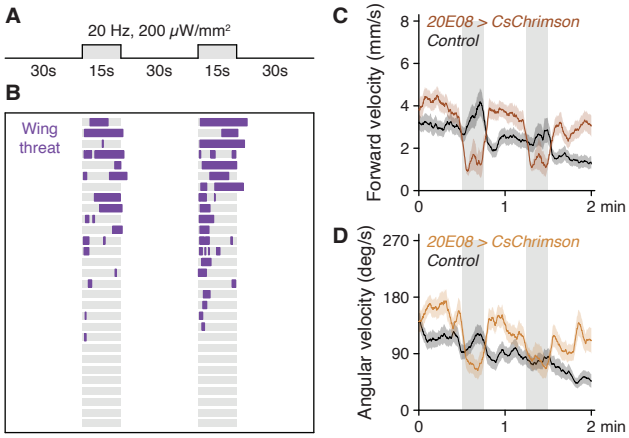
A
20 Hz, 200 μW/mm²
30s
15s
30s
15s
30s
B
Wing threat
C
20E08 > CsChrimson
Control
Forward velocity (mm/s)
8
6
4
2
0
0
1
2 min
D
20E08 > CsChrimson
Control
Angular velocity (deg/s)
270
180
90
0
0
1
2 min

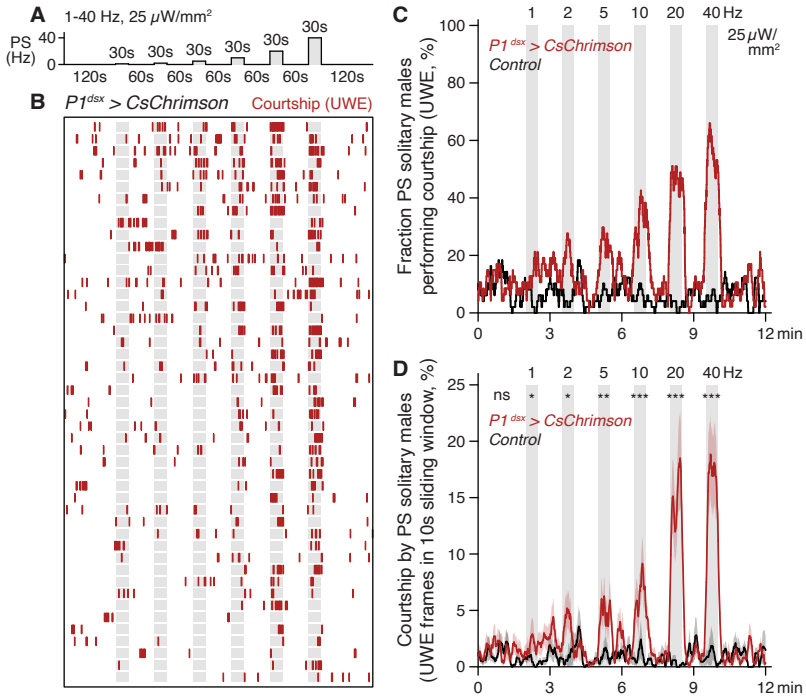
A
1-40 Hz, 25 μW/mm²
PS (Hz)
40
0
30s
120s
60s
B
P1dsx > CsChrimson
Courtship (UWE)
C
1 2 5 10 20 40 Hz
25 μW/mm²
P1dsx > CsChrimson
Control
Fraction PS solitary males performing courtship (UWE, %)
100
80
60
40
20
0
3
6
9
12 min
D
ns * * ** *** *** ***
Courtship by PS solitary males (UWE frames in 10s sliding window, %)
25
20
15
10
5

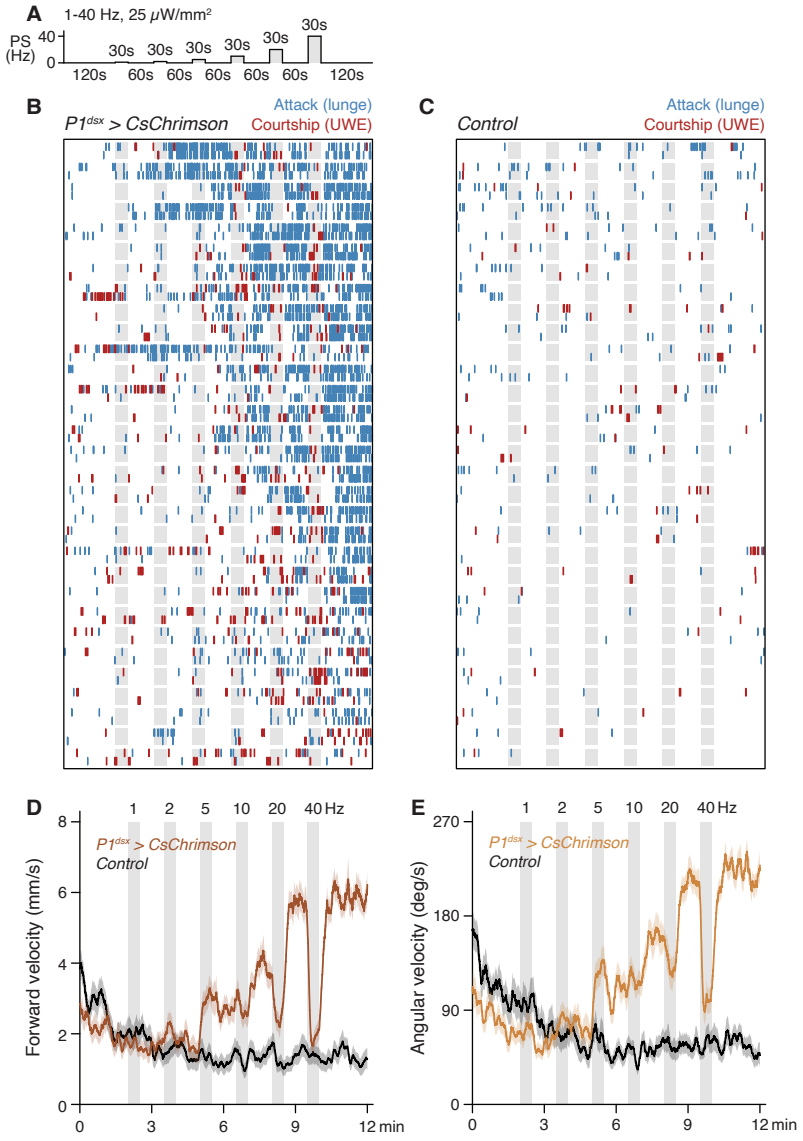
A
1-40 Hz, 25 μW/mm²
PS (Hz)
40
0
30s
30s
30s
30s
30s
30s
120s
60s
60s
60s
60s
60s
120s
B
P1dsx > CsChrimson
Attack (lunge)
Courtship (UWE)
C
Control
Attack (lunge)
Courtship (UWE)
D
1
2
5
10
20
40 Hz
P1dsx > CsChrimson
Control
Forward velocity (mm/s)
8
6
4
2
0
0
3
6
9
12 min
E
1
2
5
10
20
40 Hz
P1dsx > CsChrimson
Control
Angular velocity (deg/s)
270
180
90
0
0
3
6
9
12 min

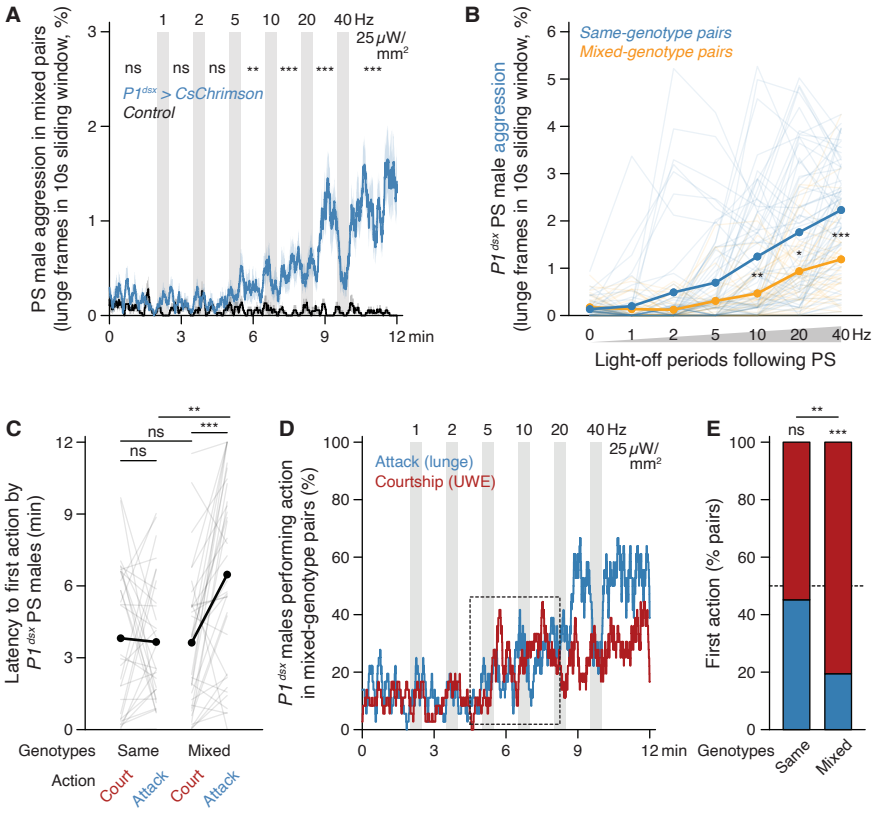
A
PS male aggression in mixed pairs (lunge frames in 10s sliding window, %)
1 2 5 10 20 40 Hz
25 μW/mm²
ns ns ns ** *** *** ***
P1dsx > CsChrimson
Control
0 3 6 9 12 min
B
P1 dsx PS male aggression (lunge frames in 10s sliding window, %)
Same-genotype pairs
Mixed-genotype pairs
0 1 2 5 10 20 40 Hz
Light-off periods following PS
C
Latency to first action by P1 dsx PS males (min)
ns
ns
***
**
Genotypes Same Mixed
Action Court Attack Court Attack
D
P1 dsx males performing action in mixed-genotype pairs (%)
1 2 5 10 20 40 Hz
25 μW/mm²
Attack (lunge)
Courtship (UWE)
0 3 6 9 12 min
E
First action (% pairs)
ns
***
**
Genotypes Same Mixed

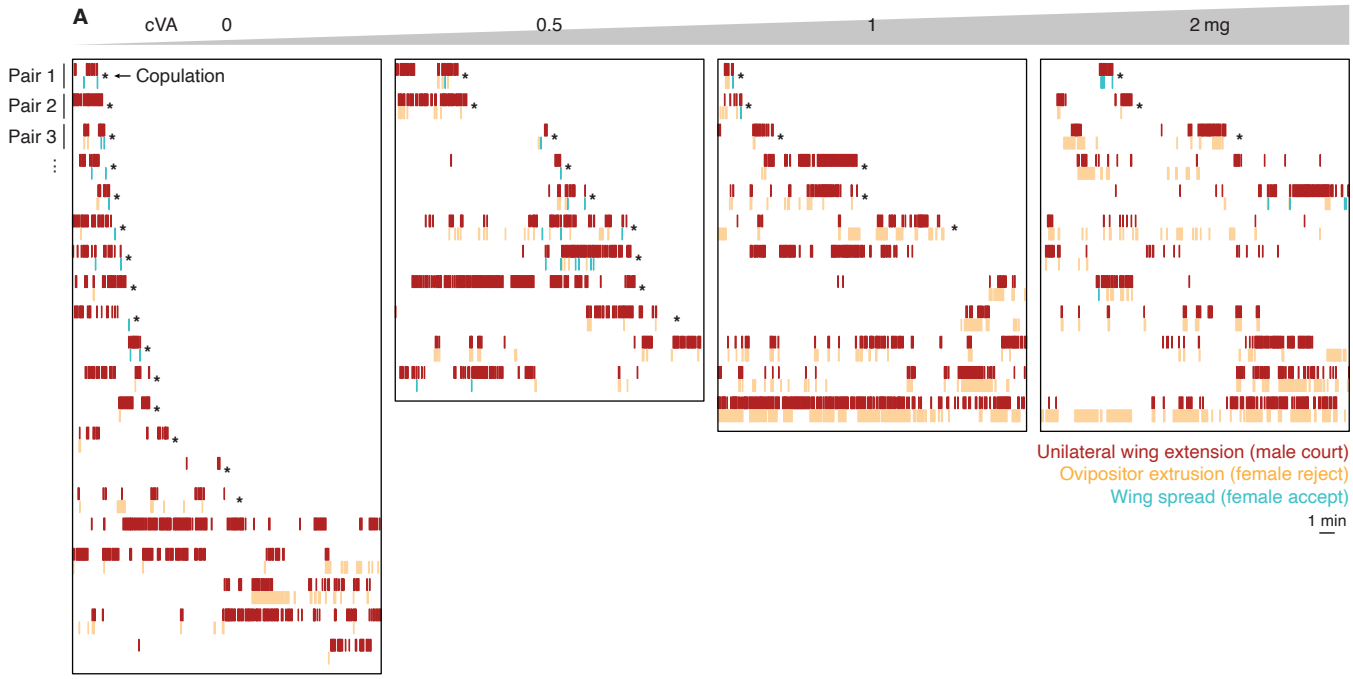
A
cVA
0
0.5
1
2 mg
Pair 1
Pair 2
Pair 3
← Copulation
Unilateral wing extension (male court)
Ovipositor extrusion (female reject)
Wing spread (female accept)
1 min

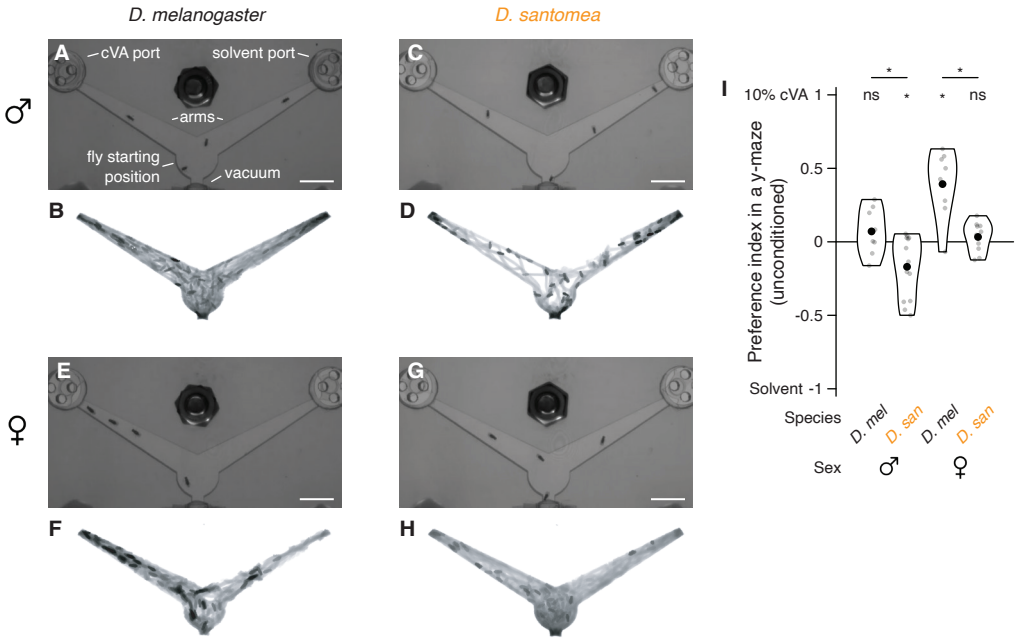
D. melanogaster
D. santomea
A
cVA port
solvent port
arms
fly starting position
vacuum
B
C
D
E
F
G
H
♂
♀
I
10% cVA 1
Solvent -1
0.5
0
-0.5
Preference index in a y-maze (unconditioned)
ns
*
*
*
ns
Species
D. mel
D. san
D. mel
D. san
Sex
♂
♀

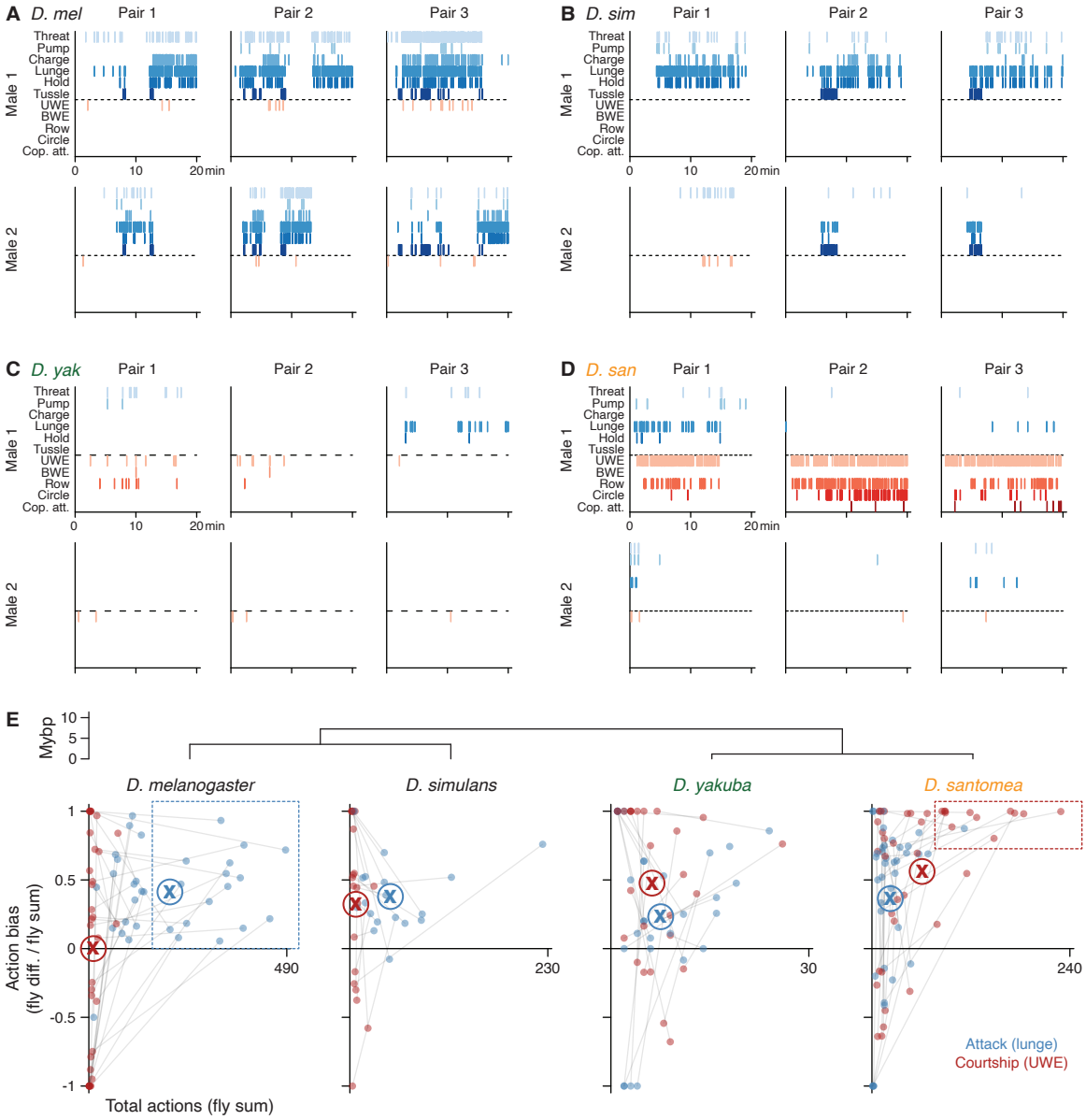
A D. mel
B D. sim
C D. yak
D D. san
Pair 1
Pair 2
Pair 3
Threat
Pump
Charge
Lunge
Hold
Tussle
UWE
BWE
Row
Circle
Cop. att.
Male 1
Male 2
0
10
20 min
E
Mybp
10
5
0
D. melanogaster
D. simulans
D. yakuba
D. santomea
Action bias
(fly diff. / fly sum)
1
0.5
0
-0.5
-1
490
230
30
240
Total actions (fly sum)
Attack (lunge)
Courtship (UWE)

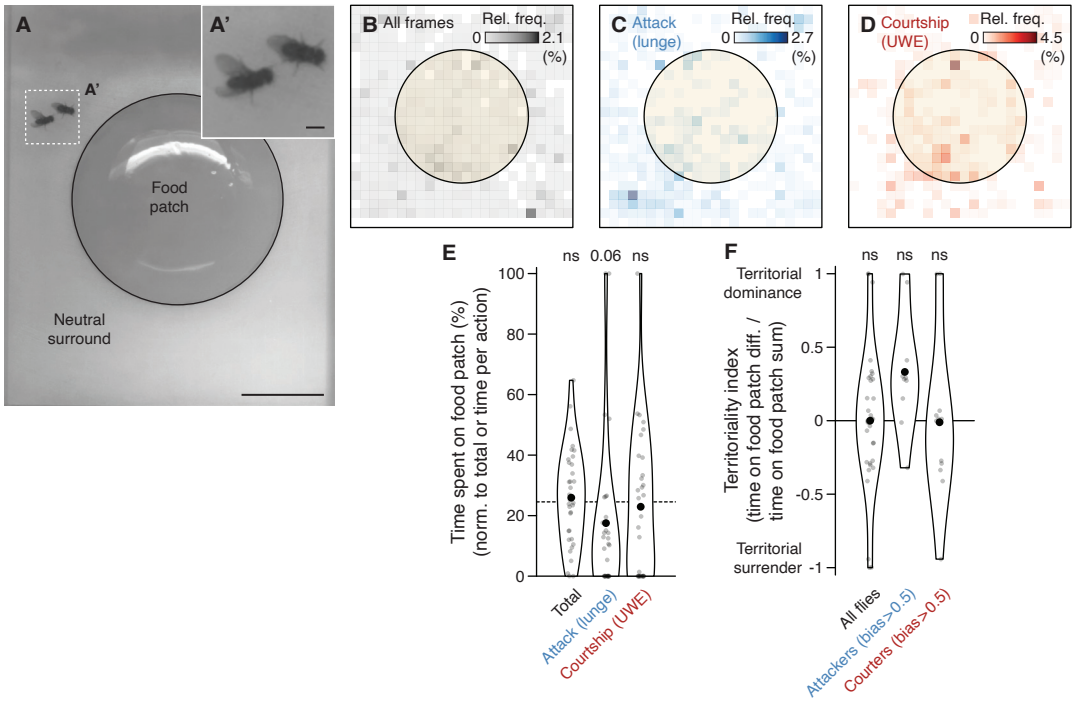
A
A'
A'
Food patch
Neutral surround
B All frames
Rel. freq.
0
2.1
(%)
C Attack (lunge)
Rel. freq.
0
2.7
(%)
D Courtship (UWE)
Rel. freq.
0
4.5
(%)
E
ns
0.06
ns
Time spent on food patch (%)
(norm. to total or time per action)
100
80
60
40
20
0
Total
Attack (lunge)
Courtship (UWE)
F
ns
ns
ns
Territorial dominance
Territoriality index
(time on food patch diff. / time on food patch sum)
1
0.5
0
-0.5
Territorial surrender
-1
All flies
Attackers (bias>0.5)
Courters (bias>0.5)

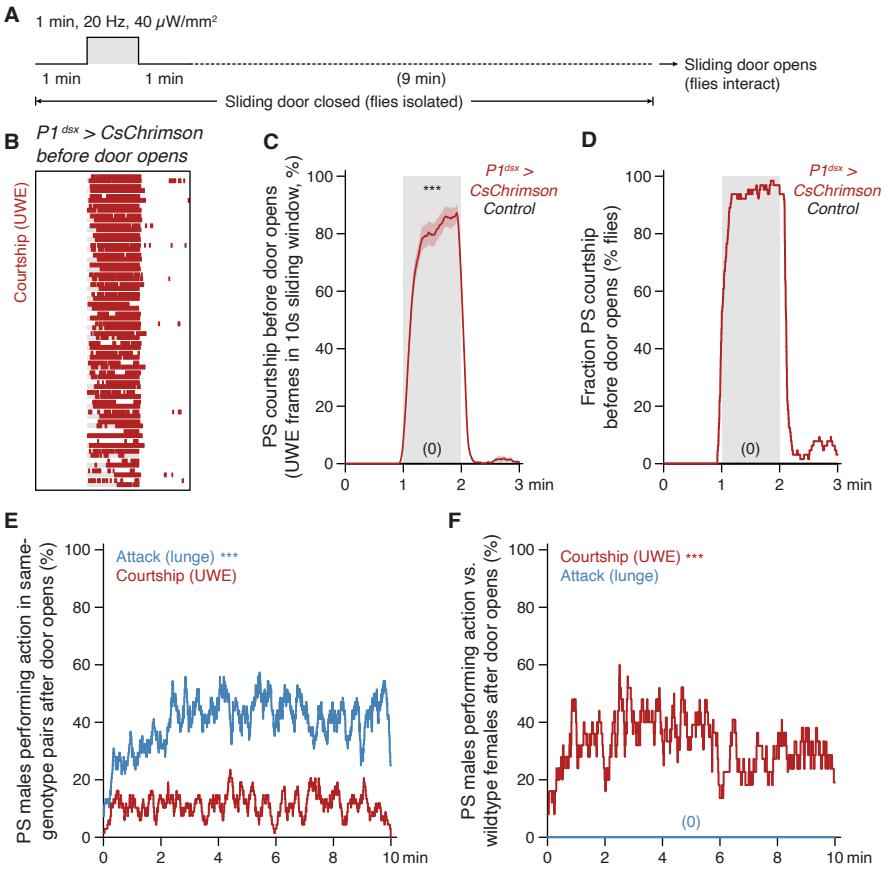
A
1 min, 20 Hz, 40 μW/mm²
1 min
1 min
(9 min)
Sliding door opens
(flies interact)
Sliding door closed (flies isolated)
B
P1dsx > CsChrimson
before door opens
Courtship (UWE)
C
PS courtship before door opens
(UWE frames in 10s sliding window, %)
P1dsx >
CsChrimson
Control
***
(0)
3 min
D
Fraction PS courtship
before door opens (% flies)
P1dsx >
CsChrimson
Control
(0)
3 min
E
PS males performing action in same-genotype pairs after door opens (%)
Attack (lunge) ***
Courtship (UWE)
10 min
F
PS males performing action vs. wildtype females after door opens (%)
Courtship (UWE) ***
Attack (lunge)
(0)
10 min

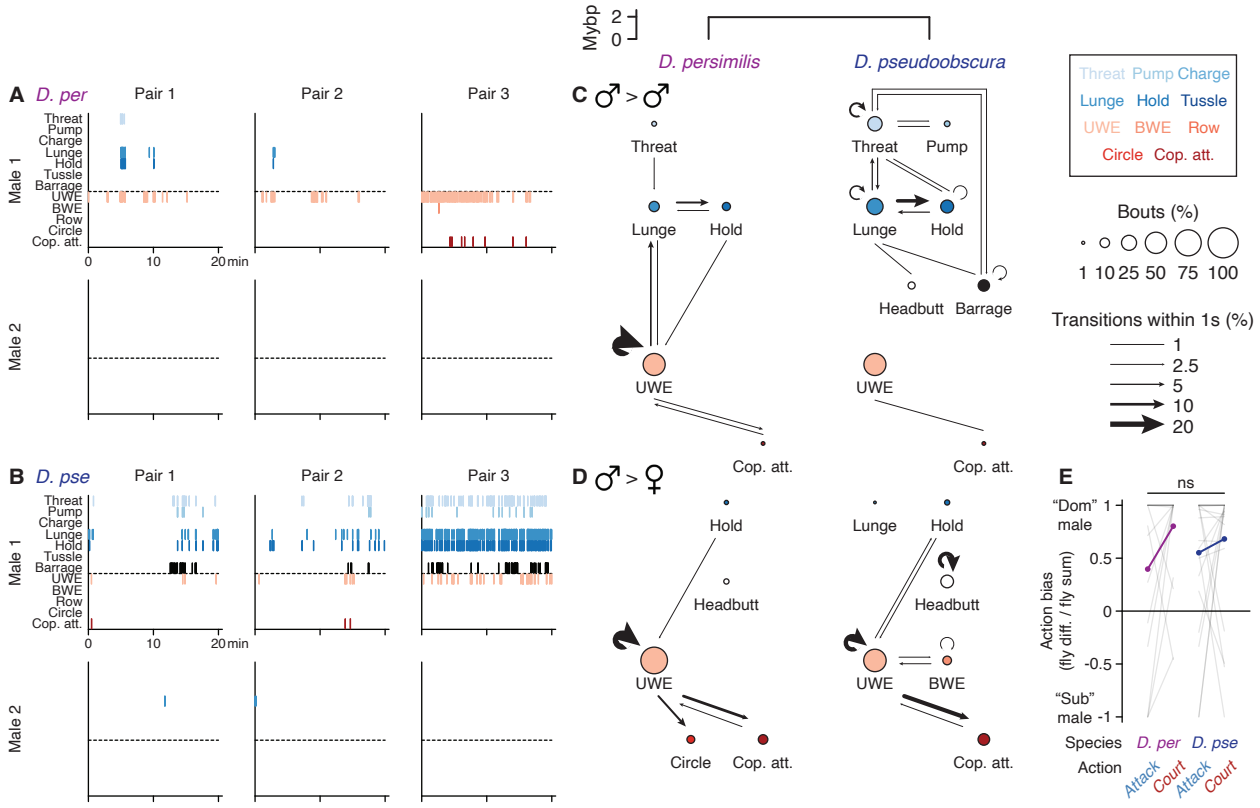
A D. per
Pair 1
Pair 2
Pair 3
Threat
Pump
Charge
Lunge
Hold
Tussle
Barrage
UWE
BWE
Row
Circle
Cop. att.
Male 1
Male 2
0
10
20 min
B D. pse
Mybp
2
0
D. persimilis
D. pseudoobscura
C ♂ > ♂
Threat
Lunge
Hold
UWE
Cop. att.
Headbutt
Barrage
D ♂ > ♀
Circle
BWE
Bouts (%)
1 10 25 50 75 100
Transitions within 1s (%)
1
2.5
5
10
20
E
ns
"Dom" male
"Sub" male
Action bias (fly diff. / fly sum)
Species
Action
Attack
Court